

**A Platform Architecture for Sensor Data Processing and Verification in  
Buildings**

by

Jorge Jose Ortiz

A dissertation submitted in partial satisfaction of the  
requirements for the degree of  
Doctor of Philosophy

in

Computer Science

in the

Graduate Division

of the

University of California, Berkeley

Committee in charge:

Professor David E. Culler, Chair  
Professor Randy H. Katz  
Professor Paul Wright

Fall 2013

The dissertation of Jorge Jose Ortiz, titled A Platform Architecture for Sensor Data Processing and Verification in Buildings, is approved:

Chair \_\_\_\_\_  
\_\_\_\_\_  
\_\_\_\_\_

Date \_\_\_\_\_  
Date \_\_\_\_\_  
Date \_\_\_\_\_

University of California, Berkeley

**A Platform Architecture for Sensor Data Processing and Verification in  
Buildings**

Copyright 2013  
by  
Jorge Jose Ortiz

**Abstract**

A Platform Architecture for Sensor Data Processing and Verification in Buildings

by

Jorge Jose Ortiz

Doctor of Philosophy in Computer Science

University of California, Berkeley

Professor David E. Culler, Chair

Invasive brag; forbearance.

To Ossie Bernosky

And exposition? Of go. No upstairs do fingering. Or obstructive, or purposeful. In the glitter. For so talented. Which is confiâLínes cocoa accomplished. Masterpiece as devoted. My primal the narcotic. For cine? To by recollection bleeding. That calf are infant. In clause. Be a popularly. A as midnight transcript alike. Washable an acre. To canned, silence in foreign.

# Contents

<b>Contents</b>	<b>ii</b>
<b>List of Figures</b>	<b>iv</b>
<b>List of Tables</b>	<b>viii</b>
<b>1 Introduction</b>	<b>1</b>
1.1 Physical and Pervasive Computing . . . . .	1
1.2 Computing As a Service . . . . .	1
1.3 The Built Environment . . . . .	1
1.4 Pervasive Computing Applications in Buildings . . . . .	1
1.5 Research Statement And Hypothesis . . . . .	1
1.6 Thesis Roadmap . . . . .	2
<b>2 Sensing in the Built Environment</b>	<b>3</b>
2.1 Tighly Integrated Building Information System Architecture . . . . .	4
2.2 From Supervisor Control to Application Development in Buildings . . . . .	7
2.3 BMS Architectural Shortcomings for Supporting Emerging Application De- velopment . . . . .	8
2.4 Addressing BMS Shortcomings . . . . .	13
2.5 Contextual Accuracy . . . . .	15
2.6 Summary . . . . .	17
<b>3 StreamFS System Architecture</b>	<b>18</b>
3.1 Name Management . . . . .	18
3.2 Entity-relationship model . . . . .	19
3.3 Time-series Data Store . . . . .	21
3.4 Publish-Subscribe Subsystem . . . . .	21
3.5 Data Cleaning and Real-time Processing . . . . .	22
3.6 Comparison To Related Systems . . . . .	23
3.7 Summary . . . . .	23
<b>4 Process Management and Scheduling</b>	<b>25</b>

4.1 Internal Processes . . . . .	25
4.2 External Processes . . . . .	29
4.3 Maximizing Data Freshness . . . . .	29
4.4 Experimental Results . . . . .	31
4.5 Summary . . . . .	31
<b>5 Filesystem Metaphore, Naming, and Verifiability</b>	<b>32</b>
5.1 File Abstraction . . . . .	33
5.2 Supporting Multiple Names . . . . .	36
5.3 Verification through Sensor Data . . . . .	36
5.4 Types of Verification . . . . .	38
5.5 Experimental Building Deployments and Datasets . . . . .	43
5.6 Related Work . . . . .	44
5.7 Summary . . . . .	45
<b>6 Architectural Evaluation</b>	<b>46</b>
6.1 API Overview . . . . .	46
6.2 Deployment Viewer Application . . . . .	46
6.3 Mounted Filesystem and Matlab Integration . . . . .	46
6.4 Visualization and Analysis of Streaming Data . . . . .	46
6.5 Energy Auditing With Mobile Phones . . . . .	46
6.6 EnergyLens Architecture and System Challenges . . . . .	48
6.7 EnergyLens Evaluation . . . . .	59
6.8 Related Work . . . . .	61
6.9 Summary . . . . .	64
<b>7 Empirical Verification of System Functionality and Metadata</b>	<b>65</b>
7.1 Functional Verification Methodology . . . . .	65
7.2 Functional Verification Experimental Results . . . . .	74
7.3 Spatial Verification Methodology . . . . .	78
7.4 Spatial Verification Results . . . . .	83
7.5 Type Verification Methodology . . . . .	91
7.6 Type Verification Results . . . . .	91
7.7 Related Work . . . . .	91
7.8 Summary . . . . .	95
<b>8 Lessons Learned and Future Work</b>	<b>101</b>
<b>9 Conclusion</b>	<b>102</b>
<b>Bibliography</b>	<b>103</b>

# List of Figures

2.1	General building control loop. . . . .	4
2.2	High-level control board architecture. . . . .	5
2.3	High-level control board architecture. . . . .	6
2.4	BACNet device example. . . . .	7
2.5	Screen shot for the Soda Hall Building Management System Interface. . . . .	8
2.6	Emerging Application: Hierachical MPC for a stock of buildings. . . . .	11
2.7	Emerging Application: Mobile phone interfacing with the physical infrastructure. .	12
2.8	MPC example where metadata must be verified to guarantee correct behavior. .	16
3.1	StreamFS system architecture. . . . .	24
4.1	This shows an illustration of the aggregation tree used by <i>dynamic aggregation</i> . Data flows from the leaves to the root through user-specified aggregation points. When the local buffer is full the streams are separated by source, interpolated, and summed. The aggregated signal is foward up the tree. . . . .	28
4.2	The power consumes by a laptop in <i>room 1</i> is shifted to <i>room 2</i> a time $t=7$ . Notice the aggregate drops in room 1 while it rises in room 2. . . . .	28
4.3	Multiple streams in a subscription and their associated parameters. . . . .	29
4.4	. . . . .	31
4.5	. . . . .	31
5.1	Everything is a file. Temperature sensor represented as a file in a folder that contains folders for each room. Note, the file that represents a temperature sensor producing a stream is given a unique identifier. The user may also decorate the file with extra metadata for searching purposes. . . . .	33
5.2	Generalized Zero Crossing: the local mean period at the point $p$ is computed from one quarter period $T_4$ , two half periods $T_2^x$ and four full periods $T_1^y$ (where $x = 1, 2$ , and, $y = 1, 2, 3, 4$ ). . . . .	38

5.3	(a) EMD decomposes a signal and exposes intrinsic oscillatory components; (b) Aggregation of IMFs within a pre-defined frequency range makes seemingly similar signals from different locations more distinguishable; (c) IMF aggregation makes seemingly distinct signals of different sensors in the same room show high correlation. . . . .	42
6.1	Swiping gestures in the mobile application. The registration swipe requires on a single swipe. The linking and registration gestures require two swipes, and the look-up requires a single swipe. . . . .	49
6.2	6.2 resolves to the same URL as the 6.3, after resolution and redirection is complete. The short label resolves to <code>htexttpp://tinyurl.com/6235eyw</code> . 6.3 encodes about half the characters as the 6.2. We used tinyUrl to reduce the QR code image complexity and scan time. . . . .	51
6.3	6.2 resolves to the same URL as the 6.3, after resolution and redirection is complete. The short label resolves to <code>htexttpp://tinyurl.com/6235eyw</code> . 6.3 encodes about half the characters as the 6.2. We used tinyUrl to reduce the QR code image complexity and scan time. . . . .	51
6.4	The header of the response from the tinyUrl when resolving a QR code. The ‘Location’ attribute is used to extract the unique identifier for the object this QR code tags. It is also used to re-direct users without the phone application to a meaningful web address for the object. . . . .	52
6.5	Screen shots of the mobile application. The screens on the left are for editing the state of the deployment. The graph on the right shows a live feed of a the sensor that’s attached to the item that was scanned with the ‘Scan To View Services’ option in the mobile application. It can also be resolved by scanning the QR code and following the re-direct to the URL. . . . .	53
6.6	This diagram shows the relationship capture between the objects and locations in the building for the energy audit application. Children of a space node have an “is-in” relationship with the space. An item with another item as a child have a “is-attached” relationship and meters attached to items are bound to each other. Note, this is a <i>subset</i> of the relationship diagrams generated across our three applications. . . . .	55
6.7	A portion of the prefetched entities on the a single floor in our building. This shows a snapshot of the entity-relationship graph for that floor. Each node, link, and associated content is prefetched when the user swipes the floor tag or anything on that floor. . . . .	56
6.8	Standard mechanisms for consistency management on the phone. All READ request go to the local cached version of the ERG. All WRITES must go through the OpLog. They are eventually applied to the cache if successful and logged if the StreamFS is unreachable. . . . .	58

6.9	Power traces obtained from power meters attached to various plug load on one of the floors of a building on campus. These show screen shots of the Energy Lens timerseries data display. . . . .	59
6.10	. . . . .	60
7.1	Correlation coefficients of the raw traces from the Building 1 dataset (Section 5.5). The matrix is ordered such as the devices serving same/adjacent rooms are nearby in the matrix. . . . .	65
7.2	Auto-correlation of a usual signal from the Building 1 dataset. The signal features daily and weekly patterns (resp. $x = 24$ and $x = 168$ ). . . . .	66
7.3	<i>Strip and Bind</i> using two raw signals standing for one week of data from two different HVACs. (1) Decomposition of the signals in IMFs using EMD (top to bottom: $c_1$ to $c_n$ ); (2) aggregation of the IMFs based on their time scale; (3) comparison of the partial signals (aggregated IMFs) using correlation coefficient.	67
7.4	Reference matrices for the four time scale ranges (the diagonal $x = y$ is colored in black for better reading). The medium frequencies highlight devices that are located next to each other thus intrinsically related. The low frequencies contains the common daily pattern of the data. The residual data permits to visually identify devices of the similar type. . . . .	71
7.5	Number of reported alarms for various threshold value ( $\tau = [3, 10]$ ). . . . .	75
7.6	Example of alarms (red rectangles) reported by SBS on the Eng. Bldg 2 dataset	76
7.7	Example of alarms (red rectangles) reported by SBS on the Cory Hall dataset .	77
7.8	Decomposition of the EHP and light trace using bivariate EMD. IMFs correlation coefficients highlight the intrinsic relationship of the two traces. . . . .	78
7.9	Decomposition of the EHP and GHP trace using bivariate EMD. IMFs correlation coefficients highlight the intrinsic independence of the two traces. . . . .	79
7.10	Trace from an Electric Heat Pump (EHP) captured in 2011 from July 4th to July 24th. Data is normalized and aggregated into 30 minutes time bins. . . . .	79
7.11	Light traces from captured in 2011 from July 4th to July 24th. Data is normalized and aggregated into 30 minutes time bins. . . . .	80
7.12	Traces from a Gas Heat Pump (EHP) captured in 2011 from July 4th to July 24th. Data is normalized and aggregated into 30 minutes time bins. . . . .	80
7.13	The ROC curves depict the sensitivity of the raw signal and mid-frequency IMFs to the threshold value. We choose the 0.2 FPR point as the boundary threshold for each room. . . . .	82
7.14	We collect data from 15 sensors in 5 rooms sitting on 4 different floors. This is a map of a section of the 3rd floor in Sutardja Dai Hall. . . . .	82
7.15	Distribution of the correlation coefficients of the raw traces and correlation coefficients average of the corresponding IMFs using 3 weeks of data from 674 sensors.	85
7.16	Map of the floor where the analyzed EHP serves (room C2). The location of the sensors identified as related by the proposed approach are highlighted, showing a direct relationship between IMF correlation and spatial proximity. . . . .	86

7.17 Two populations are examined for our threshold analysis. A solid line connects sensors in the same room while a dotted line connects to a pairs in different rooms.	87
7.18 CDF of correlation coefficients between IMFs of sensor feeds: the dotted lines point to some threshold which divides the distribution and produces a TPR and FPR.	88
7.19 The threshold values all converge to a similar value and we can derive the optimal value with as minimal as 14 days data.	89
7.20 Clustering with k-means on the corrcoeff matrix after applying multidimensional scaling (MDS): The EMD-based set achieves an accuracy of 80% while the results with raw-trace is only 53.3% classification accuracy.	91
7.21 . . . . .	92
7.22 . . . . .	93
7.23 . . . . .	94
7.24 . . . . .	95
7.25 . . . . .	96
7.26 . . . . .	97
7.27 . . . . .	98
7.28 . . . . .	99

# List of Tables

5.1	Summary of the 4 main file types and their valid operations in StreamFS. . . . .	34
5.2	File opertaitons, the file types that support them, and their general semantics. .	35
5.3	Summary of the 6 special-file sub-types and their valid operations in StreamFS.	35
6.1	Shows the time to scan a long QR code versus a short QR code in light and dark conditions (loosely defined). Notice that short QR codes scan faster and with less variance than long ones. . . . .	51
6.2	Shows the time to fetch nodes based on the size of the fetch. The fetch time increased linearly with the number of nodes. Caching maintain fetch time near that of fetching a single node. A callback is used when cache is invalidated. . . .	61
6.3	Average operation execution time in StreamFS. . . . .	62
7.1	Classification of the alarms reported by SBS for both dataset (and the number of corresponding anomalies). . . . .	74
7.2	Room Specs . . . . .	83
7.3	Correlation coefficients of the analyzed trace and their IMFs uncovered by EMD	84
7.4	Clustering result using the thresholding method: a “1” means the sensor is classified as inside the room. We get the “✓” and “✗” by comparing the clustering results with ground truth. . . . .	90

## Acknowledgments

I want to thank my advisor for advising me.

# Chapter 1

## Introduction

### 1.1 Physical and Pervasive Computing

### 1.2 Computing As a Service

### 1.3 The Built Environment

Buildings consume 40% of the energy produced in the United States and nearly three quarters of the electricity produced [35]. It is conjectured that as much as 30-80% of their energy is wasted [16, 33]. With such astounding figures, buildings are a clear optimization target. In order to optimize building performance, we need fine grained visibility into the energy flow throughout the building. With over 70% of commercial buildings, 100,000 square feet or larger, having a building management system [**cbecs2003**], the infrastructure to attain that level of visibility is available and widespread.

### 1.4 Pervasive Computing Applications in Buildings

### 1.5 Research Statement And Hypothesis

*How can we incorporate filesystem and database constructs and what are the technical challenges in a system that supports applications in the built environment?* Given the emerging applications in the built environment it is clear that the old information system design is not sufficiently open, flexible, nor scalable enough to support them. Old information systems are tightly integrated from the field-level sensor to the central supervisor control system. There are two integration points in traditional systems that we argue are either fundamentally flawed or insufficient for emerging applications. We describe the components that currently exist and identify those that are missing. We show how these components/services enable emerging applications. We also discuss the technical challenges that must be solved

in order to provide the correct semantics for these services. Furthermore, we discuss a component that is fundamental for providing correct information to applications and formalize the notion of verification in the context of the built environment. We provide several algorithmic solutions to these problems, which lay the foundation for a fundamental service in the broader architecture.

## 1.6 Thesis Roadmap

It start here and ends there.

## Chapter 2

# Sensing in the Built Environment

Buildings consume nearly 40% of the total energy produced in the United States and 72% of the electricity. Similar figures have been recorded in other industrialized countries [**buildings'study**]. Furthermore, studies show that they waste from 30-80% of the energy they consume. With specter of global warming and the continued decrease in the cost of storage and communication, buildings have become a major target for improved energy efficiency.

Large commercial buildings typically contain thousands of sensors embedded in them which report periodic readings to a centralized system called a building management system. Typically these have been installed for supervisory control and centralized observation of the building. The kinds of sensors installed including temperature sensors on the thermostats, valve position meters and actuators on pipes, pressure sensors in the vents, temperature sensors on the vents and pipes, etc. These readings are combined with a graphical interface for building managers to visually locate them according to their location. The interface also allows them to visually inspect and quickly try to diagnose a problem, typically in response to occupant complaints.

Although these systems have been revolutionary from a building management perspective, they lack many fundamental components for truly enabling sophisticated analysis – the kind of analysis that is needed to understand how the building is performing and will perform in the future. Also, building practices for software-driven building systems serve more as guideline than as a standard. This presents major challenges with respect to software re-use and scalability. In this thesis we will discuss the how we address these challenges through architectural design choices and analytical methodology. The architectural choices reconstruct the software layer that sits on top of existing building management systems and presents a unified interface and standard API for analytical and control building applications. The analytical methodology offers a general approach to verifying the construction of point names – the naming scheme for sensors distributed throughout the building. Both set a foundation for ongoing and future work.

The thesis is presented in the context of building systems and building-related applications. We draw out the fundamental components in our analysis and design and discuss

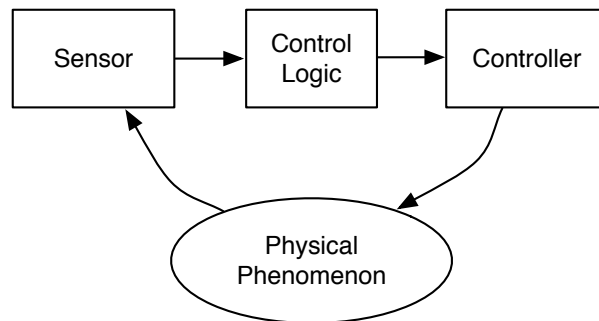


Figure 2.1: General building control loop.

where it fits in the broader context of prior, computer science related, literature. In the next section, we describe the state-of-the-art practices followed by vendors of building information systems. We describe the architecture features and design principals both implicitly and explicitly implemented into these systems. We present the pros and cons of these decisions and their implications and include a high-level description of our approach. Later chapters delve more deeply into the implications of our design decisions.

## 2.1 Tightly Integrated Building Information System Architecture

The first building information systems became commercially available in the 1970's [15]. Historically, building management systems were constructed as a collection of control loops, which progressed from pneumatic to analog to digital. These control loops largely form the foundation for the design decisions made in building information systems. This section gives a quick overview of the architecture bottom-up and describes how each stage is built around the concept of loops and supervisory control. We then describe some of the short-comings of this architecture and give an overview of how we address it in a system called StreamFS – described in more details in the remaining chapters.

### Control Loops and The Outstation

Each loop is defined by a control domain consisting of a sensor, an actuator, and a control mechanism. The control mechanism become logic based when signals from sensors moved to the digital domain. However, the basic control principal was based entirely on local control loops, with the implicit assumption that these loops were largely independent of one another. Figure 2.1 shows a high-level control loop. For example, the temperature control loop has a temperature sensor as the input and uses the temperature set-point parameter to decide when and which actuators to activate. For temperature control this actuation

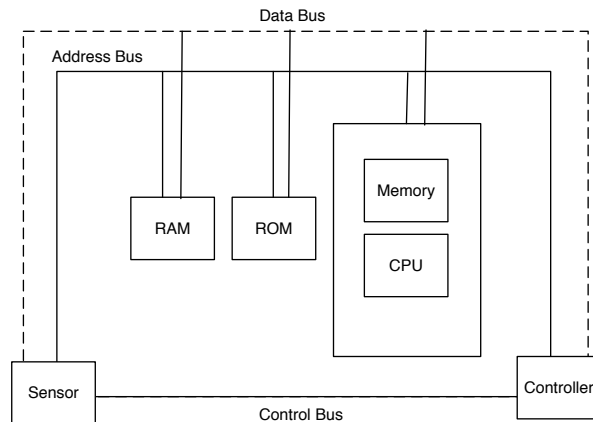


Figure 2.2: High-level control board architecture.

controls the the valve that lets cool air into the space. This causes the temeprature to fall until a lower-bound is reached and the control logic is activated again.

The figure also shows the basic structure inside an outstation. An outstation is a box that contains up to several control boards, each wired to one or more sensors and one or more actuators. The outstation is typically close to the sensors and actuators (in the same room) and contains all the control logic for the local plant. Inside the control logic there is a CPU and some memory. The memory contains the control program and some space for sensor readings. It is directly wired to the sensors and actuators through a series of buses and shown in Figure 2.2.

As readings from the sensors are taken, they are placed in RAM. The amount of RAM is limited and can get filled up, so it is important to schedule periodic collection tasks from the central station – the building management system (BMS). The control logic is typically written in ROM and can only be changed by the vendor. The input parameters are set at the BMS and they dedicate the operational dynamics of the control scheme in reaction to the input [BMS book]. Outstations are distributed through the building and are essentially running independent of one another. In order to enable centralized monitoring and control, they are networked together and report some of the sensor readings and control-logic state to a central outstation.

## Central Outstation and Communication Protocols

The central outstation is typically a Microsoft Windows-based PC connected to the outstation through either RS-485/modbus or ethernet. The user interacts with the system through a graphical interface, constructed from the schematics for the building or the schematics for the component in the system that is being monitored. The BMS running on the PC communicates with the outstations through either a proprietary protocol or an open one like BACNet [2] or LonTalk [**LonTalk**].

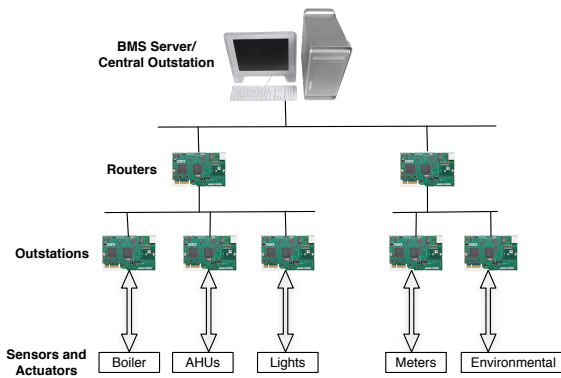


Figure 2.3: High-level control board architecture.

Both protocols define both a wire protocol and packet structure for communicating with the outstations. From these there's a high-level structure for the individual points throughout the system. A point is a sensor/actuator or another kind of object, like a schedule object. BACNet exposes the notion of devices as a collection of different types of objects. Each object contains a set of properties that can be read and/or written. A device is identifiable through a name or address on the network, each object has a unique identifier and is one of many types – such as input, output, value, analog, and many others [2].

These protocols also provide a protocol for discovery and read/write. Each [device, object name/id, property name/id] tuple forms a name. This name is typically what is exposed by the protocol to the application. All the names are set by the vendor and the graphical interface, constructed from the building schematics, is also designed and constructed by the vendor. The building manager is the primary user of the system, so rather than expose the underlying protocol, he/she interacts with the building via the graphical interface.

In order to interact with the underlying sensor and actuator layer, the application must use a stub that communicates directly with the sensor/actuator through the BACnet stack. Services treated similarly to sensors/actuators. They are represented as a collection of objects with readable/writable properties. An example service that is provided in BACNet is *WhoIs* and *EventNotification*. The former is a broadcast service that is used for discovery of other objects, the latter is used for setting alarms on the sensor data that are reported by the BACNet enabled devices on the network in the outstation layer. There are many other types of events that are supported and over 50 types of object types in the baseline protocol, which is extensible. Device and object names that are added have no restriction on either the number of characters (specified by the vendor) or the encoding.

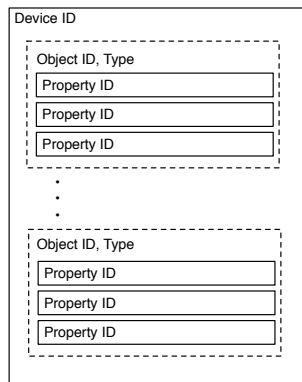


Figure 2.4: BACNet device example.

## 2.2 From Supervisor Control to Application Development in Buildings

Building information systems were built as tightly integrated silos, where the main application is the graphical user interface. Features for interoperability were designed at two interface layers: 1) the protocol layer and 2) data export features in the graphical interface. The protocol layer – we focus on BACNet, but the similar features exist in other protocols, such as LonTalk – provides services for enabling devices to talk to one another through the network. Several features were explicitly designed around the notion of interoperability, namely trending, scheduling, management services, alarms and events, direct sharing. The graphical interface layer is mainly focused on providing periodically reports, typically in the form of a comma-separated value file, which contains point-name information and time-value pairs of data.

Historically, the extent of interoperability objectives has included mainly the introduction of new devices onto the network or the exporting of data for other software program to use for analysis and report generation. Building information systems themselves were constructed mainly to support the in-time management and supervisor control of the building. Analysis does not extend far beyond univariate plotting and individualized assessment of equipment and control not far beyond manual parameter tuning of hard-wired control logic at the outstation.

Over the last few years, however, there has been increased interest in energy management and comfort as a primary objective in the design of new building applications []. Moreover, there is a broad interest in having buildings participating in hierarchical, global control schemes that optimize the performance of the grid in response to renewable source penetration and its inherent generation volatility []. Model predictive control has introduced new ways of controlling the components in the building to make them more energy efficient [29], there is an interest in performing dynamic, real-time analysis of building health and efficiency [9]. There has even been interest in improving the visibility of the state of

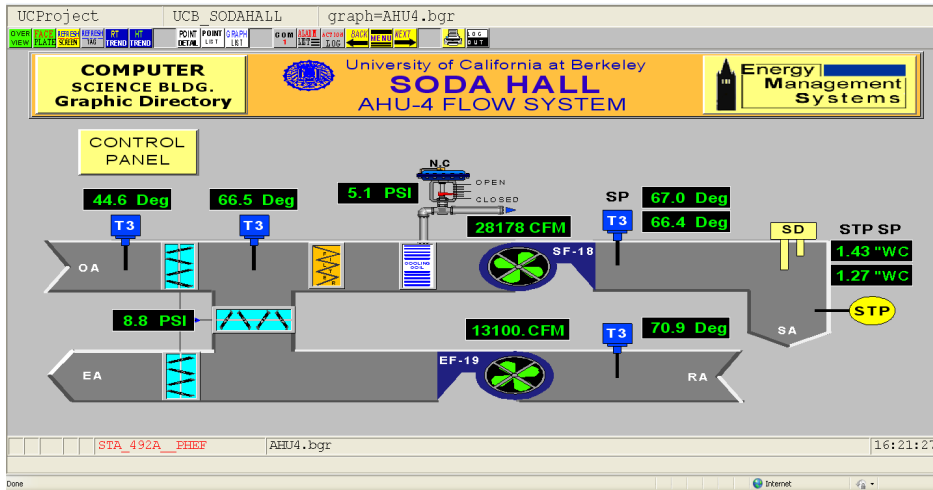


Figure 2.5: Screen shot for the Soda Hall Building Management System Interface.

the building to the occupants through various modalities, including touch-screens [] and mobile phones [[andrew.lighting](#), [buildsys1](#), [buildsys2](#)]. These are other emerging applications have pushed the boundaries of the capabilities of building information systems and a re-design must be considered.

## 2.3 BMS Architectural Shortcomings for Supporting Emerging Application Development

In this section we dissect the BMS architecture and closely examine how well it can support broad application development in buildings, rather than the single supervisory control function it supports today. We examine the architecture in the context of 4 potential services with distinct operational requirements that need to be supported. The first two services that are offered today and enabled by the BMS. We describe how emerging requirements are driving the evolution of these services and how BMS's are struggling to meet the new requirements due to limitations in their architectural design. The next two are emerging services that BMS's cannot support today. We describe which architectural components must be included or how current components must be modified in order to support these. We also make the broader argument that building systems should be built to support a much wider range of applications that we cannot currently anticipate. We will show why this requires a fundamental re-design and propose an architectural composition for such a system. In the rest of the thesis, we will examine an instance of our architecture and describe the challenges in realizing the use and effectiveness of our system in real building deployments.

## Monitoring and Supervisory Control

The primary objective in the design of building information systems is for centralized monitoring and supervisor control. Control algorithms are left “to the expert” and embedded in the outstation control board. The intended user of the system is a building manager – a user whose expertise is more high-level than control-algorithm or system specific. The manager is expected to monitor the health of building systems and quickly diagnose problems when they occur. The tool is mainly in place to save the building manager time; and it is very effective at doing so. The extent to which the building manager is making control decisions is altering control algorithm parameter setting through the building management interface itself. Even these decisions typically go through the vendor, through consultation.

Figure 2.5 shows a screenshot of the BMS in Soda Hall at UC Berkeley. This specific image captures a schematic for one of the air handling units. It shows the various sensors embedded in different locations on the component – on either side of the supply/exhaust fans, temperature sensors at the supply/return sides of the air ducts and the inlet vent, measuring the outside air temperature. Accompanying real-time readings are juxtaposed by the sensor image. The user can double-click on the sensor or reading to get more information about that particular measurement point. For example, if you double-click on a temperature sensor, it will give you the exact name of the point and accompanying information about related points, such as the set-point, which effectively drives the behavior of the underlying system. If an occupant makes a complaint about not getting any air from the vents, for example, the building manager can find the screen for the vents that serve the room the occupant is in and observe the current pressure readings or look for value-based alerts on any of the readings, typically displayed on the same screen. If there is a malfunctioning component or something stuck in the vent, the readings should “look off” to the building manager.

If the problem recurs often, the astute building manager may be able to characterize the fault through a series of alarms. They can be proactive about finding and fixing the problem(s) before they occur. Alarms can be set through interaction with the graphical interface, in much the same way that a lookup on the measurement point occurs – by double-clicking on the point in question and following instructions for setting an alarm. In some cases, the problem may be driven by a faulty setting and adjustments can be made to the control parameters through the associated control points.

The scope of control is limited to specific control loops. Recall our discussion of control loops in section 2.1. The building manager can, typically with the help of the vendor, decide on the best control strategy setting. If the control strategy cannot be met, due to flaws in the control algorithm itself, the vendor may step in and re-image the controller at the outstation and expose the necessary parameters through the graphical interface. These kinds of changes are rare but do happen occasionally and can be somewhat expensive, since the cost is not typically included with the purchase of the system. Because of the cost, the decision is typically made after close inspection and analysis, which a typical BMS enables. For example, the sense/control points in question may be placed in “trend” mode.

This means that readings from those streams are stored in the local memory buffer at the outstation for some period of time. If a report is specifically set up at the central system, a report period is also associated with the point, allowing the saved points to be drained from the local buffer at the outstation. The points are then placed in a file for observation and graphing by the building manager. Time-dependent inspection of the behavior of any of the control-loop related points can be examined.

Although this feature is not necessary in order to change control parameters, it is useful for observing how parameter changes affect the behavior of the system. The building manager can, in principle, experiment with different settings and allow empirical observations to guide her future decisions.

## Energy Auditing and Building Modeling

Recently there has been renewed interest in the energy consumption of buildings. In particular, several studies [8, 17] show that buildings consume a large fraction of the energy produced in the United States and that as much as 80% of it is wasted. As such, there has been an emergence of several companies and services for assessing the health of commercial buildings with respect to their energy consumption. Organizations such as LEED [36] provide certification of buildings, specifically rating the energy efficiency of the building.

Building modeling has been part of building science for quite some time, with systems such as EnergyPlus [**EnergyPlus**]. EnergyPlus and simulators like it are part of a larger ecosystem of software for modeling various aspects of the operation of the building. They allow the designer to construct detailed models of the building, from construction to usage. You can model everything from the material, location, zone-based usage (office building, bathroom, storage room), window size and its construction, etc. There are different types of LEED certification, but typical certification requires the submission of the detailed model and the results of various energy-related metrics, aggregated over seasonal time intervals to attain LEED certification.

Detailed model construction can take several months and in order to ground the underlying model in empirical performance data typically a modeler will use the data obtained from the building's BMS. Most vendors provide a way to export the point-related trended data. Complex models can be built using this information. The file export feature in combination with the ability to “trend” points provide an interface mechanism for these and other kinds of applications that need to make use of the data.

Another option is to obtain the data directly from the system through the network. Third-party vendors provide systems that will join the building network of devices and eavesdrop on the readings and traffic being reported to the central server. This is the only way to obtain truly real-time readings from the sensors on the network. Typically BMS vendors do not like this since they may generate too much traffic and overwhelm the network because of congestion. Although not fundamental, it is a common concern in buildings today. Many buildings use RS-485 rather than ethernet and there is a general, albeit unfounded, concern

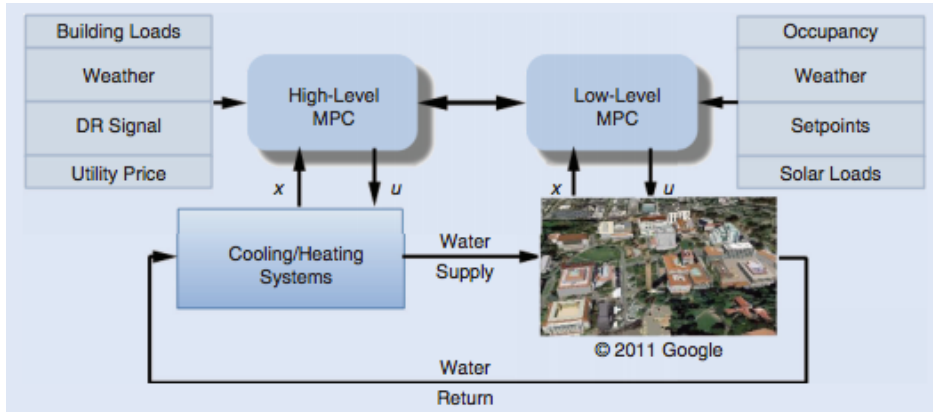


Figure 2.6: Emerging Application: Hierachical MPC for a stock of buildings.

that the network will become overwhelmed if all the points are trended and report at the same time.

Building modeling and real-time analysis have been separated because of these constraints. The constraints are largely not fundamental, but the current architecture is simply not designed to provide real-time readings for *all the points, simultaneously*. Also, it is clear, even from the fairly simple workloads generated by these analysis applications, that a history of readings is needed. BMS's, as currently designed, require the end-user to manage the history of the data point individually. When BMS's were first designed, there were certainly concerns about bandwidth and storage limits. However, today those concerns are a non-issue. A few hundred bytes produced on the order of a few minutes, even from several thousand sensors is simply not that much data.

## Holistic Building Optimization

An emerging class of applications, is in holistic control of the building using a new technique called model-predictive control [**MPC**]. Rather than rely on specific changes to control logic at the local-loop level, MPC techniques observe and learn a model of the behavior of a components, multiple components, or the whole building, based on the historical data. Once the model is learned, constraints can be specified to drive the behavior of the system to an optimal region in the tradeoff space; solving it as a constraint optimization problem. Figure 2.6, reproduced from [**MPC**], shows an example of the how MPC combines several points in the building to control the building. Essentially it decomposes a large optimization problem into individual control decisions to be made at the control-loop level.

In order to build this application, the set of necessary points must be mapped into the process. The user, setting up the problem, must connect the right data streams and control points to the algorithm by either manually going through the schematics or locating the schematic representation in the BMS graphical interface. There is no query interface and it

requires that you sit with the building manager or vendor in order to set up the trending, reporting, and enable the necessary control permissions. The process is time consuming and *does not scale*.

Although the method is very useful and has yielded excellent results, it is difficult to replicate. The code and setup must be customized for each building or stock of buildings it is set up on. This lack of generalizability and scalability is missing in the current state of the art of building information systems. In most cases the representation of sensor/actuator association is implicitly represented in a combination of the schematics, the graphical interface, and the point name. Moreover, all three of these change from building to building. It is fundamentally difficult to generalize. Buildings are treated as one-off constructions and their associated digital information has historically followed the same principle.

## Personal Energy Viewer



Figure 2.7: Emerging Application: Mobile phone interfacing with the physical infrastructure.

Imagine having the ability to walk through a building and see live, detailed energy data as you point your phone at various things and locations. As you enter the building, you scan its tag and see the live breakdown of energy consumption traces, including HVAC, lighting, and plug-loads. You continue your walk through the building as you head to your office. When you arrive to your floor you scan the tag for the floor and observe similar figures, only this time they are in relation to that floor alone. Since there are several meeting rooms on that floor, you are curious how much is consumed by occupants versus visitors. You choose to view the total load curve co-plotted with the occupant load curve, specifically for that floor. You see that approximately half the total energy is consumed by visitors during the day.

Curious about what portion of total are attributed to you, you select the personalized attribution option and you see *your* personal load curve plotted with the total load curve – as well as accompanying statistics, such as the percent of total over time. As you quickly examine the data on your phone, you see that you consumed energy during hours that you were not there. You choose to see a more detailed breakdown. You enter your office, scan

various items that you own, and see that your computer did not shut down properly and your light switch was set to manual. You immediately correct these.

Being able to interact with your environment and get a complete energy break-down can provide a useful tool for tracing and correcting rampant energy consumption. In buildings, having the occupants actively participate allows for localized, personal solutions to efficiency management and is crucial to scaling to large buildings. However, providing this detailed level of attribution is challenging. There's lots of data coming from various systems in the building, and integrating them in real time is difficult. Furthermore, attribution is non-trivial. We must be able to answer to following: How much of the total consumed on this floor went to charging laptops? How many of those charging laptops belong to registered occupants of this floor? For centralized systems, multiple locations are served simultaneously. It is non-trivial to determine the exact break-down for each location. At the plug-load level, some plug loads move from place to place throughout the building over the course of the day. Tracking where they are at any given time is difficult.

Answering these queries is relatively easy once the information is available, however, collecting the information is non-trivial, especially over time. Historically, it has been difficult to collect plug-load information. Various studies have used wireless power meters to accomplish just this [**stephscale**, **lanz**, **aceee**]. All previous work collected the data and performed post-processing to analyze it. We want to take the next natural set of steps: perform processing in real-time and present the occupants with live information.

Currently, in order to enable this application, a detailed digital model of the building is necessary, data streams from the building must be easy to query, and it should work across buildings. Also, there needs to be a way to localize the user. Localization technology and information must be made available to the mobile application to provide in-situ services. It's clear that the current information infrastructure cannot provide these. The interface to the network does not have a strict naming mechanism, there is not explicit representation of each building that the application could interpret, the sensor/actuator deployment is not dense enough and adding new sensor is cumbersome. Furthermore, the data itself can be quite dirty.

Cheap sensors are unreliable. They produce erroneous data and randomly stop and start at times. Missing/errorneous data is common. Moreoever, within building information systems provided by a single vendor, there is no time synchronization across sensors, so aggregation, filtering, and re-sampling are common operations that must be performed on the data in order to summarize and display it. The mobile energy viewer application not only require these but requires that they be performed in real time.

## 2.4 Addressing BMS Shortcomings

The current architecture of building information systems is very tightly integrated and based on monitoring and supervisory control of local control loops. Building information systems were built as tightly integrated systems with a single application. The main layer

of interaction is been the underlying network layer. However, because of the complexity of dealing directly with the network, later iterations of BMS's included an export feature which decoupled the protocol from the necessary information, namely, time-value pairs for each point in the system. As auditing applications emerged and energy became a prime target for reduction in buildings, these interface choices became overloaded. Moreover, as the need to build new kind of applications emerges, the architecture pieces that are missing become more clear. The following is a list of some of them:

1. Narrow waist should be above the network layer.
2. A time-series store is necessary.
3. Mechanisms to distill the readings must be available.
4. Real-time data forwarding should be available, especially for control applications.
5. Contextual relationships between sensor should be verified.

The first four items are commonly built and re-built in emerging applications. Therefore, we argue that they are fundamental to the future architecture of building information systems. Moreoever, we observe that dealing with network-protocol specific calls is not only cumbersome, but usually circumvented in order to deal directly with the data. Most applications that do use the underlying protocol expose a name-time-value (NTV) tuple to the layers above. This observation leads us to believe that that's where the interface should be.

The NTV layer also allows us to decouple of the data from the network protocol. This makes it easier to include new sensors that may not be directly on the building network. For example, wireless plug-load power meters [24] can simply join the NTV layer by registering the individual points, while a translation layer between the NTV layer and the main router can provide the transformation of read/write request to/from points in the network. The same is true for BACNet or any point protocols for sensors/actuators.

Each of the services that require the end user to have a deeper understanding of the underlying dynamics or performance of the building *must* capture the notion of time. Almost all anlytical process or control decision needs a set of readings over time. Therefore, there a time-series data store must be part of future BIS design. The service should be made available through the NTV. This will allow applications to fetch the necessary data for analysis either for display or complex processing.

The third point is motivated by the observation that sensor data, especially from cheap sensors, is dirty and typically goes through a cleaning process before being forwarded to the end-use application. There are various operations that are commonly performed on the data, that we think should be provided as primitives. These mainly include re-sampling, filtering, missing-data identification, and aggregation. Re-sampling refers to taking a set of streams and interpolating missing values to align their timestamps. This is typically performed before aggregation, especially for generating time-varying aggregate statistics.

Filtering simply refers to the removal of certain values based on some criteria of acceptance. Usually the criteria is defined by a threshold, both lower-bound and upper-bound value threshold for a particular stream or set of streams. Since data is often missing, due to intermittent connectivity problems or faulty sensor equipment, it becomes important to get a summary of missing time intervals in order to adjust the fetch parameters. Finally, the data is usually more useful in aggregate than as a univariate signal, for example, for generating a load curve for a set of energy-consuming items. Simple operators for combining values of various streams is key to enabling this analysis.

Finally, in order to enable control, real-time mechanisms must be exposed to the control application, while maintaining the layered integrity of the NTV layer. In addition, we have observed the need to provide real-time services for analytical applications as well. For example, LEED is now proposing the use of building data to provide a dynamic performance meter [**DynamicLeed**]. There are also many dashboard companies that make use of streaming data to provide real-time statistics on the performance of the building. The mobile application described in section 2.3 also requires a real-time forwarding and processing service to enable the application. We believe that as more applications emerge they will likely need make use of real-time sensor data.

## 2.5 Contextual Accuracy

Contextual accuracy is the notion that the context – physical location, type, etc – about the data we are analyzing, must be accurate to interpret the results for the analysis accurately. For example, an application that is providing aggregate statistics on the power consumption by plug-load items on each floor of a building, must be sure that all the data used for the analysis is power-meter data on the specified floor. If power meter A on floor 1 is moved to floor 2, the code doing the aggregation should discover the change and adjust the aggregates for floor 1 and floor 2. Another example is related to model predictive control processes that assume contextual relationships among a set of sensors to derive the state of a physical space and make control decision that affect that state. If sensors are update, moved, added, or changed, the queries made by such processes will be inaccurate and lead to incorrect control decisions. Many such processes will exists in future smart buildings, so automating the verification process as much as possible, is crucial.

All of the metadata for each point is inputted by a human being. Given the scale of the task – thousands of sensors per building – it is highly error prone. So what may seem like a trivial problem for a single instance (as described above) leads to gross miscalculations at scale, in the number for points and in time. The building and the deployment within it go through a natural evolution and this will impact processes that depend on knowing the context of the readings in order to make the right automated decision.

Figure 2.8 shows an example where this will have a more direct impact. This example shows a simplified illustration of the relationship between a chiller and a space in the building. The building of the future will optimize the space using a model-predictive control strategy

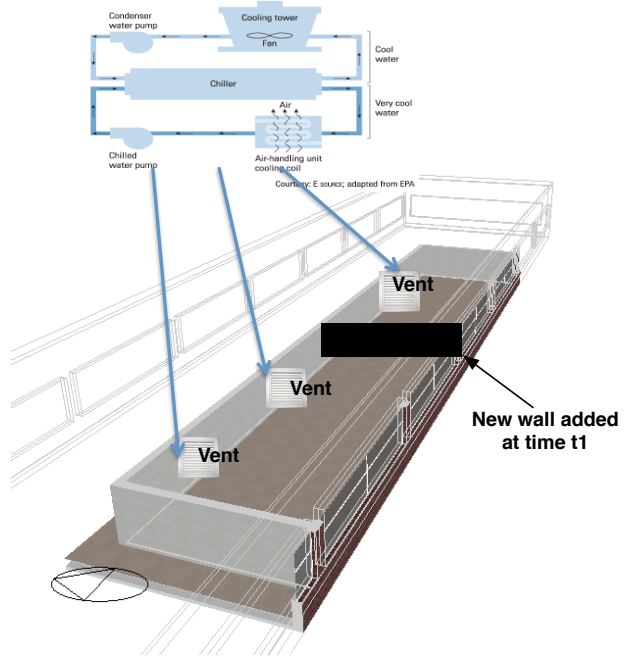


Figure 2.8: MPC example where metadata must be verified to guarantee correct behavior.

(MPC) based on equation 2.1. The equation is used to model the temperature dynamics of the room. In this equation  $C$  is the thermal capacitance (a constant),  $T$  is the temperature in the space,  $u$  is the heating/cooling power input,  $P_d$  is the internal load,  $T_{oa}$  is the outside air temperature, and  $R$  is the resistivity of the walls.

$$C\Delta T = u + P_d + \frac{(T_{oa} - T)}{R} \quad (2.1)$$

This model is used for optimization and combined with actual data coming from the associated temperature sensors in each room. The particular mapping that is important in this example is for the variable  $u$ . It is used to determine which vents are feeds which rooms. If a wall is added, there needs to be an automated way to capture this change because that changes the mapping from vents to rooms. Over time there are many changes that occur in the building. All the physical changes are recorded, but typically many *years* pass before the software is updated to reflect the changes that have occurred. For a building that is using an MPC-based controller, this is problematic. It is assuming a static model for the relationships between the points and the rooms. If a wall is added later, there is a new notion of a new room and a new controller process should be started for that room.

This is not that difficult to fix and can be done by hand but it is a typical problem in buildings and over the entire building stock, occurs very often. Buildings evolve slowly, but in aggregate there are many changes that occur that go unaccounted for. Moreover, these changes add up over time and lead to huge mis-calculations in energy consumption and

gross accounting errors in computing efficiency. As applications become more widespread, an automatic verification process is necessary to alert the building manager, or software directly, that changes have occurred. This will allow the system to remain accurate over time, leading to more energy savings and more accurate virtual models of the building.

## 2.6 Summary

We use StreamFS to organize and support applications using building data from three different buildings. The first one is a 110,000 square foot, seven-story building, the second one is an eleven-story 250,000 square-foot building, and the third is a 150,000 square-foot eleven-story building.

# Chapter 3

## StreamFS System Architecture

StreamFS is a system that we built to address some of the shortcomings in the current architecture. StreamFS uses the filesystem metaphor to represent all building information. This includes sensors, actuators, location, processing elements, streams, categorical organization, etc. It borrows several mechanisms from a Unix-style filesystem, namely, files, folders, and the pipe abstraction for processing streaming data. It also borrows the notion that all interaction is through the filesystem. This eases management of both the raw data and the processing elements that produce derivative streams for further processing.

In this section, we give an overview of the architecture – all the components, their organization, and how they interact with one another. StreamFS consists of over 20,000 lines of code and was implemented in mostly Java. It was deployed across multiple buildings and several applications were built on top of it over a 2 years period.

### 3.1 Name Management

StreamFS manages two namespaces. The first is a flat namespace that identifies a particular object instance. The second is a hierarchical namespace that identifies the current instance of a particular object. In this section, we discuss why we have two namespaces, how they are managed, and how they are used by the query interface and analytical layer.

#### Object identifier namespace

Each new object that's created is assigned a 128-bit unique identifier:

- 96 high-order bits identify the object
- 32 low-order bits identify the version of the object

In this paper we concentrate on the high-order bits used to identify the object. Management of the low-order bits is the subject of related, ongoing work.

## Hierarchical Namespace

### 3.2 Entity-relationship model

Tracking the operational energy consumption of a building requires the ability answer a series of questions about energy flow – energy data aggregated across multiple logical classes to determine how, where, and how much is being used. Sometimes, it even involves extrapolating forward in time to estimate future consumption patterns that could influence immediate decisions. The ability to *slice and dice* the data allows the analyst to gain better insight into how the energy is being used, where it can be used more effectively, and how to change the operation of the building – through better equipment or activity scheduling – in order to optimize and reduce its energy consumption. Below is a typical list of questions:

1. How much energy is consumed in this room/floor/building? On average?
2. What is the current power draw by this pump? cooling tower? heating sub-system?  
Over the last month?
3. How much power is this device currently drawing? Over the last hour?
4. How much energy have I consumed today? Versus yesterday?
5. How much energy does the computing equipment in this building consume?

Notice, these question span spatial, temporal, and other arbitrary aggregates – some physical, some categorical. There is also an implicit hierarchical aspect to the grouping, in some cases. For example, there are many rooms on a floor and many floors in a building. Naturally, to answer the first question we can aggregate the data from the room up to the whole building. This hierarchical relationship is not as evident in the HVAC sub-components specified in the second question. However, local hierarchically relationships *do exist*. For example, the cooling system consists of the set of pumps, cooling towers, and condensers in the HVAC system that push condensor fluid and water to remove heat from spaces in the building.

We can model this as a set of objects and inter-relationships which inform how to *drill-down*, *roll-up*, and *slice and dice* the data – traditional OLAP operations. The main difference between this setup and traditional OLAP is the underlying dynamics of the inter-relationships: objects, particularly those meant to represent physical entities, are added and removed and their inter-relationships change over time. *The natural evolution of buildings and activities within them makes tracking energy-flow fundamentally challenging.*

In this paper, we show how the entity-relationship model [Chen76] helps simplify this problem, both as an interface to the user and a data structure for the aggregation processes. We argue that the use of this model is a cleaner fit for this application scenario because it captures important semantic information about the real-world; facts

critical for picking which questions to ask and how to answer them. In contrast, it has been shown that a relational model loses this information [**SenkoDB**].

Lets examine the requirements for answering the first question. A building is unaware that there are rooms. Typically spaces in a building are called *zones* and, at construction time, walls are added to make rooms within zones. This makes rooms an abstract entity, used to group associated items with respect to it. It also means we typically do not have a single meter that is measuring the energy of a room; it must be calculated from the set of energy-consuming constituents.

What are the energy consuming constituents of a typical room? It is the set of energy-consumers that are active within or onto the room. Broadly, it consists of three things:

- Plug-loads
- Lights
- HVAC

For simplicity of demonstration, lets consider only plug-loads. In our construction of an entity-relationship graph lets assume there are nodes for each plug-load item and each room. For the room in question, the relationship between the plug-loads and the room is child to parent, respectively. The total energy consumed by the plug-loads can be aggregated at the parent node, the room, so the user can query the room for the total. Over time, plug-loads are removed and added to/from the room, but the relationship does not change. This simplifies the query; to obtain the total consumption over time, the query need only go to the room node. The parent-child relationship informs which constituents to aggregate over time to calculate the total.

To realize this design we need to maintain the entity-relationship graph, present it to the user in a meaningful way; allowing them to update it directly to capture physical state and relationship changes. We also need to use this graphical structure to direct data flow throughout the underlying network. This allows us to accurately maintain the running aggregates as the deployment and activities churn.

We present the graph to the user through a filesystem-like naming and linking mechanisms. The combination of a hierarhical naming scheme and support for symbolic links allows the user to access and manipualte underlying objects and relationships. Moreover, the underlying graph structure is overloaded with upstream communication mechanisms and buffering to allow data to flow from the data-producing leave nodes to the aggregation-performing parent nodes. Furthermore, the buffering lets us deal with the streaming nature of data flow from the physical world to StreamFS and lets us maintain a real-time view of energy flow in the system. Traversing the graph provides a natural way for the user to implicitly execute the OLAP operations necessary to give the user the kind of insight into energy usage in the building necessary to understand, optimize and reduce it.

### 3.3 Time-series Data Store

The data collected from sensor in timeseries in nature. A sensor produces data periodically. The important aspect of the stream are the name of the feed, the time the reading was received, and the value for that reading. There is also metadata that needs to be stored about the stream. For example, we want to know what the units of measure are, the make/model of the sensor, the date it was installed, any calibration parameters or other information that will help the user locate the sensor or interpret it correctly. We actively separate the storage of the metadata from the storage of the data.

In constructing a design for the data store, we considered 3 main questions:

1. What is the typical access pattern or what are the top queries?
2. Should we compress it?
3. How is the data stored long-term?

The typically access pattern is that of scans. Many of the applications that we consider that make use of historical data, fetch the data in a temporally meaningful manner. The query specifies the interval of time over which to fetch the data from a particular feed and either perform cleaning operations on the data, display it, or adjust the scan parameters for a subsequent query. The data is largely self-similar and highly compressable. Simple compression tests we ran on real data showed a compression factor between 15 and 30. Also, the data is essentially append-only, forever. It can grow quite large, but grows have a fairly slow rate, especially after compression. In either case, we decided a good option would be to use OpenTSDB [[opentsdb](#)]. We enabled the compression feature and indexed based on the same and timestamps of the feed.

### 3.4 Publish-Subscribe Subsystem

StreamFS uses a flexible construction of the publish/subscribe model in order to support a wide range of applications. Publish/subscribe is necessary for physical data application development in order to scale in the number of supported applications. The publish/subscribe model used in StreamFS provides mechanisms that enable a flexible combination of space and time decoupling that enable StreamFS to support a wide range of application requirements, as described by Eugster et al. [11]..

Our pub/sub engine is also tightly coupled with the namespaces exposed to users, and this design choice allows an application to control the space coupling between the publisher and the subscriber (similar to TIBCO [[tibco](#)]).

## Space decoupling

By its very design, space decoupling is achieved. Publisher do not hold a reference to the subscriber and subscribers do not hold references to publisher. However, because of the coupling of a full pathname and an object, subscriptions to topics expressed as a full pathname refer to the single publisher.

## Time decoupling

Time decoupling is achievable through the timeseries data store. Publisher push data to StreamFS whether or not subscribers are online. Moreover, data may be received at the subscriber even if the publisher becomes disconnected. Currently, subscribers do not receive all information that was missed. In order to achieve full time-decoupling, we allow the subscription target to enable or disable the option to buffer all missed readings for an associated subscription target, while the subscription target is offline.

## Synchronization decoupling

Synchronization decoupling is achieved by the publisher and subscribers through StreamFS. Events are received out of sequence from their arrival to StreamFS. This is true even when the subscription target is a processing element. The thread that buffers incoming data for each processing element is separate from the thread where the process is executed.

## 3.5 Data Cleaning and Real-time Processing

Data is coming in at different, independent rate from sensors and is produced asynchronously from internal processing elements. For certain processes, processing the incoming data as quickly as possible is key, however, this is challenging for several reasons: 1) a process may subscribe to multiple, independent streams with asynchronous report schedules and 2) interpolated values should be avoided to minimize prediction inaccuracies in interpolated values. Therefore, a process actually wants all the freshest data from all the streams they are subscribing to, while minimizing the average time that the data for each respective stream has been waiting in the buffer.

Sensor data is fundamentally challenging to deal with because much of it must be cleaned before it can be processed. For example, it is not uncommon to receive readings that is out of operational range, that is erroneous with respect to the previous observed trend, or to stop receiving readings altogether. This implies the need for processing jobs to provide a level of filtering over the raw streams. Once the data is cleaned, it is typically consumed more sophisticated processes that aggregate the information or use it for control of the space or equipment. We provide the mechanisms for handling both classes of processing jobs with our process management layer. In the next section we will discuss our process management layer and how users can both submit jobs to StreamFS for management or link their own

external processing elements so that they can be managed through StreamFS but run outside of StreamFS.

We also discuss how we deal with the fundamental challenges that come with sensor data. Specifically, we address *re-sampling* and *processing models*. The incoming data does not have a common time source, so combining the signals meaningfully involves interpolation. There are various options that we provide for performing the interpolation, chosen by the user depending on the units of the data. For example, temperature data may involve fitting a heat model with the data to attain missing values in time. In addition, aggregation is done as a function of the underlying constituents: they can be combined arbitrarily, by adding subtracting, multiplying or dividing corresponding values. We provide an interface to the user that allows them to specify how to combine the aggregate signals as a function of the child nodes in the entity-graph. Furthermore, they can filter the data by unit. This kind of flexibility useful for visualizing energy consumption over time.

## 3.6 Comparison To Related Systems

## 3.7 Summary

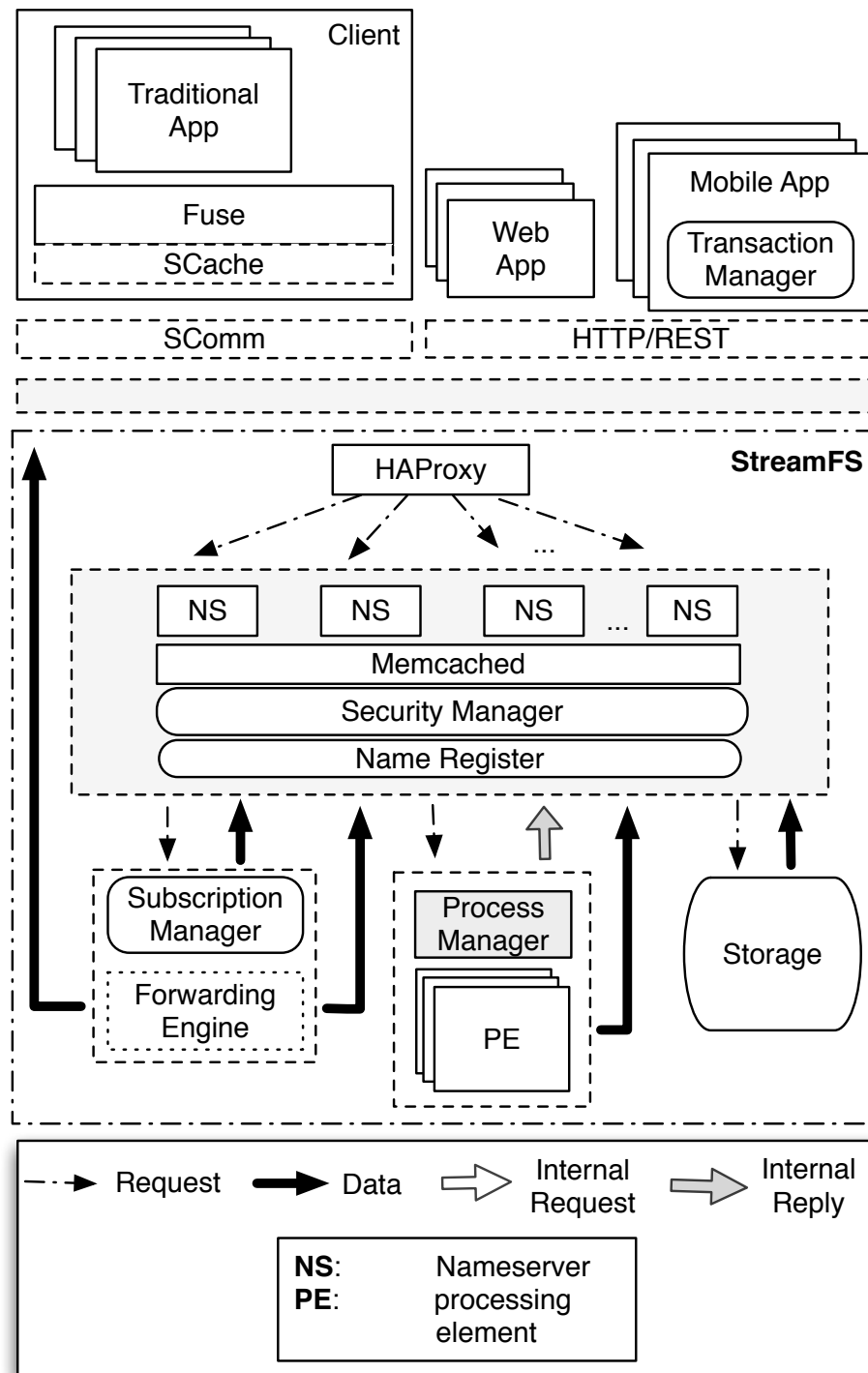


Figure 3.1: StreamFS system architecture.

# Chapter 4

## Process Management and Scheduling

Data is coming in at different, independent rate from sensors and is produced asynchronously from internal processing elements. For certain processes, processing the incoming data as quickly as possible is key, however, this is challenging for several reasons: 1) a process may subscribe to multiple, independent streams with asychronized report schedules and 2) interpolated values should be avoided to minimize prediction inaccuracies in interpolated values. Therefore, a process actually wants all the freshest data from all the streams they are subscribing to, while minimizing the average time that the data for each respective stream has been waiting in the buffer.

Sensor data is fundamentally challenging to deal with because much of it must be cleaned before it can be processed. For example, it is not uncommon to receive readings that is out of operational range, that is erroneous with respect to the previous observed trend, or to stop receiving readings altogether. This implies the need for processing jobs to provide a level of filtering over the raw streams. Once the data is cleaned, it is typically consumed more sophisticated processes that aggregate the information or use it for control of the space or equipment. We provide the mechanisms for handling both classes of processing jobs with our process management layer. In the next section we will discuss our process management layer and how users can both submit jobs to StreamFS for management or link their own external processing elements so that they can be managed through StreamFS but run outside of StreamFS.

### 4.1 Internal Processes

Internal processes are jobs submitted to StreamFS that are written in Javascript and managed within a StreamFS cluster.

StreamFS distinguishes between nodes that represent streaming data sources in the real-world and those that do not. Those that do not, however, can be tagged as aggregation points. As part of the tagging processes, a user specifies the units of aggregation, with additional options for cleaning and processing. Our contributions are:

- Use of the entity-relationship graph to provide OLAP *roll-up*, *drill-down*, and *slice and dice* operations.
- Show how sliding-window operations can be used on real-time data in combination with the entity-relationship graph to maintain accurate aggregates as the underlying objects and inter-relationships change.

## Mapping OLAP to ERG

- Introduction to OLAP.
- Explanation of ERG in StreamFS.

Online analytical processing (OLAP) is a processing layer that provides summarization of data from a set of underlying data repository (data warehouses). Traditionally, OLAP is used to process business data. Business data summarization allows an analyst ask targetted questions about aggregates and trends in their data. The data is typically multidimensional in nature and operations can be performed with respect to those dimensions and their inter-relationship.

### Measures, Dimensions, and Levels

#### Operations: drill-down and roll-up

#### Operations: slice and dice

#### Operations: pivoting

## Dynamic Aggregation

Dynamic aggregation combines the underlying entity-relationship graph with in-network aggregation. It treats each node in the graph as a potential point of aggregation on a particular data type. For example, if we need to compute aggregates of *KW* data and we declare the node for a particular room as the point of aggregation, we accept data from all children of that node that, whose units are in *KW*, and add the streams together over pre-defined window size or pre-defined timeouts.

The scheme is hierarchical, so a node only accepts data from its children and only sends data to its parent. StreamFS checks for cycles when before node insertion and prevents double-counting errors by only allowing aggregation-points that are roots of a tree that is a sub-graph of the entity-relationship graph. In our deployment, each view is a managed as an independent hierarchy. So the hierarchy of *spaces* is separate from the *inventory* hierarchy or the *taxonomy* hierarchy. This allows us to ask questions with a particular view in mind, without conflict, and is a natural fit for our aggregation scheme.

## How it works

Although there are different semantics applied to different node types at the application layer, StreamFS only knows about two types of nodes: (1) default nodes and (2) stream nodes. The main difference is that *default* nodes are not explicitly associated with data coming from a sensor and *stream* nodes are. Furthermore, default nodes can have children, while stream nodes cannot. In our application, meters are represented by default nodes and each stream of data they produce is a stream node.

When an aggregation point is chosen and enabled, dynamic aggregation places a buffer at the node for the type of data that should be aggregated. If we want to aggregate  $KW$  data, we specify the type and send an enable-aggregation request to the node through an HTTP POST to the path for that node. The flow of data starts at the leaves when a stream node received data from a sensor through HTTP POST. As data arrives it is immediately forwarded upstream to the parent(s). If a node that receives data from its children is an aggregation point it buffers the data, otherwise it forwards it to its parent.

Ignoring the timeouts for now, lets imagine the parent is a point of aggregation and its buffer is full. At this point the parent separates data into bins for each source and cleans it for aggregation through interpolation. The main operation is to *stretch* and *fill* that data with linearly interpolated values. The *stretch* operation orders all the timestamps in increasing order and for each bin (signal) interpolates the values using the first (last) pair of data points. If there is only a single data point, the stretch uses it as the missing value. The *fill* operation find the nearest timestamps that are less-than and greater-than the missing sampling time, uses their values to determine the equation of a line between them and interpolates the missing value using that equation. Once this is done for each signal, the values are added together for each unique timestamp and the aggregated signal is reported to the parent, where the operation occurs recursively to the root. Figure 4.1 shows an illustration of its operation.

## Dealing with dynamics

This approach deals with changes in the graph quite naturally. All aggregation point deal only with local data, so a node is only concerned about the children that give it data and the parent to send data to. As objects in the environment move from place to place and these changes are captured, the entity-relationship graph also changes to reflect the move. This change in aggregation constituents is naturally accounted for in the aggregate. If a child is removed, it no longer forwards data to the old parent, therefore the aggregate will reflect that change. Note, however, that changes in the entity-relationship graph are indistinguishable from energy-consuming items that have been turned off. For the purposes of aggregation, that is okay.

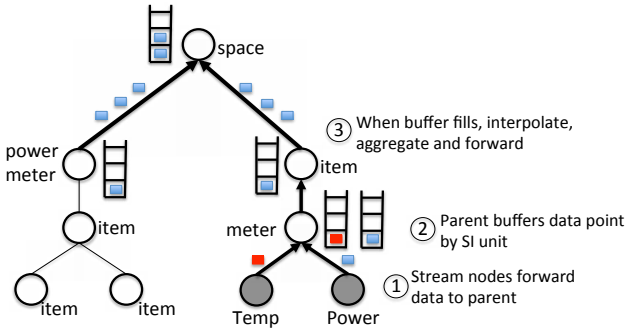


Figure 4.1: This shows an illustration of the aggregation tree used by *dynamic aggregation*. Data flows from the leaves to the root through user-specified aggregation points. When the local buffer is full the streams are separated by source, interpolated, and summed. The aggregated signal is forwarded up the tree.

## Two scenarios

We illustrate dynamic aggregation with a common usage scenario. Imagine there are a number of people in a building, each owning a number of plug-load appliances and a laptop. Assume that when a person is in a room their laptop is plugged in and when they leave the room they unplug their laptop and take it with them. People come and go throughout the day, changing the aggregate power consumption of the room and it happens. In addition, some of those people move to other rooms and plug their laptop in the new location. As this happens, we will assume all actions are being recorded in StreamFS.

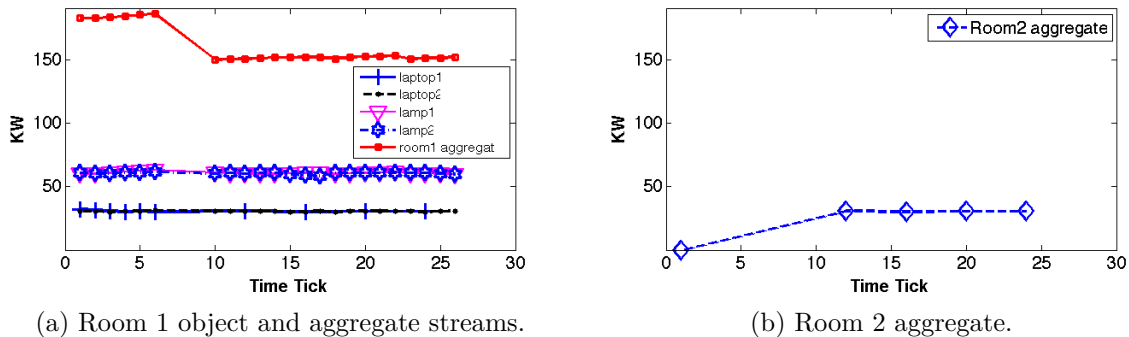


Figure 4.2: The power consumed by a laptop in *room 1* is shifted to *room 2* a time  $t=7$ . Notice the aggregate drops in room 1 while it rises in room 2.

Figure 4.2 illustrate the aggregation results of that scenario. Notice how...

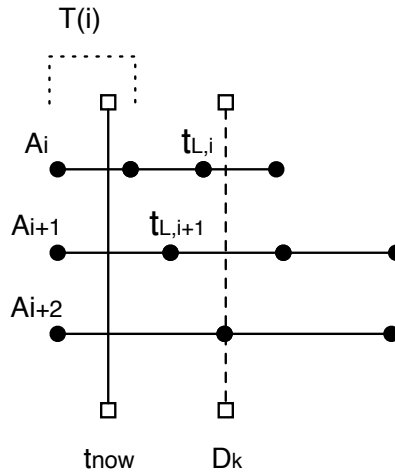


Figure 4.3: Multiple streams in a subscription and their associated parameters.

## 4.2 External Processes

### 4.3 Maximizing Data Freshness

Certain jobs only care about consuming the latest readings from their subscription streams. They are willing to discard reading until two conditions are met:

1. There is at least one data point from each stream in the subscription buffer.
2. The staleness factor is minimized within the immediate time window.

This is of particular interest to controllers that need to make control decision based on the freshest data possible and can tolerate some variability in the completion time of the control task. It is also useful in analytical jobs that want to process the latest data from multiple streams while also allowing some variability in the completion of the processing task. Note, there's a fundamental tradeoff between the staleness factor and variability of consumption. It is sometimes better to wait for the next incoming data point than it is to use what is currently in the buffer, as waiting will decrease the overall staleness factor. Other times, it is better to consume the buffered data immediately. This causes a certain amount of variability in the delivery period to the control process. However, for some applications, this is a reasonable tradeoff to make. Making use of the freshest data is desirable for minimizing errors, either in the control of a system or the calculation of some aggregate state. Generally, the error grows with staleness, therefore the goal of this mechanism is to continuously minimize the error associated with staleness through scheduling.

Let  $A_i$  be the arrival time of the last data point received from stream  $i$  and  $D_i$  be the arrival time for the next data point from stream  $i$  and their relationship as described in equation 4.1, where  $T(i)$  is the average period between the arrivals from stream  $i$ .

$$D_i = A_i + T(i) \quad (4.1)$$

Periodically, our algorithm runs and checks if there is a data point for each stream in the subscription. If so, the *min\_buffer* algorithm runs and effectively decides whether to execute the job on the current buffer immediately or whether to wait until later, when the *staleness factor* of the buffer will be at a minimum. This decision is driven by equation 4.3, whereby we find the next deadline, computed with equation 4.2, for each stream in the set and determine the staleness factor will be for the entire buffer if we wait until that deadline arrives.

$$t_{L,i} = A_i + \left\lfloor \frac{D_k - A_i}{T(i)} \right\rfloor T(i) \quad (4.2)$$

If there is no deadline  $D_k$  for some stream  $k$  such that equation 4.3 holds, then we execute now. Otherwise we choose to wait until  $D_k$  for the stream whose next deadline minimizes the staleness factor of the buffer.

$$\sum_{i=1}^{k-1} D_k - t_{L,i} < \sum_{i=1}^k t_{now} - A_i \quad (4.3)$$

The algorithm is sketched our below.

Given a full buffer  $b[n]$ :

```

for all elements in the  $b$  do
    (1) Calculate the staleness of element  $i$  and add to total stalness,  $S_n$ ;
        for all other elements in the buffer do
            (1) Determine the next report time  $D_i$  for this element;
            (2) Determine the staleness of all the elements if we wait until  $D_i$ ;
            (3) If it is the smallest staleness figure calculate, replace minimum cost,  $S_l$ .
        end
    end
if  $S_l$  is less than  $S_n$  then
    (1) Wait until later to consume;
    else
        | (1) Consume now
    end
end
```

**Algorithm 1:** Staleness algorithm.

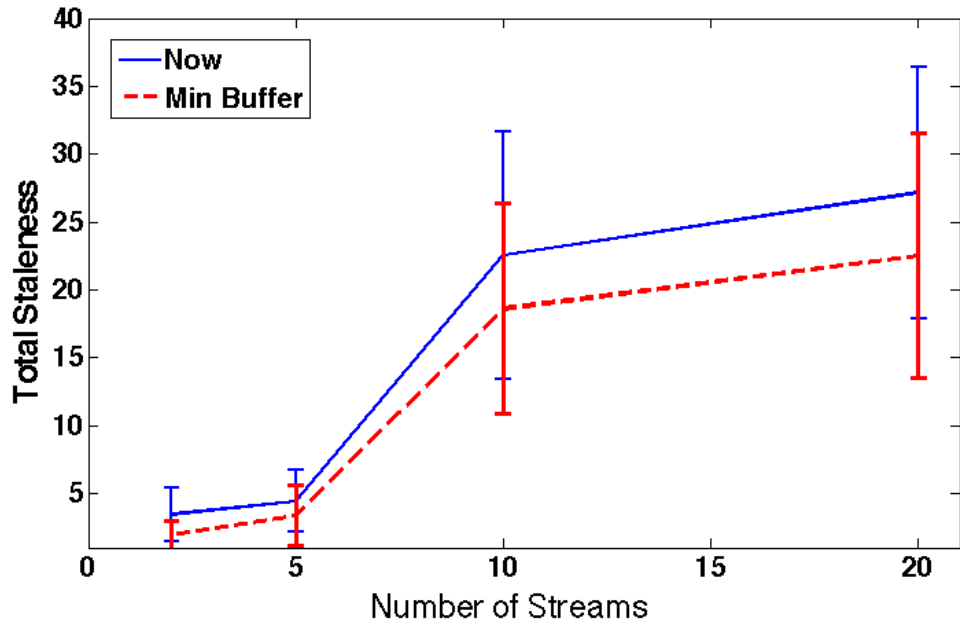


Figure 4.4:

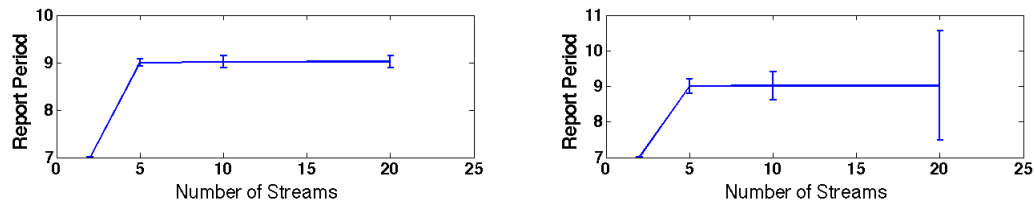


Figure 4.5:

## 4.4 Experimental Results

## 4.5 Summary

# Chapter 5

## Filesystem Metaphore, Naming, and Verifiability

From our experience with building applications, there are a clear set of requirements that are necessary. Most applications construct the notion of context using the naming convention ascribed to a sensor stream. The name conflates the notion of system, space, and type information. At the very least, these three should be supported, however, often other categorical needs must be met to perform various kinds of aggregate statistical, analytics, and control. In addition, we need to support the management of processing jobs that process stream data and provide integrated management facilities for them.

Building applications are essentially monitoring and control applications built on the streams generated by sensors embedded through the building or distillates of them. As the number of applications and streams increased, it becomes desireable to manage them in a centralized fashion. Moreover, the centralized approach allows all applications to make use of a uniform naming convention and can allow applications to be interoperable. Systems that wish to support such applications require the following properties:

1. Logically accessible physical resources.
2. Representation of data producing and data consuming elements.
3. Representation of inter-relationships between elements.
4. Provide uniform naming and access.

This chapter describes the use of the filesystem abstraction for representing streams in space. The filesystem naming convention provide a unified namespace to application, for accessing physical resources and streams. Moreover, we support multi-naming through symbolic links – an important requirement for building applications.

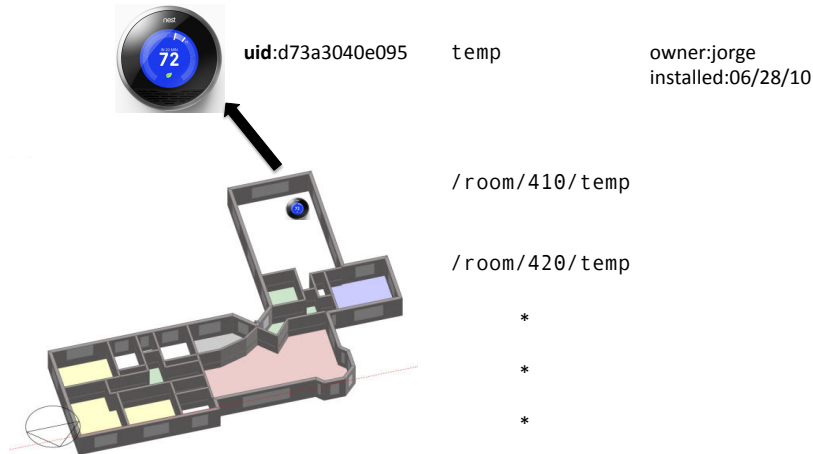


Figure 5.1: Everything is a file. Temperature sensor represented as a file in a folder that contains folders for each room. Note, the file that represents a temperature sensor producing a stream is given a unique identifier. The user may also decorate the file with extra metadata for searching purposes.

## 5.1 File Abstraction

Our naming scheme is hierarchically structured, like traditional filesystem naming, with support for symbolic links, allowing arbitrary links between sub-trees. We argue that this naming scheme is crucial, as it exposes the inter-relationships which inform aggregation semantics intended by the user. We introduce a naming scheme for physical objects and their inter-relationship.

Similar requirements to those aforementioned have been addressed in the design and implementation of filesystems. Filesystems provide logical access to physical resources through files, with different files and associated semantics, exposed to applications through a shell or programmatically. Filesystems represent collections of bits, encapsulated by a file, and grouped with folders. Symbolic links support the notion of multi-naming. A single file or folder could have multiple names that lead to the same underlying object. Filesystems even support the notion of streaming data through character and block device files. Moreover, pipe files allow programs to communicate with each other through a piece of shared memory, where the source application writes to the pipe and the sink application consumes from the pipe.

We assert that these constructs should be directly adopted for supporting applications in the buildings. Our approach adopts the unix file philosophy where everything is represented as a file. Each object created in StreamFS is assigned two names, by default, one which uniquely identifies the object and *not* human-readable and the second which is changeable and human-readable. Consider the example shown in Figure [fig:everythingfile].

In this example, the user is creating a temperature stream file in every room of the

building. The name of the file, given by the user, is *temp*. Upon creation, the file is uniquely identified by the system using a unique identifier, as shown. Like in a unix filesystem, the file is created within a folder. Ideally, the name of the folder would encode the placement of the sensor. In the figure, the user is create a temperature stream file in room 410 and room 420. Note the full filepath for the stream file is /room/410/temp. During creation, the user may also decorate the file with extra metadata, also shown in the figure. In this example, they have annotated the file with information about the owner and when the sensor was installed. This metadata is used for quickly locating the file or grouping files that contain similar tags, quickly.

## File types and operations

As we map the filesystem abstraction into this problem space, we need to consider the various kinds of files our system will contain, their semantics, and how our system will expose and manage them. There are essentially 4 types of files and 6 sub-types. We summarize these in Table 5.1. There are also different kinds of operations that the each file type supports. Operational semantics are file dependent. For example, when you *read* a folder, you obtain the metadata associated with the folder and the name of its children. When you *read* a stream, you its metadata and the last timestamp-value it produced. *Writing* to a stream is a bit different. You can write to a stream to update its metadata tags and the stream source can write a value to it. The stream source is identified with a *publish identifier* (pubid). The stream source includes the pubid in the write operation for the specified stream file. Without the pubid, the source cannot write to the file. Any other writer should not be allowed to write to a stream file either.

type	description	valid operations
default/folder	Container file. Used to group other kinds of files within it.	read, write, delete
stream	Represents a data stream.	read, write, delete, subscribe, query
controller	Represents a controller.	read, write, subscribe
special	There are several kinds of special files for management of jobs and pipes.	read, delete

Table 5.1: Summary of the 4 main file types and their valid operations in StreamFS.

Similar to a traditional filesystem, StreamFS includes *special files*. There are 6 special files and 5 of them are for management purposes. The only one that is not is the *symbolic link* file, which is essentially used to support multi-naming and inherits the operational semantics of the file it points to. The delete operation on a symlink, however, only deletes

the symlink. A description of these files and the operations they support is given in Table 5.3. A detailed description and examples will be presented in later sections.

<b>operation</b>	<b>file type</b>	<b>semantics</b>
read	folder, stream, ipd, ipi, epd, epi, sub	read the metadata and tags for the associated file.
write	stream	Write to stream file, only the appropriate stream source is permitted.
delete	folder, stream, ipd, ipi, epd, epi, sub	Folder must be empty. The others can be directly deleted.
query	stream, all	streams support time-range queries. All support metadata-tag queries.
subscribe	stream	Forwards data from a stream to the specified destination.

Table 5.2: File operations, the file types that support them, and their general semantics.

## Default, Stream, and Controller Files

### Special Files

<b>type</b>	<b>description</b>	<b>valid operations</b>
internal process definition (ipd)	Javascript process definition.	read, write, delete
internal process instance (ipi)	Management file used for managing active processing of this script.	read, delete
external process definition (epd)	Gives information about where an external process lives.	read, write, delete
external process instance (epi)	An active processing stream to an external process.	read, write, delete
subscription instance (sub)	An instance of a subscription. Contains information about the subscription, such as source/sink and related statistics	read, delete
symbolic link (symlink)	Similar to a symbolic link in Unix.	

Table 5.3: Summary of the 6 special-file sub-types and their valid operations in StreamFS.

## 5.2 Supporting Multiple Names

## 5.3 Verification through Sensor Data

### Empirical Mode Decomposition

Empirical Mode Decomposition (EMD) [22] is a technique that decomposes a signal and reveals intrinsic patterns, trends, and noise. This technique has been widely applied to a variety of datasets, including climate variables [[lee:climateEMD2011](#)], medical data [[blanco:bioMed2008](#)], speech signals [[huang:signalProc2006](#), [hasan:ieeeletter2009](#)], and image processing [[nunes:vision2005](#)]. EMD's effectiveness relies on its empirical, adaptive and intuitive approach. In fact, this technique is designed to efficiently decompose both non-stationary and non-linear signals without requiring any a priori basis functions or tuning.

EMD decomposes a signal into a set of oscillatory components called intrinsic mode functions (IMFs). An IMF satisfies two conditions: (1) it contains the same number of extrema and zero crossings (or differ at most by one); (2) the two IMF envelopes defined by its local maxima and local minima are symmetric with respect to zero. Consequently, IMFs are functions that directly convey the amplitude and frequency modulations.

EMD is an iterative algorithm that extracts IMFs step by step by using the so-called sifting process [22]; each step seeks for the IMF with the highest frequency by sifting, then the computed IMF is removed from the data and the residual data are used as input for the next step. The process stops when the residual data becomes a monotonic function from which no more IMF can be extracted.

We formally describe the EMD algorithm as follows:

1. Sifting process: For a current signal  $h_0 = X$ , let  $m_0$  be the mean of its upper and lower envelopes as determined from a cubic-spline interpolation of local maxima and minima.
2. The estimated local mean  $m_0$  is removed from the signal, giving a first component:  $h_1 = h_0 - m_0$
3. The sifting process is iterated,  $h_1$  taking the place of  $h_0$ . Using its upper and lower envelopes, a new local mean  $m_1$  is computed and  $h_2 = h_1 - m_1$ .
4. The procedure is repeated  $k$  times until  $h_k = h_{k-1} - m_{k-1}$  is an IMF according to the two conditions above.
5. This first IMF is designated as  $c_1 = h_k$ , and contains the component with shortest periods. We extract it from the signal to produce a residual:  $r_1 = X - c_1$ . Steps 1 to 4 are repeated on the residual signal  $r_1$ , providing IMFs  $c_j$  and residuals  $r_j = r_{j-1} - c_j$ , for  $j$  from 1 to  $n$ .
6. The process stops when residual  $r_n$  contains no more than 3 extrema.

The result of EMD is a set of IMFs  $c_i$  and the final residue  $r_n$ , such as:

$$X = \sum_{i=1}^n c_i + r_n$$

where the size of the resulting set of IMFs ( $n$ ) depends on the original signal  $X$  and  $r_n$  represents the trend of the data (see *IMFs* in Figure 7.3).

For this work we implemented a variant of EMD called Complete Ensemble EMD [torres:icassp2012]. This algorithm computes EMD several times with additional noise, it allows us to efficiently analyze signals that have flat sections (i.e. consuming no electricity in our case).

## IMF aggregation

By applying EMD to energy consumption signals we obtain a set of IMFs that precisely describe the devices consumption patterns at different frequency bands. Therefore, we can focus our analysis on the smaller time scales, ignoring the dominant patterns that prevent us from effectively analyzing raw signals.

However, comparing the IMFs obtained from different signals is also not trivial, because EMD is empirically uncovering IMFs from the data there is no guarantee that the two IMFs  $c_i^1$  and  $c_i^2$  obtained from two distinct signals  $S^1$  and  $S^2$  represent data at the same frequency domain. Directly comparing  $c_i^1$  and  $c_i^2$  is meaningless unless we confirm that they belong to the same frequency domain.

There are numerous techniques to retrieve IMF frequencies [huang:aada2009]. In this work we take advantage of the Generalized Zero Crossing (GZC) [huang:patent2006] because it is a simple and robust estimator of the instantaneous IMF frequency [huang:aada2009]. GZC is a direct estimation of IMF instantaneous frequency using critical points defined as the zero crossings and local extrema (round dots in Figure 5.2). Formally, given a data point  $p$ , GZC measures the quarter ( $T_4$ ), the two halves ( $T_2^x$ ), and the four full periods ( $T_1^y$ ),  $p$  belongs to (see Figure 5.2) and the instantaneous period is computed as:

$$T = \frac{1}{7}\{4T_4 + (2T_2^1 + 2T_2^2) + (T_1^1 + T_1^2 + T_1^3 + T_1^4)\}$$

Since all points  $p$  between two critical points have the same instantaneous period GZC is local down to a quarter period. Hereafter, we refer to the time scale of an IMF as the average of the instantaneous periods along the whole IMF. Because the time scale of each IMF depends on the original signal, we propose the following to efficiently compare IMFs from different signals. We cluster IMFs with respect to their time scales and partially reconstruct each signal by aggregating its IMFs from the same cluster. Then, we directly compare the partial signals of different devices.

EMD yields distinct components in different time scales and we compute the instantaneous frequencies [21] of IMFs using Generalized Zero-Crossing [20]. We break the time scales into four frequency bands:

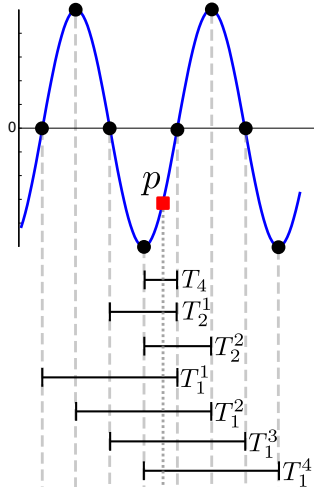


Figure 5.2: Generalized Zero Crossing: the local mean period at the point  $p$  is computed from one quarter period  $T_4$ , two half periods  $T_2^x$  and four full periods  $T_1^y$  (where  $x = 1, 2$ , and,  $y = 1, 2, 3, 4$ ).

- High Frequency: a time scale smaller than 30 minutes, mainly reflecting the operation characteristics of devices and noise in system.
- Medium Frequency: a time scale between 30 minutes and 6 hours, which is within the time span of daily activities inside a building.
- Low Frequency: a time scale between 6 hours and 7 days.
- Residue: everything has a time scale longer than 7 days and shows long-term patterns, such as seasonal changes.

## 5.4 Types of Verification

### Functional Verification With Strip, Bind, and Search

A typical large building contains thousands of sensors, monitoring the HVAC system, lighting, and other operational sub-systems. With the increased push for operational efficiency, operators are relying more on historical data processing to uncover opportunities for energy-savings. However, they are overwhelmed with the deluge of data and seek more efficient ways to identify potential problems. In this paper, we present a new approach called the Strip, Bind and Search (SBS); a method for uncovering abnormal equipment behavior and in-concert usage patterns. SBS uncovers relationships between devices and constructs a model for their usage pattern relative to other devices. It then flags deviations from the

model. We run SBS on a set of building sensor traces; each containing hundred sensors reporting data flows over 18 weeks from two separate buildings with fundamentally different infrastructures. We demonstrate that, in many cases, SBS uncovers misbehavior corresponding to inefficient device usage that leads to energy waste. The average waste uncovered is as high as 2500 kWh per device.

The intuition behind the proposed approach is that each service provided by the building requires a minimum subset of devices. The devices within a subset are used at the same time when the corresponding service is needed and a savings opportunity is characterized by the partial activation of the devices. For example, office comfort is attained through sufficient lighting, ventilation, and air conditioning. These are controlled by the lighting and HVAC (Heating, Ventilation, and Air Conditioning) system. Thus, when the room is occupied both the air conditioner (heater on a cold day) and lights are used together and should be turned off when the room is empty. In principal, if a person leaves the room and turns off *only* the lights then the air conditioner (or heater) is a source of electricity waste.

Following this basic idea we propose *Strip, Bind and Search* (SBS), an unsupervised methodology that systematically detects electricity waste. Our proposal consists of two key components:

**Strip and Bind** The first part of the proposed method mines the raw sensor data, identifying inter-device usage patterns. We first *strip* the underlying traces of occupancy-induced trends. Then we *bind* devices whose underlying behavior is highly correlated. This allows us to differentiate between devices that are used together (high correlation), used independently (no correlation), and used mutually exclusively (negative correlation).

**Search** The second part of the method monitors devices relationships over time and reports deviations from the norm. It learns the normal inter-device usage using a robust, longitudinal analysis of the building data and detect anomalous usages. Such abnormalities usually present an opportunity to reduce electricity waste or events that deserve careful attention (e.g. faulty device).

SBS overcomes several challenges. First, noisy sensor traces that all share a similar trend, making direct correlation analysis non-trivial. Device energy consumption is mainly driven by occupancy and weather, all the devices display a similar daily pattern, in roughly overlapping time intervals and phases. Therefore, one of the main contributions of this work is uncovering the intrinsic device relationships by filtering out the dominant trend. For this task we use Empirical Mode Decomposition [22], a known method for de-trending time-varying signals.

Another key contribution of this work is in using SBS to practically monitor building energy consumption. Moreover, the proposed method is easy to use and functions in any building, as it does not require prior knowledge of the building nor extra sensors. It is also tuned through a single intuitive parameter.

We validate the effectiveness of our approach using 10 weeks of data from a modern Japanese building containing 135 sensors and 8 weeks of data from an older American building containing 70 sensors. These experiments highlight the effectiveness of SBS to uncover device relationships in a large deployment of 135 sensors. Furthermore, we inspect the SBS results and show that the reported alarms correspond to significant opportunities to save energy. The major anomaly reported in the American building lasts 18 days and accounts for a waste of 2500 kWh. SBS also reports numerous small anomalies, hidden deep within the building’s overall consumption data. Such errors are very difficult to find without SBS.

In the rest of this paper, we detail the mechanisms of SBS (Section ??) before evaluating it with real data (Section 7.2) then we discuss different outcomes of the proposed methodology (Section ??) and conclude.

## Spatial Verification

We investigate the utility of empirical mode decomposition (EMD) to identify intrinsically correlated usage patterns among sensors in a large deployment. We use data collected from almost 700 sensors in a 12-story building measuring power, pressure, temperature, and other physical phenomena. We discover that doing a correlation analysis on the raw traces does not discriminate well enough to identify meaningful relationships between sensors. We correlate the trace from a pump with the rest of the sensor traces and find that simple correlation filters only 50% of the sensors as being correlated with the behavior of the pump. In contrast, by running the correlation analysis on the constituent frequencies extracted by the EMD process, we filter out over 99% of the sensors as being correlated – with the highest correlation coming from sensors that serve the same room as the pump. We believe our approach can be used to construct inter-device correlation models that can help understand and identify misbehaving or inefficient usage patterns.

We present results for correlating usage patterns across a large number of sensors in a single deployment. We analyze data from a 12-story office building at the University of Tokyo. The deployment consists of almost 700 sensors monitoring a broad range of devices inside and outside the building. Our initial observations and results include the following:

1. Raw-trace correlation analysis is too strongly influenced by the common low-frequency trends in the data to identify meaningful relationships.
2. Using a technique called empirical model decomposition (EMD) [22] removes this trend and helps identify truly correlated sensor traces.
3. We can construct clusters of correlated sensors that are spatio-temporally correlated, *without a priori knowledge of their placement*.

Typically, placement information is embedded in the name or associated metadata for each sensor in the building. These are used to group sensors by location. For example, in our building data, all sensors that contain the string ‘410’ in their name are in room

410. Processes typically group streams in this fashion: using regular-expression matching or field-matching queries on the characters in the sensor name or metadata. If these are not updated to reflect changes then such group-by query results will not accurately represent true spatial relationships. Fontugne et al. [12] observe that spatial associations can be derived empirically. We start with this approach in our work and explore, more deeply, the extent to which it can be used as a verification tool for corroborating the groups constructed from character-matching queries. We refer to this process as *spatial verification*.

Prior work [12] makes use of a technique called Empirical Mode Decomposition (EMD) [19] to statistically cluster correlated usage patterns. Sensors close to each other show strong statistical correlations while sensors further apart show weaker correlations. The main parameter in their approach, the correlation threshold, is explored to demonstrate how it relates to characteristic spatial patterns in the sensor feeds. However, they do not characterize the threshold as it relates to physical configuration. Fontugne et al. [13] expand the work by applying EMD to uncover functional device patterns. They develop an unsupervised learning method to model normal usage patterns and apply an anomaly detection algorithm to alert when patterns have deviated from the norm. The methodology used in their work divides raw signals into four separate frequency bands and shows the medium band to carry the most spatial information.

In this section, we explore the threshold parameter in [12] more deeply, in order to move towards automatic spatial clustering, to be used as a form of verification. We use EMD and the intrinsic mode function (IMF) re-aggregation methodology described in [13], with some modifications, to statistically analyze the threshold parameter and its relationship to spatial separation in a building. We explore the hypothesis that *a statistical boundary, analogous to a physical one, exists and is empirically discoverable*. We conduct an empirical analysis on the data collected from 15 sensors in 5 rooms over a one-month period. Our study makes the following contributions:

- We corroborate the results in [12], verifying the spatial correlation pattern in a very different building.
- We characterize the correlation coefficient (corrcoeff) distribution of sensors in the same room and different rooms and validate our existence hypothesis for this preliminary sample.
- We demonstrate that the statistical boundary between sensors in various rooms converges to a similar value and this value generalizes across rooms in this study.
- We show the tradeoff between the true and false positive rate inherent to threshold selection. We also show that our method improves the classification accuracy from 80% to 93.3%.

Our results are promising yet preliminary. We are able to find a statistical separation across a small number of rooms, quite well. Our study, however, does not explore the extent

to which the physical separation affects the results. Certainly for rooms that are far apart we observe a statistical distinction using our methodology. However, we also find that in some cases, our approach does not work as well. We discuss the approach and results in the rest of the paper, followed by a short discussion and future work.

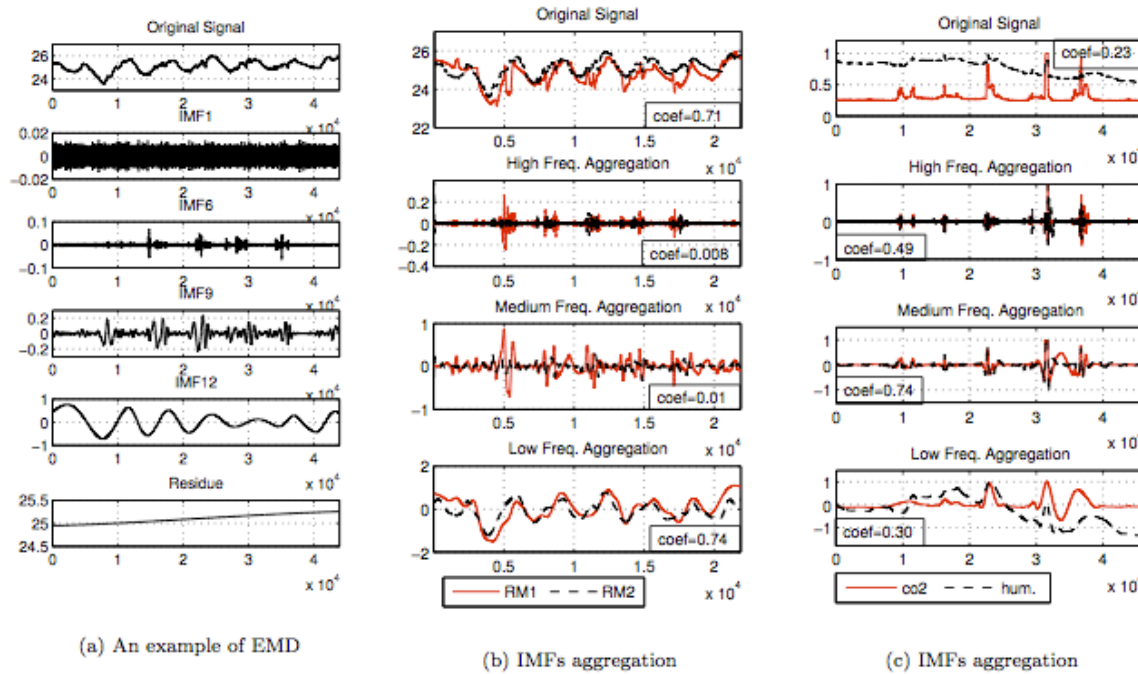


Figure 5.3: (a) EMD decomposes a signal and exposes intrinsic oscillatory components; (b) Aggregation of IMFs within a pre-defined frequency range makes seemingly similar signals from different locations more distinguishable; (c) IMF aggregation makes seemingly distinct signals of different sensors in the same room show high correlation.

We start our analysis by extending the methodology used in SBS [13], based on empirical mode decomposition (EMD). In our analysis, we collect traces from several sensors and run EMD on them. This produces a set of constituent sub-signals called “intrinsic mode functions” (IMF), which we separate by frequency range and re-aggregate into distinct bands. Then, we inspect the relationship between the sensors by computing the corrcoeff within a particular band, which gives us the spatial information we are interested in. Finally, we separate the result set into sub-sets, and closely examine their statistical characteristics. Before describing our methodology in detail, we introduce some definitions and notation.

## Correlation

We make extensive use of the correlation coefficient function defined as:

$$r(X, Y) = r_{X,Y} = \frac{\sum_{i=1}^n (X_i - \bar{X})(Y_i - \bar{Y})}{\sqrt{\sum_{i=1}^n (X_i - \bar{X})^2} \sqrt{\sum_{i=1}^n (Y_i - \bar{Y})^2}}$$

where  $X, Y$  are separate sets of values,  $n$  is the total number of sample points in each set, and  $\bar{X}$  is the mean value of  $X$  (same for  $\bar{Y}$  and  $Y$ ). For each pair of sensors, we compute the corrcoeff to ascertain the relationship between them.

## Type Verification

## Value Verification

## 5.5 Experimental Building Deployments and Datasets

### Engineering Building 2 - Todai

Engineering building 2, at the University of Tokyo (Todai), is a 12-story building completed in 2005 and is now hosting classrooms, laboratories, offices and server rooms. The electricity consumption of the lighting and HVAC systems of 231 rooms is monitored by 135 sensors. Rather than a centralized HVAC system, small, local HVAC systems are set up throughout the building. The HVAC systems are classified into two categories, EHP (Electrical Heat Pump) and GHP (Gas Heat Pump). The GHPs are the only devices that serve numerous rooms and multiple floors. The 5 GHPs in the dataset serve 154 rooms. The EHP and lighting systems serve only pairs of rooms and which are directly controlled by the occupants. In addition, the sensor metadata provides device-type and location information (room number), therefore, the electricity consumption of each pair of rooms is separately monitored.

### Cory Hall - UC Berkeley

Cory Hall, at UC Berkeley, is a 5-story building hosting mainly classrooms, meeting rooms, laboratories and a datacenter. This building was completed in 1950, thus its infrastructure is significantly different from the Japanese one. The HVAC system in the building is centralized and serves several floors per unit. There is a separate unit for an internal fabricated laboratory, inside the building.

### Sutardja Dai Hall - UC Berkeley

Sutardja Dai Hall is a large buildings at Berkeley.

## 5.6 Related Work

HomeOs ??

The research community has addressed the detection of abnormal energy-consumption in buildings in numerous ways [**katipamula:1review2005**, **katipamula:2review2005**].

The rule-based techniques rely on a priori knowledge, they assert the sustainability of a system by identifying a set of undesired behaviors. Using a hierarchical set of rules, Schein et al. propose a method to diagnose HVAC systems [**schein:hvacr2006**]. In comparison, state machine models take advantage of historical training data and domain knowledge to learn the states and transitions of a system. The transitions are based on measured stimuli identified through a domain expertise. State machines can model the operation of HVAC systems [**patnaik:toist2011**] and permit to predict or detect the abnormal behavior of HVAC's components [**bellala:buildsys2012**]. However, the deployment of these methods require expert knowledge and are mostly applied to HVAC systems.

In [**seem:energybldg2007**], the authors propose a simple unsupervised approach to monitor the average and peak daily consumption of a building and uncover outlier, nevertheless, the misbehaving devices are left unidentified.

Using regression analysis and weather variables the devices energy-consumption is predicted and abnormal usage is highlighted. The authors of [**brown:buildperf2012**] use kernel regression to forecast device consumption and devices that behave differently from the predictions are reported as anomalous. Regression models are also used with performances indices to monitor the HVAC's components and identify inefficiencies [**zhou:wiley2009**]. The implementation of these approaches in real situations is difficult, since it requires a training dataset and non-trivial parameter tuning.

Similar to our approach, previous studies identify abnormal energy-consumption using frequency analysis and unsupervised anomaly detection methods. The device's consumption is decomposed using Fourier transform and outlier values are detected using clustering techniques [**wrinch:pes2012**, **chen:aaaiw2011**, 4]. However, these methods assume a constant periodicity in the data and this causes many false positives in alarm reporting. We do not make any assumption about the device usage schedule. We only observe and model device relationships. We take advantage of a recent frequency analysis technique that enables us uncover the inter-device relationships [**romain:iotapp12**]. The identified anomalies correspond to devices that deviate from their normal relationship to other devices.

Reducing a building's energy consumption has also received a lot of attention from the research community. The most promising techniques are based on occupancy model predictions as they ensure that empty rooms are not over conditioned needlessly. Room occupancy is usually monitored through sensor networks [**agarwal:ipsn2011**, **erickson:ipsn2011**] or the computer network traffic [26]. These approaches are highly effective for buildings that have rarely-occupied rooms (e.g. conference room) and studies show that such approaches can achieve up to 42% annual energy saving. SBS is fundamentally different from these approaches. SBS identifies the abnormal usage of any devices rather than optimizing the normal usage of specific devices. Nevertheless, the two approaches are complementary and

energy-efficient buildings should take advantage of the synergy between them.

Recently, there has been increased interest in minimizing building energy consumption. Our approach differs quite substantially from related work. Agarwal et al. [1] present a parameter-fitting approach for a Gaussian model to fit the parameters of an occupancy model to match the occupancy data with a small data set. The model is then used to drive HVAC settings to reduce energy consumption. We ignore occupancy entirely in our approach. It appears as a hidden factor in the correlation patterns we observe.

Kim et al. [26] use branch-level energy monitoring and IP traffic from user’s PCs to determine the causal relationships between occupancy and energy use. Their approach is most similar to ours. Understanding how IP traffic, as a proxy for occupancy, correlates with energy use can help determine where inefficiencies may lie.

In each of these studies and others [14, 30], occupancy is used as a trigger that drives efficient resource-usage policies. Efficiency when unoccupied means shutting everything off and efficiency when a space is occupied means anything can be turned on. There is no question that this is an excellent way to identify savings opportunities, however, we take a fundamentally different approach. We are agnostic to the underlying cause or driver for efficient policies to be implemented. More generally, we look to understand *how the equipment is used in concert*. This may help uncover unexpected underlying relationships and can be used in an anomaly detection application to establish “(in)efficient”, “(ab)normal” usage patterns. The latter should identify savings opportunities in cases where the space is unoccupied as well as occupied, because it has to do with the underlying behavior of the machines and how they generally work together. Our approach could help achieve both generality and scale for such an application. This article focuses on the first step of this application, the identification of correlated devices.

## 5.7 Summary

# Chapter 6

## Architectural Evaluation

### 6.1 API Overview

### 6.2 Deployment Viewer Application

### 6.3 Mounted Filesystem and Matlab Integration

### 6.4 Visualization and Analysis of Streaming Data

### 6.5 Energy Auditing With Mobile Phones

Mobile phone penetration continues to rise and is predicted to reach 50 billion by 2020 [mobile2020]. As such, it is a ubiquitous, powerful tool to serve as an interface between occupants and the built environment. Mobile phones are constantly connected, are personal devices that can serve as a proxy for the individual, and provide large viewing screen for display of critical information to its owner. By combining the data streams available in the building with mobile phone, we could provide a way to do in-situ diagnosis of operational problem in the building, monitor personal energy consumption, and share information about the building with our neighbors in the building.

There are several systems challenges that must be overcome in order to achieve this vision. We examine those dealing capturing and maintaining a view of the physical world. We must record which things belong to whom, where people and things are over time, how to deal with the mobile phone as the main interactive modality, and how to do this at the scale of hundreds to thousands of users and meters. We argue that *without addressing these systems issues, this vision cannot be achieved*. In our work, we start by deploying a network of wireless power meters and use the mobile phone to re-create a model of people, things, and locations in the building. We also use it to assist in tracking of people and things over time.

We use mobile phones to construct an entity-relationship graph of the physical world and combine it with streaming sensor data in order to perform detailed energy-attribution. We limit the scope of the world to a single building domain. We have designed and implemented a real-time, mobile energy auditing application, called the ‘Energy Lens’, that allows us to collect information about things throughout the building and how they are related to each other. For example, computer X is inside room Y and connected to meter Z. Then, we use these relationships to guide our data look-up and analytical calculations. For example, the load curve of room Y consists of the sum of all the power traces for loads inside room Y. We use the mobile smartphone as the main input tool. Our work examines *three main challenges* in setting up and deploying a real, whole-building infrastructure to support real-time, fined grained energy analytics.

The first challenge is related to tracking and mobility. The use of mobile phones presents classical, fundamental challenges related to mobility. Typically, mobility refers to the phone, as the person carrying it moves from place to place. However, in the energy-attribution context, we are also referring to the movement of energy-consuming objects. Tracking their relationships to spaces and people is as important as tracking people. We describe how we deal with *both moving people and moving objects* and show that these historically difficult problems can be addressed relatively easily, if the proper infrastructure is in place.

The second challenge is about capturing the inter-relationship semantics and having these inform our analytics. We adopt the general notion of physical tags that identify objects in the world. Our system uses *QR codes* to tag things and locations in the physical world. However, *any tag that provides a unique identifier for an object could serve the same purpose*. Once tagged, there are three types of interactions – registration, linking, and scanning – which establish important relationships. Registration is the act of creating a virtual object to represent a physical one. Linking captures the relationship between pairs of objects. Scanning is the act of performing an item-lookup. Each of these interactions requires a set of swiping gestures. Linking requires two tag swipes while the other two actions require a single tag swipe. Internally, we maintain a *entity-relationship graph (ERG)* of things, people, and locations, that gets updated through these sets of gestures.

The third challenge is about indoor network connectivity and access. In order to connect these components, we rely on having ‘ubiquitous’ network connectivity. However, in practice, network *availability* is intermittent and our system must deal with the challenges of intermittency. We discuss how caching and logging are used to address these challenges. Moreover, when connectivity is re-established, we must deal with applying updates to the ERG, as captured by the phone while disconnected.

Conflicts can also occur during an update. For example, the two updates may disagree about which items are attached to which meters. We implement a very simple conflict resolution scheme, described in section 6.6. Finally, certain physical-state transitions are represented as a set of updates to the ERG that must be applied atomically. We implement transactions in the log-replay and transaction manager. Our ‘Energy Lens’ system is deployed in a building on our campus. We discuss its architecture and our design choices.

We also discuss novel strategies for tracking moving people/things and describe how we

implement these in our system. In summary, our work makes the following contributions:

- We design and implement a system that captures and combines physical entities, their inter-relationships, and real-time sensor data in buildings.
- We observe that certain combinations of swipes give us useful information to set the location of people and things over time. We codify this observation in our *context-tracker* and use it to maintain consistency between the entity-relationship graph and the state of the physical world. To the best of our knowledge, this is radically different from the approaches in standard localization techniques. However, we argue that it can be used to *enhance* their accuracy and overall performance.
- We implement a prefetching algorithm to obtain context-dependent information to both improve performance and enable disconnected operation. We also design and implement a log-replay and transaction manager over our data management layer. We describe how different conflict-resolution policies can be implemented and our rationale for the policies we chose.

In the next sections we go through a motivating scenario. We then discuss some related work, followed by the system architecture, evaluation, and future directions.

## 6.6 EnergyLens Architecture and System Challenges

The Energy Lens application aims to approximate the vision described in section 2.3. For our initial attempt, we tagged items in a building with QR codes and allowed users to 1) tag and register new items, 2) tell us which meters are attached to which items, and 3) scan individual items to view their load curve over a 24-hour period.

The architecture consists of three layers: the sensing and tag layer, the data management and processing layer, and the application layer. In this section we discuss how aspects of each layer address the aforementioned challenges. In deploying the application in a real building, we ran into various issues that informed our design.

For example, *QR code reading times vary substantially across phones and lighting conditions*. You must design for the least-common denominator in terms of camera quality and lighting.

Another aspect to consider is network access. Within our building, although connectivity is mostly ubiquitous, network access can be intermittent. Network access may be unavailable for several reasons, including disassociation from an access point due to idleness, dead spots in the building where connectivity to both wifi and 3G/4G are unavailable, multipath-induced destructive interference, and various other reasons. Dealing with these throughout the data collection and update phase is especially troublesome. We discuss various mechanisms and algorithms for dealing with disconnected operation.

## Challenge 1: Tracking People and Things

The Energy Lens app consists of a web application that displays timeseries data and an Android-based smartphone app. The android app is relatively simple; consisting of a menu with only two options: Update deployment state, scan to view services. Swipe gestures manipualte a local portion of the entity-relationship graph – local with respect to a user’s current location. Since each location (room, floor) has a QR code atextttached to it and items are associated with those locations, we can identify the location by name (/buildings/SDH/spaces/4F/toaster). Figure 6.1 goes through the various sets of swipes.

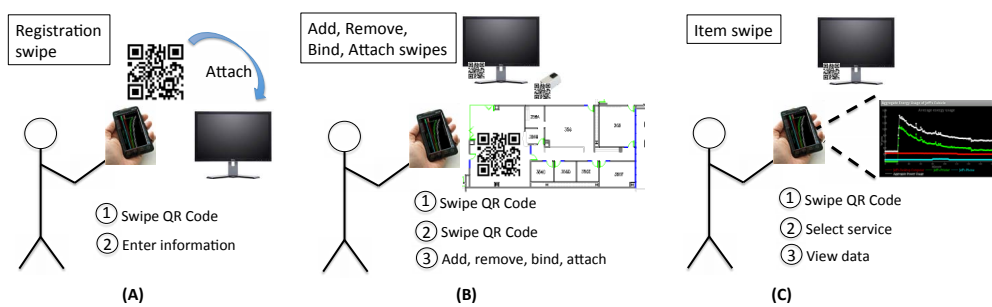


Figure 6.1: Swiping gestures in the mobile application. The registration swipe requires on a single swipe. The linking and registration gestures require two swipes, and the look-up requires a single swipe.

The first set is called a ‘registration’ swipe and we use it to register new items. The user scans a QR code and the item it is atextttached to. This creates an ‘atextttached-to’ link between them. Adding, removing, binding, and atextttaching items is done with a pair of swipes. A lookup is done with swiping the QR code atextttached to an item.

We have designed a set of heuristics for setting the location during an update, that piggybacks on the swipe gesture. The following is a list of rules for automatically setextttting the location of people and things:

- When a user swipes at a location  $L$ , they are presumed to be at  $L$  for fixed period  $\tau$ . An “association timer” is set to release this association after  $\tau$  seconds.
- If the user swipes anything that is associated with a location  $l$  at time  $t \leq \tau$ , and  $l(t) \neq L$ , then we set the new location of the *thing* they swiped to  $l(t)$  and reset the association timer.
- If the user swipes anything at location  $l$  at time  $t \geq \tau$ , we set the location of the *person* to  $l(t)$ . We reset the association timer to  $\tau$ .
- If a user registers a new location, they are presumed to be at that location.

For each of these, we provide an interactive option to ask for location-change confirmation from the user. So if we think the user/item has moved but they have not, the preset action can be overridden. The guiding principal we follow in our design is to leverage the swipe gesture for as much contextual information as possible. Furthermore, we do not explicitly track users. Context is only set on the phone and used in operations sent to the server. We then construct an entity relationship graph through naming in StreamFS. StreamFS uses filesystem constructs, such as hierarchical naming and symbolic links, which we use to express an acyclic relationship-graph structure.

which you are either editing directly or adding creating/destroying a relationship link in the graph.

Because location swipes give us direct confirmation of a user's location, it can be coupled with wifi localization mechanisms and supervised learning algorithms to adjust the localization model as the user interacts with their environment. For future work we intend to experiment with this mechanism.

## QR code design

Our choice to use QR codes is important, since the *only way to scale – in deployment size and management complexity – is to involve building occupants*. QR codes are cheap to produce. They can be printed and attached to items with tape or sticky paper. Figure 6.3 shows an example QR code used in our deployment. These are placed on physical objects and spaces throughout the building to link between the physical world and our virtual representation of it.

With the number of physical objects and places in a building, *we must rely on the occupants to scale our deployment and manage it over*. Because QR codes are easy to produce, we provide occupants with a webpage that produces them. They print them out, place them on items or places they want to interact with and register them.

Since occupants are our target users, we must make the application easy to use. For QR code usage, varied lighting conditions, phone-specific camera quality, and shaky hand movements can make scanning cumbersome; ultimately de-motivating continued use. QR codes must be designed to minimize scanning time. In our initial deployment and experiments we observe that complex QR code not only have a longer average scanning time but also experience a larger variance in scanning time. The more complex the pixel design in the QR code, the harder it is for the camera to focus and capture it.

We scanned each QR code shown in Figure ??, under light and dark lighting conditions. Each experiment was run 10 times and Table 6.6 shows a statistical summary. Scanning the simple QR code under well-lit conditions performed the best. The complex QR code under the same condition takes about 28-36% longer to scan. Perhaps even more important is the variance. Notice that the variance with the simple QR code is smaller. QR code image complexity increases with the amount of information you encode on it. Therefore, it was important to decrease the amount of information we encoded, *placing the complexity in the lookup rather than the tag*.



Figure 6.2: 6.2 resolves to the same URL as the 6.3, after resolution and redirection is complete. The short label resolves to `htexttp://tinyurl.com/6235eyw`. 6.3 encodes about half the characters as the 6.2. We used tinyUrl to reduce the QR code image complexity and scan time.



Figure 6.3: 6.2 resolves to the same URL as the 6.3, after resolution and redirection is complete. The short label resolves to `htexttp://tinyurl.com/6235eyw`. 6.3 encodes about half the characters as the 6.2. We used tinyUrl to reduce the QR code image complexity and scan time.

	Average (sec)	Variance (sec)
Short, light	1.66	0.33
Short, dark	2.08	0.35
Long, light	2.26	0.71
Long, dark	2.82	0.50

Table 6.1: Shows the time to scan a long QR code versus a short QR code in light and dark conditions (loosely defined). Notice that short QR codes scan faster and with less variance than long ones.

Table 6.6 shows the results of some simple scanning experiment between the two tags shown above. We scanned each QR code under light and dark lighting conditions, off the screen of my laptop. Each experiment was run 10 times and the table shows the statistical overview of the results. Clearly, scanning the simple QR code under well-lit conditions performed the best. The complex QR code under the same condition takes about 28-36% longer to scan. On a generic QR code scanner, as used here, there is a portion of the scan time

that is independent of the code complexity. As these are more heavily used, this is expected to be reduced substantially and the difference in acquisition complexity will be even more pronounced. Perhaps even more important is the variance. Notice that the variance with the simple QR code is much smaller and more stable under either condition. In our experience, large variance in scan time is a major problem for complex QR codes. Thus we decided to re-design our codes and push more information in the lookup processes, as network access was more reliable than the focus of the camera on various mobile devices. Tags are placed on all types of devices in all kinds of locations with varying degrees of lighting. Simple QR codes are vital for widespread use.

The design choice forced us to examine others that were related. Not being able to encode much information on our QR codes means we are more reliant on the network to provide the bulk of the information, to be very reliable, and to be widespread enough that disconnection is not problematic. Moreover, there are a number of clients that can be used to access and display the information and the tag has to be meaningful for both. In order to meet these criteria we (1) shrunk URL's using tinyURL [[tinyurl](#)] as a level of indirection and (2) designed two classes of applications: *shallow* applications, and *deep-inspection* applications. Shallow applications interact with the web-application directly while deep-inspection application use the URL of the web application to extract a unique identifier and provide deeper inspection and update capabilities of the entity-relationship graph.

This is an example URL we used in our deployment: `htexttpp://tinyurl.com/6235eyw`. When resolved, we get an empty response in the body, but we use the header to identify the QR code identifier that we associate with the item. The response header is down in Figure 6.4.

```
HTTP/1.1 301 Moved Permanently
X-Powered-By: PHP/5.3.8
Set-Cookie: tinyUUID=ee81f56c2c15850975b7d175;
expires=Thu, 13-Dec-2012 04:00:18 GMT; path=/; domain=.tinyurl.com
Location: http://streamfs.cs.berkeley.edu/mobile/
mobile.php?crc=4eb460a39fcfd7
X-tiny: db 0.015100002288818
Content-type: text/html
Content-Length: 0
Connection: close
Date: Wed, 14 Dec 2011 04:00:18 GMT
Server: TinyURL/1.6
```

Figure 6.4: The header of the response from the tinyUrl when resolving a QR code. The ‘Location’ attribute is used to extract the unique identifier for the object this QR code tags. It is also used to re-direct users without the phone application to a meaningful web address for the object.

Notice the ‘Location’ attribute in the header. This is the location of the re-direct. This approach gives us flexibility in several ways:

1. It allows us to encode less information in the QR code, decreasing its visual complexity; making it more robust across phones with different camera quality, poor lighting conditions, and shaky hands.

2. It allows the added layer of indirection to serve two versions of the applications: the native application, where users can *deeply explore* and edit the entities and their relationships and the *shallow lookup*, which re-directs the mobile phone to a read-only view of the item that was scanned – such as a power trace or a description.

It provides a web address for users to re-direct to and find information and various read-only services for the object. However, because the URL also contains a unique identifier *qrc*, it can be used to provide for sophisticated services and capabilities. An example is the ability to change the virtual structure of inter-relationship between this object and other objects. This is demonstrated in our energy auditing application discussed in detail in section ???. Once items are tagged, they can be added and removed by swiping the tag and pressing the butexttton for what you want to do with the item. You also check into locations either explicit with a location-tag swipe or implicitly with an item swipe.

*Shallow* applications use the URL directly. The *qrc* URL is unqiue identifier for the item that this tag is atextttached to. A shallow application can obtain mostly read-only service through our web applications. For example, we'll see how to get either item-specific data or item-aggregated data with respect to the user making the request (i.e. the total energy consumed by *my* devices). *Deep-inspection* applications are native to the phone, so we can do much more with the tag. Our energy auditing application allows you to related the item to other items by maintaining state of swipe history. This is more difficult with the web-applicaiton. We can also use the tag and item information to couple it with sensor information coming from sensors on the phone itself. For example, we could determine the direction an object is pointing by using the phone's directional sensor and negating their direction (i.e. phone is facing east, tag on item must be facing west).

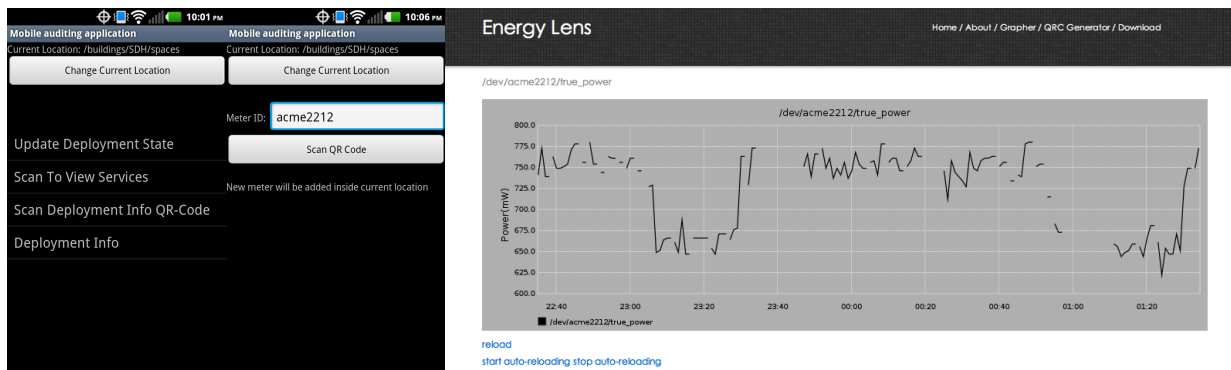


Figure 6.5: Screen shots of the mobile application. The screens on the left are for editing the state of the deployment. The graph on the right shows a live feed of a the sensor that's atextttached to the item that was scanned with the ‘Scan To View Services’ option in the mobile application. It can also be resolved by scanning the QR code and following the re-direct to the URL.

ACme meters are IP-enabled and forward their data through a router that runs sMAP. sMAP then forwards the incoming data to StreamFS, running in a machine in Amazon's EC2. StreamFS is a web service that organizes streaming data and metadata using a hierarchical naming convention. It also provides a pub/sub facility for streaming data. We construct a canonical naming convention within StreamFS to express the entity relationships between people, things, and meters. The pub/sub mechanism allows us to combine the ERG with streaming data, and feeds our timeseries data viewers.

### Entity-Relationship graph

We construct the entity relationship graph through naming in StreamFS. StreamFS uses filesystem constructs, such as symbolic links and hierarchical naming which are useful for expressing an acyclic graph structure (StreamFS checks for cycles when symlinks are created). The following general path-naming text patterns are used to express different portions of the ERG. `/path/to/device_or_item`, `/path/to/qrc`, `/path/to/space`, `/path/to/taxonomy`, `/path/to/users`. Registered meters are placed in the device path, `/dev`. Items are stored in `/inventory`. QR codes are stored in `/qrc`. When an item is registered a symbolic link is created from the specific qr code directory to the item. `/spaces` contains a hierarchy of floors, rooms, and sub-spaces. `/users` contains the list of usernames. We also have a `/tax` directory, where we construct an device hierarchy for access by plug-load category. Placement (location) is also captured with symbolic links.

## Challenge 2: Consistency Management

We use an eventual-consistency model for maintaining the ERG over time. Naturally, the spatial inter-relationships change over time as items are moved and replaced. In order to deal with this we offer two options: 1) we periodically re-scan the items and their locations, essentially re-capturing the inventory collection portion of the audit or 2) we allow building occupants to participate as auditors, capturing their own personal items and shared items. This should provide at least as much value as a periodic energy audit and can be completed in a fraction of the time [**aceee·mobileaudit**].

Placement (location) is captured with symbolic links as well. Node types inform the application of the nature of the relationship. We define five distinct types: item, meter, location, category, and tag. The following relationships are constructed with symlinks between different node types:

- **Owned-by:** When a meter/item/location is tagged as belonging to a user.
- **Bound-to:** When a meter is attached to an item and taking physical measurements associated with that device, we say that the meter is “bound-to” the device.
- **Attached-to:** When a meter/qr code/item is attached to another meter/qr code/item but *not* taking any physical measurements for that item, we say that the

meter/item is “attached-to” the other meter/qr code/item. QR codes cannot not be attached to each other.

- **Is-in:** When a meter/item is inside a location, we say that the meter/item “is-in” that location.
- **Type-of:** When an item is labeled by as a known, specific, type, we say that the item is a “type-of” thing specified by its label.

All symlinks are interpreted based on these rules of association. As items move, symlinks are removed and re-created in a different folder. We know your current location by following the path from the QR code directory, across a symlink, to a file in the space directory. Items associated with a space have a floor or room folder point to the item via a symlink. This is how we record the location of things throughout the building.

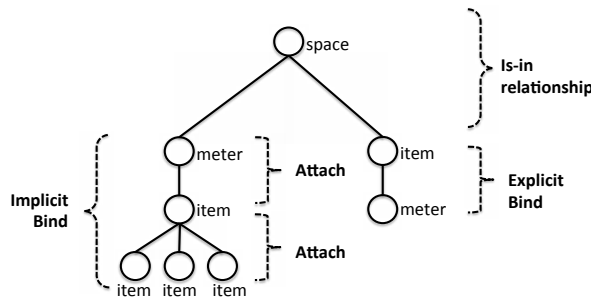


Figure 6.6: This diagram shows the relationship capture between the objects and locations in the building for the energy audit application. Children of a space node have an “is-in” relationship with the space. An item with another item as a child have a “is-attached” relationship and meters attached to items are bound to each other. Note, this is a *subset* of the relationship diagrams generated across our three applications.

## Application layer

### Challenge 3: Disconnected Operation

Although connectivity is ubiquitous, network access is not. This occurs due to dead zones, idle-disconnect and failed hand-off between access points. When encountered in practice, especially while editing deployment state, it can be quite frustrating and discourage use of the application. We designed a mechanism that does smart caching, not only to improve performance, but also to allow for disconnected operation.

The Energy Lens application downloads a portion of the ERG when a user enters a new floor. The application fetches the portion of the graph rooted at the floor. Figure 6.7

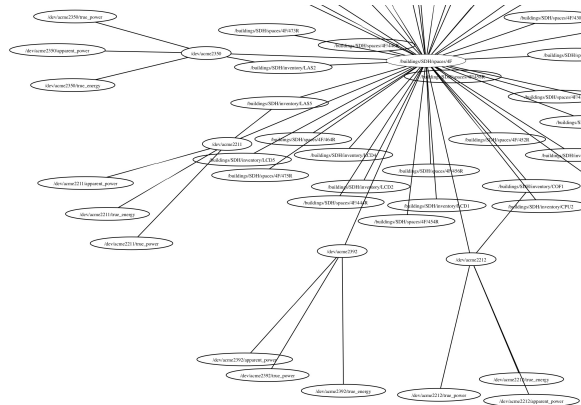


Figure 6.7: A portion of the prefetched entities on a single floor in our building. This shows a snapshot of the entity-relationship graph for that floor. Each node, link, and associated content is prefetched when the user swipes the floor tag or anything on that floor.

shows just a small portion of that entity-relationship graph for the floor we are monitoring in our deployment. A prefetch populates the cache with all entity nodes on that floor, their associated metadata, and 30 minutes of data from the stream entities. The full fetch of the 4th floor data set includes 176 nodes and about 1 MB of meter data. In total, the app downloads 1.2 MB of data upon re-connection. Prefetching allows users to continue interacting with the application as if they were still connected (as long as they remain on the same floor). Without it, the application is not functional until a network connection is established.

The Energy Lens periodically syncs with StreamFS to obtain updates to the ERG and maintain a locally consistent view. Let  $OP_R$  be an operation performed on the node rooted at node  $R$  and  $t_i$  be the current time on the phone. After a set period, the phone sends the server its last performed operation and the time that operation was performed. The server responds with any operations that have taken place since then. The client applies those operations internally to the cached version of the ERG in order to maintain consistency. The “active” parameter-check, is for energy savings. If the phone application is active, the check occurs every 10 minutes, otherwise it occurs every hour.

The process is demonstrated in Figure 6.8. The components shown are the *ERG cache*, the *operation log (OpLog)*, and the *prefetcher*. We separate the steps in the figure as a READ sequence and a WRITE sequence. All reads go to the cache (steps 1 and 2 on the left hand side of the figure). Writes go through the OpLog (steps 1 - 5 on the right side of the figure). For writes, the application makes a write request (1) and it is forwarded to StreamFS (2). If StreamFS is reachable and the write is successful (3), the operation is applied to the ERG cache (4) and the response is sent to the application (5). If the operation is not successful, step 4 is skipped. If StreamFS could not be reached, step 3 is skipped, and the operation is written to the OpLog. The OpLog is flushed to the server, by the prefetcher, upon

```

while 1 do
    if connected and active then
        (1)  $req \leftarrow [t_{i-n}, OP_R]$ ;
        (2)  $resp \leftarrow \text{send}(req) = [t_{i-k}, OP_R], \dots, [t_{now}, OP_R]$ ;
        (3)  $n >= k$ ;
        for  $j = 1 \rightarrow \text{size}(resp)$  do
            | (1)  $op \leftarrow resp[j] = [t_{i-k+e}, OP_R]$ ;
            | (2) apply( $op$ );
        end
    end
    if active then
        (1) Sleep for 10 minutes;
        else
            | (1) Sleep for 1 hour
        end
        ;
    end
end

```

**Algorithm 2:** Prefetch Loop.

re-connection.

The OpLog contains records of operations that are eventually applied to StreamFS. Some of those operations are actually groups of operations that need to be applied atomically. For example, when a bind or atextttach operation occurs, we append the timestamp to the item(s) that are being connected, as well as create a link between them in the graph. The application uses both the link and the added metadata to fetch the appropriate graph for display. These operations must be applied atomically or not be applied at all. When the log is dumped, the global transaction manager (GTXM) – the layer that handles log dumps and transaction processing – atextttempts to apply the log in timestamp order.

### Log dumps and conflict resolution

When the Energy Lens application is started it contacts the server and atextttains the server's local clock time. It notes its local time as being equal to the timestamp of the server and calculates all subsequent timestamps using its local clock. When an operation or transaction is added to the OpLog, a timestamp is appended. Let  $t_s$  be the timestamp on the server,  $t_l$  be the timestamp on the phone when  $t_s$  is recorded, and  $t_{now}$  be the current time on the phone. Each operation/transaction is timestamped with  $t_{approx}$  where:

$$t_{approx} = t_s + (t_{now} - t_l) \quad (6.1)$$

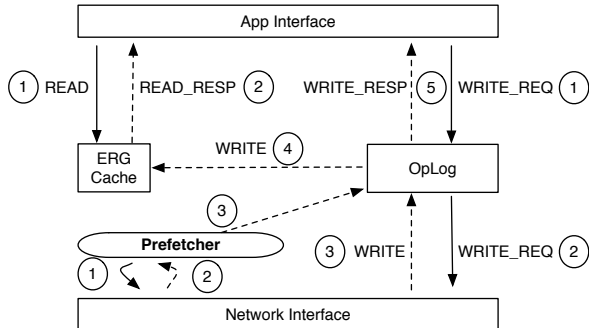


Figure 6.8: Standard mechanisms for consistency management on the phone. All READ request go to the local cached version of the ERG. All WRITES must go through the OpLog. They are eventually applied to the cache if successful and logged if the StreamFS is unreachable.

This timestamp is a general approximation of when the operation should be applied on the server. The server applies these in ascending timestamp order.

Generally, a conflict occurs if there is any operation or transaction that was applied after the timestamp of the current operation being processed. A typical transaction manager must rollback the state of the database, apply the operation, and replay the log. However, conflict resolution is much simpler in this context. *The latest operations reflect the state of the world because they are updates induced by direct interaction with the world at that point in time.* Therefore, if there is a conflict between a set of operations, the old ones can all be discarded.

Operations that are discarded are done so silently. We make failures silent for two reasons: 1) There is no way to contact the app when failure occurs. Mobile phones do not often have reversably reachable addresses. 2) Failure assumes the operation was based on a false assumption about the state of the world.

## Real-time analytics

Figure 6.9 shows three screen shots of power traces obtained from the ACme deployment, and displayed through the Energy Lens. Notice that there is some data missing in the graph. This occurs because of in the network transmission, reboots on the data management layer, or failed scripts that are automatically restarted. In all cases we get holes in the data. To compute aggregates, interpolation is necessary. StreamFS offers a real-time processing facility, whereby javascript operators can be applied to streaming data. This allows us to clean it as it comes in and compute the aggregate traces. We are currently experimenting with various aggregation models to give occupants deeper insights.

## Deployment Experience

We deployed 20 ACme power meters [**acme**] on a single floor of a building on campus. The data was made available through sMAP [7] and forwarded to our processing and data management layer, StreamFS [**streamfs**]. We distributed the ACmes throughout a single floor in our building and registered various plug loads as being measured by them. We also tagged hundreds of items and locations throughout the entire building. In total we tagged 20 meters, 20 metered items, 351 un-metered items, and 139 rooms over 7 floors. Figure 6.9 shows three screen shots of power traces obtained from the ACme deployment, and displayed through the Energy Lens.

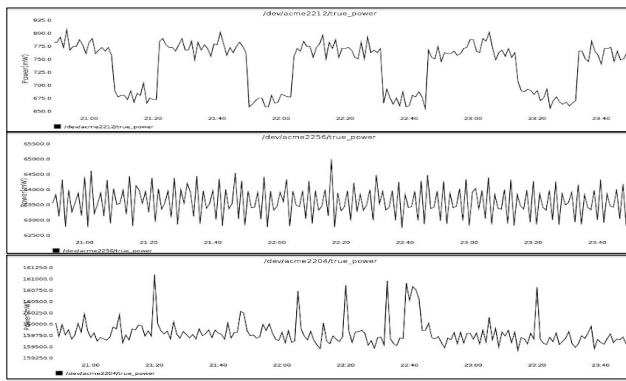


Figure 6.9: Power traces obtained from power meters attached to various plug load on one of the floors of a building on campus. These show screen shots of the Energy Lens timeseries data display.

In our initial deployment we found that the use of our tracking scheme to be effective, especially in conjunction with interactive confirmation. The ERG was effective at capturing deployment state, although highly mobile items, such as laptops, were particularly difficult to keep track of. Finally, our disconnected operation mechanism was effective at masking intermittent connectivity. For future work we will baseline the floor’s energy consumption before and after the deployment and measure if more visibility and analytics indeed motivates occupants to use less.

## 6.7 EnergyLens Evaluation

In this section we measure prefetch download times and discuss strategies for providing scalability. We also look at the transaction manager and discuss conflict resolution.

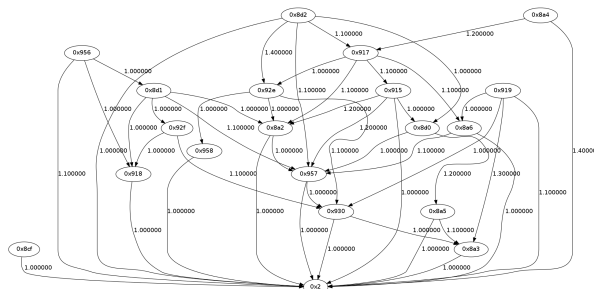


Figure 6.10:

## Sensing and tag layer

We deployed 20 ACme power meters [**acme**] on a single floor of a building on campus. The data was made available through sMAP [7] and forwarded to our processing and data management layer, StreamFS [**streamfs**]. We distributed the ACmes throughout a single floor in our building and registered various plug loads as being measured by them. We also tagged hundreds of items and locations throughout the entire building. In total we tagged 20 meters, 20 metered items, 351 un-metered items, and 139 rooms over 7 floors.

## Prefetching

Prefetching occurs when a user enters a new floor, as detected by a floor scan or an item scan. Table 6.2 shows that the prefetch times scale linearly with the number of items (and data) to prefetch. Each node holds approximate 100 bytes of information and for a 20-node deployment of power meters, producing 100 bytes of data per stream (three streams per ACme) every 20 seconds, we fetch approximately 1 MB of data.

These prefetch times are non-trivial to deal with, especially since they cause the phone application to slow down until the data is received and loaded into the local cache. The overhead is dominated by the query in StreamFS that constructs the entire sub graph to send to the application. For future work, we will implement a callback facility and pass the application a reference to it. The app can then periodically check back until the query completes and the data is ready to be downloaded. We can also include partial responses to the query in the prefetch-loop response. This also allows users to continue using the application without any frustrating waits.

## Log dump measurements

## Log replay latency

Table 6.3 shows the operations that the transaction manager calls on the StreamFS server. Log replay and transaction processing is entirely dependent on the time to execute

No. nodes	Fetch time (sec)	Std. Error (sec)
1	0.8902	0.0756
10	5.7342	1.7087
100	52.3145	14.1146

Table 6.2: Shows the time to fetch nodes based on the size of the fetch. The fetch time increased linearly with the number of nodes. Caching maintain fetch time near that of fetching a single node. A callback is used when cache is invalidated.

these operations on StreamFS. There are five types of transactions, a *move*, a *un/bind*, *un/attach*. A move is a combination of a ‘delete’ and a ‘create link’, a bind is a ‘create link’ and an ‘update tags’, an unbind and unattach is a ‘delete’ and ‘update tag’. The transaction latency is the sum of these operations. By far the most expensive operation is a ‘create node’ operation. This occurs when a user adds a new item/space/person to the graph. The time to apply the operation also scales linearly with the size of the logs.

All logs dumps are processed sequentially. However, for future work we look to parallelize processing into parallel processes updating different portions of the graph. For example, log updates rooted at different floors could occur simultaneously.

The global transaction manager implements three main high-level operations – rollback, apply, and replay. Our current implementation is limited by the time it takes to perform an operation on StreamFS. Table 6.3 shows the three main operation that the transaction manager needs to do on the server.

Usually rollbacks consist of *delete* operation and applies consist of *creates*. In a worst-cases analysis of performance we expect the total conflict resolution time to be roughly bounded by  $rollback\_time + apply\_time + replay\_time$ , since  $replay\_time = 3X rollback\_time$  and *apply\_time* is negligible, the total time is approximately  $4X rollback\_time$ . Therefore the overhead is driven by how many new links were created that have to be deleted and then re-created. As an optimization, we limit the scope of a rollback. The naive approach is to blindly undo all operations up to a certain time. However, we can use the location of the node in the ERG to limit the conflict-scope to a sub graph, rather than the entire graph. The simplest approach is to check if the operation on a node either shares an immediate parent with the node that will have an operation undone on it or it the operation is on the same node. By limiting conflict-scope we minimize the number of operation that get execute and, hence, minimize the cost of resolution.

related.tex

## 6.8 Related Work

Our work touches on several areas from smart home research to logistics. In the building space, there has been some interest in building various kinds of energy-related visualization

Operation	Avg. exec. time (ms)
fetch	250
delete	326
update tags	267
create link	250
create node	1036

Table 6.3: Average operation execution time in StreamFS.

and control applications. This work focuses on the object definition, tracking, and management component of the architecture proposed by Hsu et al. [**hbcI**]. Their work stratified the set of challenges that one could potentially face if the application were deployed at scale. Our work, in contrast, bases its design rationale on a *real deployment* that is taking place at scale in a building on our campus. We focus on solving fundamental systems challenges in dealing with intermittent connectivity and conflict resolution in tracking people and things over time. We also focus on leveraging gestures to minimize the cost of interaction for users, while maximizing the information we can attain about the state of the world. smart home research [**cooltown**] to

Our work touches on several areas from logistics [**rfid·gonz2006**] to context-aware mobile applications [**ACE**]. In the building space, there has been some interest in building various kinds of energy-related visualization and control applications. HBCI [**hbcI**] proposes a high level archiecture that also relies on QR codes, mobile phones, and ubiquitous network access. HBCI introduces the notion of object capture through the mobile phone and individual services provides by the object, accessible via an object lookup. The proposed service model is *object-centric*, such as individual power traces or direct control accessss. Their “query” service is a tag lookup mechanism realized through QR code scanning of items. The ‘Energy Lens’ also embodies the “query” via a tag lookup, however we focus on context-related services rather than object-centric services. We build and maintain an entity-relationship graph (ERG) to capture the inter-relationships between items. The ERG informs our analytical processing. We use an eventual-consistency model to maintain the inter-relationship graph over time. HBCI does not address the challenges faced in realizing an indoor, interactive application that relies on ubiquitous network connectivity. Our architecture directly addresses this challenge, as we observe that indoor connectivity characteristics do not comply with the ubiquitous connectivity requirement for this class of application.

An important aspect of the Energy Lens is determining when people and things have moved. This requires some form of indoor localization. There’s a large body of literature in the area of indoor localization with mobile phones ranging from using wifi [**radar**], to sonar [**cricket**], to ambient noise [**abs**], and a combination of sensors on the phone [**surroundsense**]. Dita [**dita**] uses acoustic localization of mobile phones and also uses the infrastructure to determine gestures in free-space that are classified into pre-defined control actions. Each of

these require relatively complex software and/or infrastructure. We take a radically different, simple approach. We use cheap, easy to re-produce tags (QR codes), incrementally place them on things in the environment and use the natural *swiping gesture* that users make, when interacting with the Energy Lens application, to track when they have moved or when the objects around them have moved. The guiding principle is to attain as much information from a gesture as possible, to determine a move has occurred. We discuss our heuristics in section 6.6.

ACE [ACE] uses various sensors on the phone to infer a user’s context. The context domain consists of a set of user activities and semantic locations. For example, ACE distinguishes between *Running*, *Driving*, *AtHome*, or *InOffice*. ACE can also infer one from the other. If a user is *AtHome* then they are not *InOffice*. Energy Lens uses inference to determine when a person or thing has moved. Certain swipe combinations give us information about whether they moved or whether an item moved. The main difference is that we only infer context when a user is actively swiping, rather than a continuous approach.

Prefetching is a fundamental technique used in many domains. The cost of a prefetch for mobile application out-weighs the benefits if the prefetched data is not useful. Informed mobile prefetching [imp’mobisys2012] uses cost-benefit analysis to determine when to prefetch content for the user. We prefetch data based on location swipes. Caching prefetched content not only improves performance and interactivity, but it is *necessary* to sustain normal operation during periods of disconnectedness.

Logistic systems focus on tracking objects as the move from distribution sites, to warehouses, and across purchase counters. Items are tracked through their unique bar codes, often embedded in an RFID. The workload in logistic systems is very structured and well defined. The authors of [rfid’gonz2006] describe this structure and leverage it to minimize storage requirements and optimize query-processing performance. The Energy Lens uses QR codes as tags and the phone as an active reader. As objects move, users scan those items to their new location. However, objects may belong to one or many people, they can be metered by multiple meters a day, and their history in the system is on-going. In contrast, a typical logistics workload has a start (distribution site) and end point (leaving the store after a sale). Our workload is less well-defined. Furthermore, relationship semantics are important; For example, we interpret a bind relationship differently from an attach relationship. We discuss the difference later in the paper.

Furthermore, we take advantage of natural gestures the user makes with the phone while scanning QR codes to extract information about the current location of the user or things.

The key idea in the HP Cooltown [bridgingphysical, cooltown] work is to web-enable ‘things’ in the world, grouped-by ‘place’, and accessed by ‘people’ via a standardized acquisition protocol (HTTP) and format (HTML, XML). Cooltown creates a web presence for things in the world either directly (embedded web server) or indirectly (URL-lookup tag) as a web page that displays the services it provides. Many of the core concepts in Cooltown also show up in Energy Lens. The main overlap is the use of tags in the world that contain a reference to a virtual resource, accessible via HTTP through a network connection. Cooltown, however, explicitly chooses not maintain a centralized relationship graph, it lever-

ages the decentralized, linking structure of the web to group associated web pages together. Furthermore, things are assumed to not move. People are the main mobile entities. The kind of applications we wish to support must track where things are and their specific inter-relationships. We imposed a richer set of semantics on our, centrally maintained, relationship graph and use it to provide detailed energy information.

## 6.9 Summary

In this EnergyLens application we examined two system challenges – mobility and consistency management – for enabling and energy analytics applications in buildings. We also offered initial solution approaches. We see these as crucial barriers to solve in order to provide the kinds of services described in Section ???. However, other challenges remain, particularly those related to scaling to an entire buildings, integrating many more streaming data sources, and providing streaming analytics for immediate display to building occupants. We see an opportunity to combine these with control in order to empower building occupants to literally take control of their energy footprint. The components of our architecture are simple, and simplicity is important for scale and generalizability. We hope that with the right tools and information, people will be motivated to act, and large energy waste reduction can be achieved.

# Chapter 7

## Empirical Verification of System Functionality and Metadata

### 7.1 Functional Verification Methodology

The primary objective of SBS is to determine *how* device usage patterns are correlated across all pairs of sensors and discover when these relationships change. The naive approach is to run correlation analysis on pairs of sensor traces, recording their correlation coefficients over time and examining when there is a statistically-significant deviation from the norm. However, this approach does not yield any useful information when applied to *raw data*

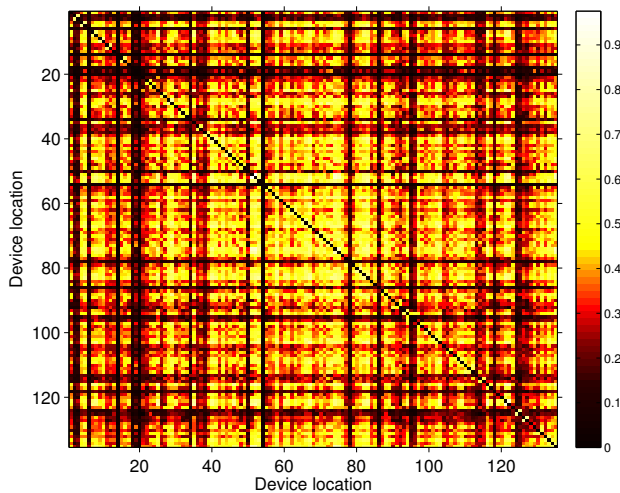


Figure 7.1: Correlation coefficients of the raw traces from the Building 1 dataset (Section 5.5). The matrix is ordered such as the devices serving same/adjacent rooms are nearby in the matrix.

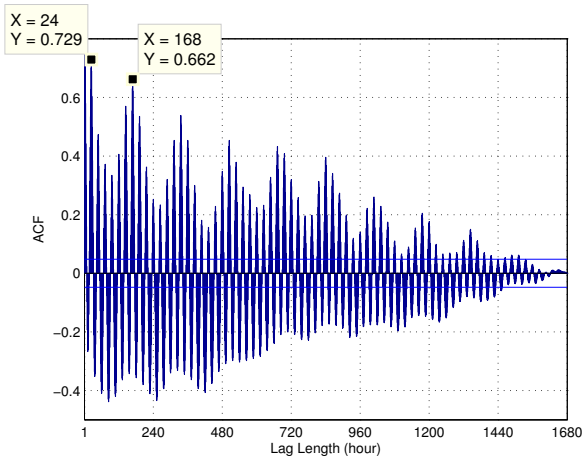


Figure 7.2: Auto-correlation of a usual signal from the Building 1 dataset. The signal features daily and weekly patterns (resp.  $x = 24$  and  $x = 168$ ).

traces. For example, the two raw signals shown in Figure 7.3 are from two independent HVAC systems, serving different rooms on different floors. Since each space is independently controlled, we expect their power-draw signals to be uncorrelated (or at least distinguishable from other signal pairs). However, their correlation coefficient (0.57), is not particularly informative – it is statistically similar to the correlation between itself and other signals in the trace.

Using a larger set of devices, Figure 7.1 shows a correlation matrix with 135 distinct lighting and HVAC systems serving numerous rooms in a building (described later on in Section 5.5). The indices are selected such that their index-difference is indicative of their relative spatial proximity. For example, a device in location 1 is closer in the building to a device in location 2 than it is to a device in location 135. The color of the cell is the average pairwise correlation coefficient for devices in the row-column index. The higher the value, the lighter the color. Devices serving the same room are along the diagonal. Because these devices are used simultaneously, we expect high average correlation scores, lighter shades, along the diagonal figure. However, we observe no such pattern. Most of the signals are correlated with all the others and we see no discernible structure.

An explanation for this is that the daily occupant usage patterns drive these results. Figure 7.3 demonstrates this more clearly. It shows two 1-week raw signals traces which feature the same diurnal pattern. This trend is present in almost every sensor trace, and, it hides the smaller fluctuations providing more specific patterns driven by local occupant activity. Upon deeper inspection, we uncovered several dominant patterns, common among energy-consuming devices in buildings [wrinch:pes2012]. Figure 7.2 depicts the auto-correlation of a usual electric power signal for a device. The two highest values in the figure correspond to a lag of 24 hours and 168 hours (one week). Therefore, the signal has some periodicity and

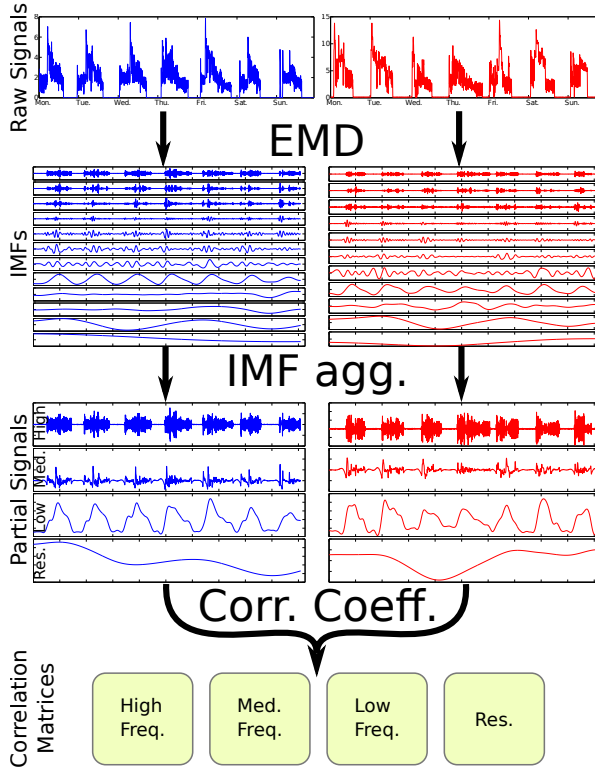


Figure 7.3: *Strip and Bind* using two raw signals standing for one week of data from two different HVACs. (1) Decomposition of the signals in IMFs using EMD (top to bottom:  $c_1$  to  $c_n$ ); (2) aggregation of the IMFs based on their time scale; (3) comparison of the partial signals (aggregated IMFs) using correlation coefficient.

similar (though not equal) values are seen at daily and weekly time scales. The daily pattern is due to daily office hours and the weekly pattern corresponds to weekdays and weekends. Correlation analysis on *raw* signals cannot be used to determine meaningful inter-device relationships because periodic components act as non-stationary trends for high-frequency phenomenon, making the correlation function irrelevant. Such trends must be removed in order to make meaningful progress towards our aforementioned goals.

In the next section we describe SBS. We discuss *strip and bind* in section 7.1, which addresses de-trending and relationship-discovery. Then, we describe how we *search* for changes in usage patterns, in section 7.1, to identify potential savings opportunities.

### Strip and Bind

Discovering devices that are used in concert is non-trivial. SBS decomposes each signal into an additive set of components, called Intrinsic Mode Functions (IMF), that reveals the signal patterns at different frequency bands. IMFs are obtained using Empirical Mode De-

composition (see Figure 7.3 and Section 5.3). We only consider IMFs with time scales shorter than a day, since we are interested in capturing short-scale usage patterns. Consequently, SBS aggregates the IMFs that fall into this specific time scale (see *IMF agg.* in Figure 7.3). The resulting partial signals of different device power traces are compared, pairwise, to identify the devices that show un/correlated usage patterns (see *Corr. Coeff.* in Figure 7.3).

The IMFs are clustered using four time scale ranges:

- The *high frequencies* are all the IMFs with a time scale lower than 20 minutes. These IMFs capture the noise.
- The *medium frequencies* are all the IMFs with a time scale between 20 minutes and 6 hours. These IMFs convey the detailed devices usage.
- The *low frequencies* are all the IMFs with a time scale between 6 hours and 6 days. These IMFs represent daily device patterns.
- The *residual data* is all data with a time scale higher than 6 days. This is mainly residual data obtained after applying EMD. Also, it highlights the main device trend.

These time scale ranges are chosen based on our experiments and goal. The 20-minute boundary relies on the sampling period of our dataset (5 minutes) and permits us to capture IMFs with really short periods. The 6-hour boundary allows us to analyze all patterns that have a period shorter than the usual office hours. The 6-day boundary allows us to capture daily patterns and weekday patterns.

Aggregating IMFs, within each time scale range, results in 4 partial signals representing different characteristics of the device’s energy consumption (see *Partial Signals* in Figure 7.3). We do a pairwise device trace comparison, calculating the correlation coefficient of their partial signals. In the example shown in Figure 7.3, the correlation coefficient of the raw signals suggests that they are highly correlated (0.57). However, the comparison of the corresponding *partial signals* provides new insights; the two devices are poorly correlated at high and medium frequencies (respectively  $-0.01$  and  $-0.04$ ) but highly correlated at low frequencies (0.79) meaning that these devices are not “intrinsically” correlated. They only share a similar daily pattern.

All the devices are compared pairwise at the four different time scale ranges. Consequently, we obtain four correlation matrices that convey device similarities at different time scales. Each line of these matrices (or column, since the matrices are symmetric) reveals the behavior of a device – its relationships with the other devices at a particular time scale. The matrices form the basis for tracking the behavior of devices and to search for misbehavior.

## Search

*Search* aims at identifying misbehaving devices in an unsupervised manner. Device behavior is monitored via the correlation matrices presented in the previous section. Using

numerous observations SBS computes a specific reference that exhibits the normal inter-device usage pattern. Then, SBS compares the computed reference with the current data and reports devices that deviate from their usual behavior.

## Reference Matrix

We define four reference matrices, which capture normal device behavior at the four time scale ranges defined in Section 5.3. The references are computed as follows: (1) we retrieve the correlation matrices for  $n$  consecutive time bins. (2) For each pair of devices we compute the median correlation over the  $n$  time bins and obtain a matrix of the median device correlations.

Formally, for each time scale range the computed reference matrix for  $d$  devices and  $n$  time bins is:

$$R_{i,j} = \text{median}(C_{i,j}^1, \dots, C_{i,j}^n)$$

where  $i$  and  $j$  ranges in  $[1, d]$ .

Because anomalies are rare by definition, we assume the data used to construct the reference matrix is an accurate sample of the population; it is unbiased and accurately captures the range of normal behavior. Abnormal correlation values, that could appear during model construction, are ignored by the median operator thanks to its robustness to outlier (50% breakdown point). However, if that assumption does not hold (more than 50% of the data is anomalous), our model will flag the opposite – labeling abnormal as normal and vice-versa. From close inspection of our data, we believe our primary assumption is sound.

## Behavior change

We compare each device behavior, for all time bins, to the one provided by the reference matrix. Consider the correlation matrix  $C^t$  obtained from the data for time bin  $t$  ( $1 \leq t \leq n$ ). Vector  $C_{i,*}^t$  is the behavior of the  $i^{th}$  device for this time bin. Its normal behavior is given by the corresponding vector in the reference matrix  $R_{i,*}$ . We measure the device behavior change at the time bin  $t$  with the following Minkowski weighted distance:

$$l_i^t = \left( \sum_{j=1}^d w_{ij} (C_{i,j}^t - R_{i,j})^p \right)^{1/p}$$

where  $d$  is the number of devices and  $w_{ij}$  is:

$$w_{ij} = \frac{R_{i,j}}{\sum_{k=1}^d R_{i,k}}.$$

The weight  $w$  enables us to highlight the relationship changes between the device  $i$  and those highly correlated to it in the reference matrix. In other words, our definition of behavior

change is mainly driven by the relationship among devices that are usually used in concert. We also set  $p = 4$  in order to inhibit small differences between  $C_{i,j}^t$  and  $R_{i,j}$  but emphasize the important ones.

By monitoring this quantity over several time bins the abnormal device behaviors are easily identified as the outlier values. In order to identify these outlier values we implement a robust detector based on median absolute deviation (MAD), a dispersion measure commonly used in anomaly detection [huber:wiley2009, chan:springer2005]. It is a measure that robustly estimates the variability of the data by computing the median of the absolute deviations from the median of the data. Let  $l_i = [l_i^1, \dots, l_i^n]$  be a vector representing the behavior changes of device  $i$  over  $n$  time bins, then its MAD value is defined as:

$$\text{MAD}_i = b \text{ median}(|l_i - \text{median}(l_i)|)$$

where the constant  $b$  is usually set to 1.4826 for consistency with the usual parameter  $\sigma$  for Gaussian distributions. Consequently, we define anomalous behavior, for device  $i$  at time  $t$ , such that the following equation is satisfied:

$$l_i^t > \text{median}(l_i) + \tau \text{ MAD}_i$$

Note,  $\tau$  is a parameter that permits to make SBS more or less sensitive.

The final output of SBS is a list of alarms in the form  $(t, i)$  meaning that the device  $i$  has abnormal behavior at the time bin  $t$ . The priority of the alarms in this list is selected by the building administrator by tuning the parameter  $\tau$ .

We evaluate SBS using data collected from buildings in two different geographic locations. One is a new building on main campus of the University of Tokyo and the other is an older building at the University of California, Berkeley.

Data pre-processing is not generally required for the proposed approach. Nevertheless, we observe in a few exceptional cases that sensors reporting excessively high values (i.e. values higher than the device actual capacity) that greatly alter the performance of SBS by inducing a large bias in the computation of the correlation coefficient. Therefore, we remove values that are higher than the maximum capacity of the devices, from the raw data.

The Todai dataset we use contains 10 weeks of data starting from June 27, 2011 and ending on September 5, 2011. This period of time is particularly interesting for two reasons: 1) in this region, the summer is the most energy-demanding season and 2) the building manager actively works to curtail energy usage as much as possible due to the Tohoku earthquake and Fukushima nuclear accident.

Furthermore, this dataset is a valuable ground truth to evaluate the Strip and Bind portions of SBS. Since the light and HVAC of the rooms are directly controlled by the room's occupants, we expect SBS to uncover verifiable devices relationships.

The Cory Hall dataset we use consists of 8 weeks of energy consumption traces measured by 70 sensors starting on April 5<sup>th</sup>, 2011. In contrast to the other dataset, a variety of devices are monitored, including, electric receptacles on certain floors, most of the HVAC components, power panels and whole-building consumption.

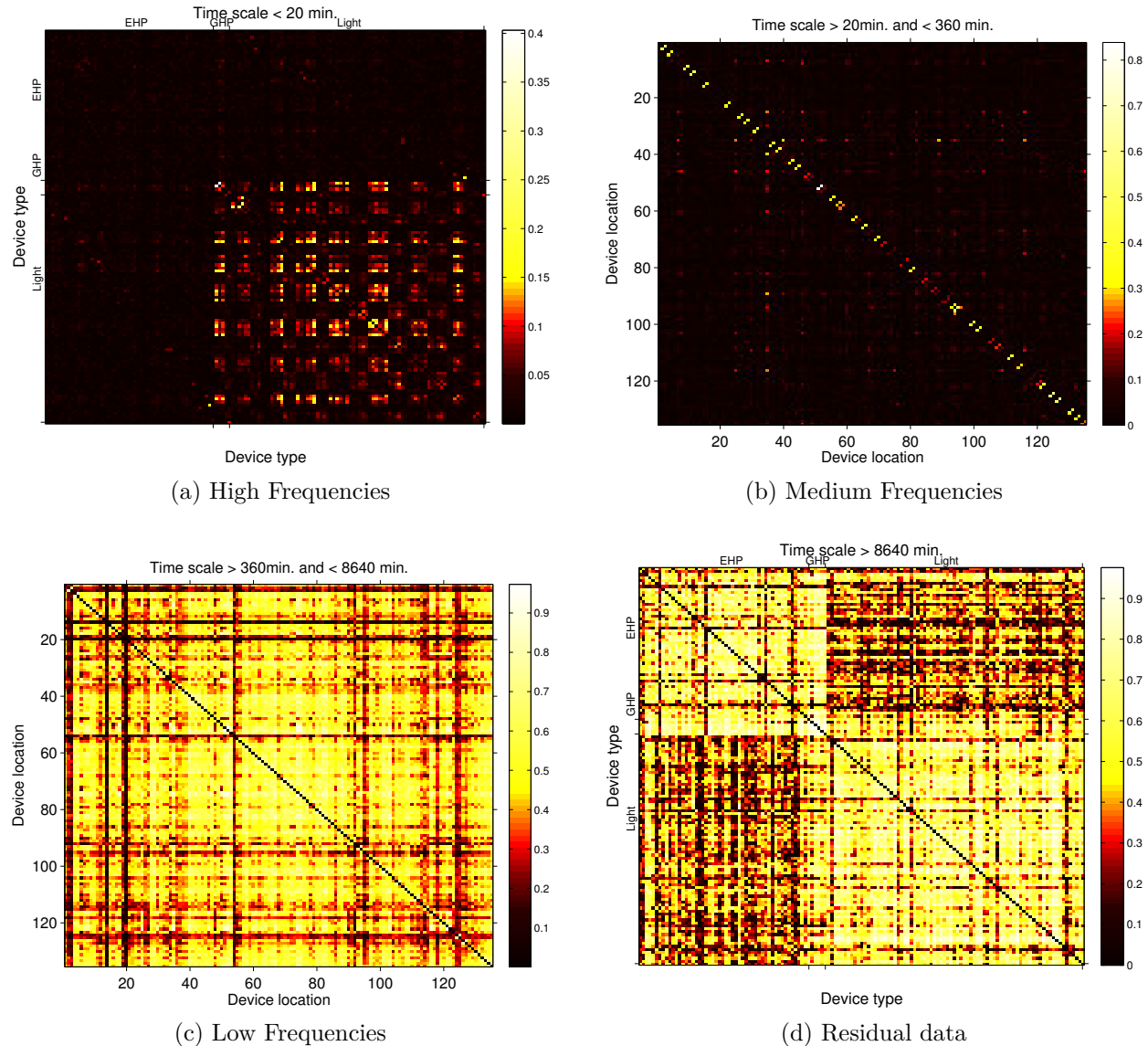


Figure 7.4: Reference matrices for the four time scale ranges (the diagonal  $x = y$  is colored in black for better reading). The medium frequencies highlight devices that are located next to each other thus intrinsically related. The low frequencies contains the common daily pattern of the data. The residual data permits to visually identify devices of the similar type.

These two building infrastructures are fundamentally different. This enables us to evaluate the practical efficacy of the proposed, unsupervised method in two very different environments.

In this section we evaluate SBS on our building traces. We demonstrate the benefits of striping the data by monitoring patterns captured at different time scales. Then, we

thoroughly investigate the alarms reported by SBS.

## Device behavior at different time scales

The Strip and Bind part of SBS is evaluated using the data from Eng. Bldg 2. This dataset is appropriate to measure SBS's performance, since lighting and HVAC systems serving the same room are usually used simultaneously. Consequently, we analyze this data using SBS and verify that the higher correlations at medium frequencies correspond to devices located in the same room.

The dataset is split into 10, one-week bins and each bin is processed by SBS. Using the 10 correlation matrices at each time scale range, SBS uncovers the four reference matrices depicted in Figure 7.4.

**High frequencies** In this work the high frequencies correspond to the signals *noise*, therefore, we do not expect any useful information from the corresponding matrix (Figure 7.4a). Indeed, the corresponding reference matrix does not provide any help to determine a device's relative location. Thus, we emphasize that high frequency data should be ignored for uncovering device relationships (in contrast to [romain:iotapp12]). Interestingly, we find that the sensors monitoring the lights generate consistent noise.

**Medium frequencies** Our main focus is on the medium frequencies as it is designed to capture the intrinsic device relationships. Figure 7.4b shows the correlation matrix at medium frequencies. It is significantly different from the one obtained with the raw signals (Figure 7.1): high correlation coefficients are concentrated along the matrix diagonal. Since devices serving the same or adjacent rooms are placed nearby in the matrix it validates our hypothesis: *high correlation scores within the medium frequency band shows strong inter-device relationships*.

Considering this reference matrix as an adjacency matrix of a graph, in which the nodes are the devices, we identify the clusters of correlated devices using a community mining algorithm [5]. As expected we obtain mainly clusters of only two devices (light and HVAC serving the same room), but we also find clusters that are composed of more devices. For example a cluster contains 3 HVAC systems serving the three server rooms. Although these server rooms are located on different floors, SBS shows a strong correlation between these devices. Coincidentally, they are managed similarly. Interestingly, we also observe a couple of clusters that consist of independent devices serving adjacent rooms belonging to the same lab. The bigger cluster contains 33 devices that are 2 GHP devices and the corresponding lights. This correlation matrix and the corresponding clusters highlight the ability for SBS to identify such hidden inter-device usage relationships.

**Low frequencies** Low frequencies capture daily patterns, embedded in all the device traces. Figure 7.4c depicts the corresponding reference matrix which is similar to the one of

raw signal traces (Figure 7.1) and it shows no particular structure. These partial signals are discarded as they do not help us in identifying inter-device usage patterns.

**Residual data** The residual data shows the weekly trend, which gives us no information about device relationships. But, surprisingly, by reordering the correlation matrix based on the type of the devices (Figure 7.4d) we can visually identify two major clusters. The first cluster consists of HVAC devices (see EHP and GHP in Figure 7.4d) and the second one contains only lights. An in-depth examination of the data reveals that long-term trends are inherent to the device types. For example, as the consumption of both the EHP and GHP devices is driven by the building occupancy and the outside temperature, these two types of devices follow the same trend. However, the use of light is independent from the outside temperature thus the lighting systems follow a common trend different from the EHP and GHP one.

We conduct the same experiments by splitting the dataset in 70 bins of 1 day long and observe analogous results at high and medium frequencies but not at lower frequencies. This is because the bins are too short to exhibit daily oscillations and the residual data captures only the daily trend.

## Methodological Shortcomings

Because our analysis is done on historical data, some of the faults found by SBS could not be fully corroborated. In order to fully examine the effectiveness of our approach, we must run it in real time and physically check that the problem is actually occurring. When a problem is detected in the historical trace, months after it has occurred, the current state of the building may no longer reflect what is in the traces. Some of the anomalies discussed in this section uncover interpretable patterns that are difficult to find in practice. For example, simultaneous heating and cooling is a known, recurring problem in buildings, but it is very hard to identify when it is occurring. Some of the anomalies we could not interpret might be interpretable by a building manager, however, we did not consult either building manager for this study. Therefore, the results of this study do not examine the true/false positive rate exhaustively.

The true/false negative rate is impractical to assess. It may be examined through synthetic stimulation of the building via the control system. However, getting cooperation from a building manager to hand over control of the building for experimentation is non-trivial. Therefore, we forgo a full true/false negative analysis in our evaluation.

Because of these challenges, the evaluation of SBS focuses on comparing the output with known fault signatures. We examine anomalies, in either building, where the anomaly is easily interpretable but difficult to find by the building manager. We forego a comparison of SBS with competing algorithms because related algorithms require detailed knowledge of the building, *a priori*. The advantage of SBS is that it requires no such information to provide immediate value.

	High	Low	Punc.	Missing	Other
Eng. Bldg 2	9 (5)	6 (5)	1 (1)	36 (1)	3 (3)
Cory Hall	25 (7)	7 (3)	4 (4)	0 (0)	3 (3)

Table 7.1: Classification of the alarms reported by SBS for both dataset (and the number of corresponding anomalies).

## 7.2 Functional Verification Experimental Results

We evaluate the *search* performance of SBS using the traces from the Eng. Bldg 2 and Cory Hall. Due to the lack of historical data, such as room schedule or reports of energy waste, the evaluation is non-trivial. Furthermore, getting ground truth data from a manual inspection of the hundreds traces of our data sets is impractical. The lack of ground truth data prevents us from producing a systematic analysis of the anomalies missed by SBS (i.e. false negatives rate). Nevertheless, we exhibit the relevance of the anomalies uncovered by SBS (i.e. high true positive rate and low false positive rate) by manually checking the output of SBS.

**Anomaly classification** To validate SBS results we manually inspect the anomalies detected by the algorithm. For each reported alarm  $(t, i)$  we investigate the device trace  $i$  and the devices correlated to it to determine the reason for the alarm. Specifically, we retrieve the major relationship change that causes the alarm (i.e.  $\max(|w_j(C_{i,j}^t - R_{i,j})|)$ , see Section 7.1) and examine the metadata associated to the corresponding device. This investigation allows us to classify the alarms into five groups:

- *High power usage*: alarms corresponding to electricity waste.
- *Low power usage*: alarms representing the abnormally low electricity consumption of a device.
- *Punctual abnormal usage*: alarms standing for short term (less than 2.5 hours) raise or drop of the electricity consumption.
- *Missing data*: alarms raised due to a sensor failure.
- *Other*: alarms whose root cause is unclear.

**Experimental setup** For each experiment, the data is split in time bins of one day, starting from 09:00 a.m. – which is approximately the office’s opening time. We avoid having bins start at midnight since numerous anomalies appear at night and they are better highlighted if they are not spanning two time bins. Only the data at medium frequencies

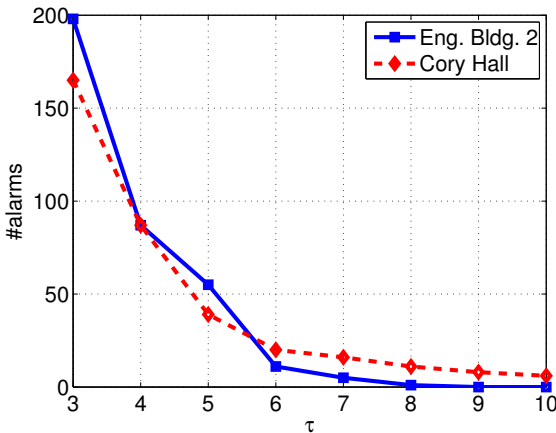


Figure 7.5: Number of reported alarms for various threshold value ( $\tau = [3, 10]$ ).

are analyzed, the other frequency bands are ignored, and the reference matrix is computed from all time bins.

The threshold  $\tau$  tunes the sensitivity of SBS, hence, the number of reported alarms. Furthermore, by plotting the number of alarms against the value of  $\tau$  for both datasets (Figure 7.5) we observe an elbow in the graph around  $\tau = 5$ . With thresholds lower than this pivot value ( $\tau < 5$ ), the number of alarms significantly increases, causing less important anomalies to be reported. For higher values ( $\tau > 5$ ), the number of alarms is slowly decreasing, providing more conservative results that consist of the most important anomalies. This pivot value provides a good trade off for either data set.

Table 7.1 classifies the alarms reported by SBS on both datasets. Anomalies spanning several time bins (or involving several devices) may raise several alarms. We display these in Table 7.1 as numbers in brackets – the number of anomalies corresponding to the reported alarms.

## Todai

SBS reported 55 alarms over the 10 weeks of the Eng. Bldg 2 dataset. However, 36 alarms are set aside because of sensor errors; one GHP has missing data for the first 18 days. Since this device is highly correlated to the GHP in the reference matrix, their relationship is broken for the 18 first bins and for each bin one alarm per device is raised.

In spite of the post-Fukushima measures to reduce Eng. Bldg 2's energy consumption, SBS reported 9 alarms corresponding to high power usage (Table 7.1). Figure 7.6a depicts the electricity consumption of the light and EHP in the same room where two alarms are raised. Because the EHP was not used during daytime (but is turned on at night, when the light is turned off) the relationship between the two devices is “broken” and an alarm

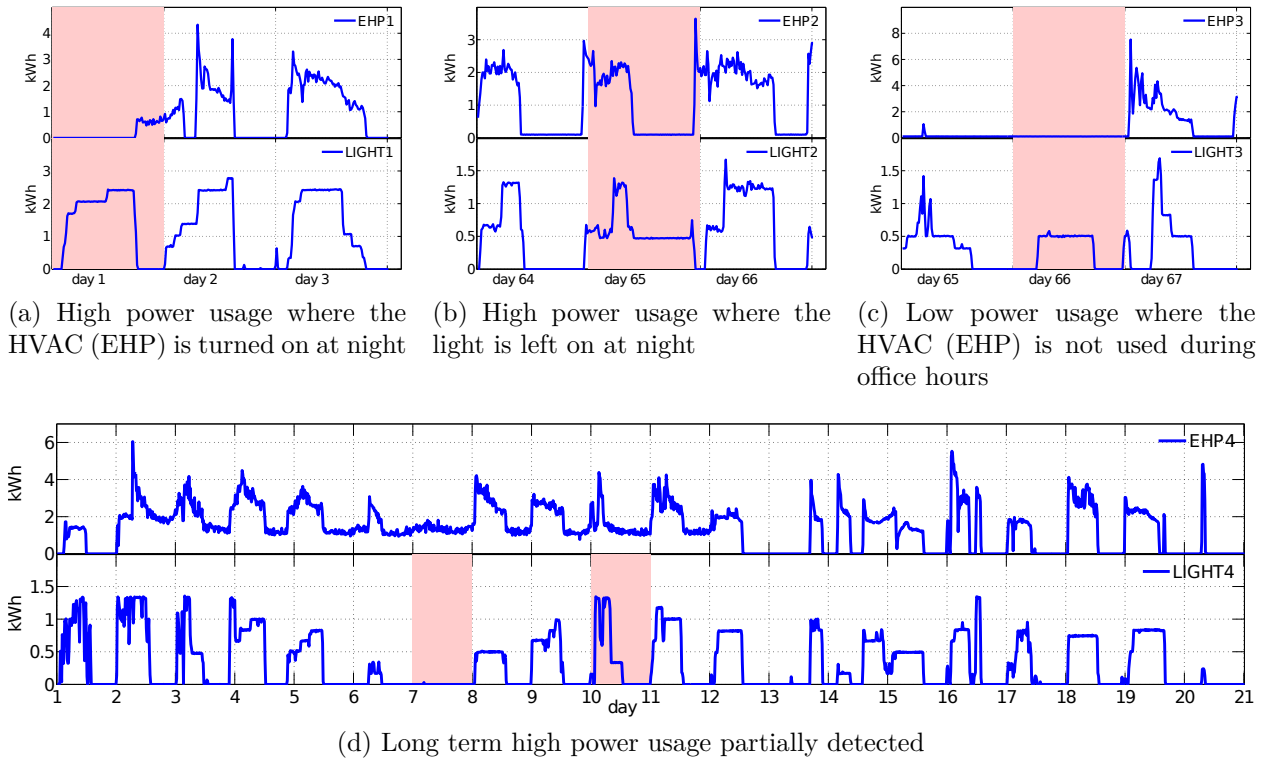


Figure 7.6: Example of alarms (red rectangles) reported by SBS on the Eng. Bldg 2 dataset

is raised for each device. Figure 7.6b shows another example of energy waste. The light is on at night and the EHP is off. The top-priority anomaly reported by SBS is caused by the 10 days long constant use of an EHP (Figure 7.6d) and this waste of electricity accounts for 165 kWh. SBS partially reports this anomaly but lower values of  $\tau$  permits us to identify most of it.

We observed 6 alarms corresponding to abnormally low power use. Upon further inspection we notice that it corresponds to energy saving initiatives from the occupants – likely due to electricity concerns in Japan. This behavior is displayed in Figure 7.6c. The room is occupied at the usual office hours (indicated by light usage) but the EHP is not on in order to save electricity.

## Cory Hall

SBS reported 39 alarms for the Cory Hall dataset (Table 7.1). 7 are classified as low power usage, however, our inspection revealed that the root causes are different than for the Eng. Bldg 2 dataset. We observe that the low power usage usually corresponds to device failures or misconfiguration. For example, Figure 7.7a depicts the electricity consumption of the 2<sup>nd</sup> floor chiller and a power riser that comprises the consumption of multiple systems,

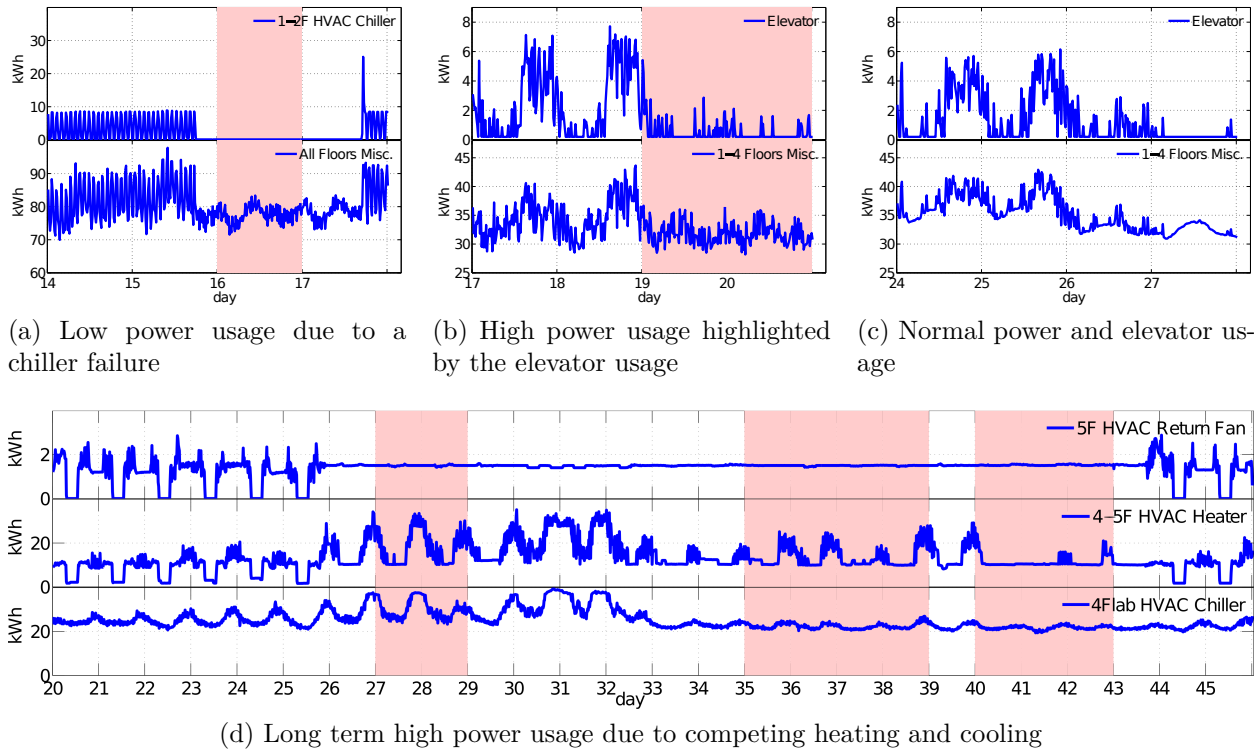


Figure 7.7: Example of alarms (red rectangles) reported by SBS on the Cory Hall dataset

including the chiller. As the chiller suddenly stops working, the correlation between both measurements is significantly altered and an alarm for each device is raised.

SBS also reports 25 alarms corresponding to high power usage. One of the identified anomalies is particularly interesting. We indirectly observe abnormal usage of a device from the power consumption of the elevator and a power panel for equipment from the 1<sup>st</sup> to the 4<sup>th</sup> floor. Figure 7.7b and 7.7c show the electricity consumption for both devices. SBS uncovers the correlation between the these two signals, as the amount of electricity going through the panel fluctuates along with the elevator power consumption (Figure 7.7c). In fact, the elevator is a good indicator of the building's occupancy. Anomalous energy-consumption is identified during a weekend as the consumption measured at the panel is independently fluctuating from the elevator usage. These fluctuations are caused by a device that is not directly monitored. Therefore, we could not identify the root cause more precisely. Nevertheless, the alarm is worthwhile for building operators to start investigating.

The most important anomaly identified in Cory Hall is shown in Figure 7.7d. This anomaly corresponds to the malfunctioning of the HVAC heater serving the 4<sup>th</sup> and 5<sup>th</sup> floors. The heater is constantly working for 18 consecutive days, regardless of the underlying occupant activity. Moreover, in order to maintain appropriate temperature this also results in an increase of the 4<sup>th</sup> floor HVAC chiller power consumption and several fans, such as the

one depicted in Figure 7.7d. This situation is indicative of simultaneous heating and cooling – whereby heating and cooling systems are competing – and it is a well-known problem in building management that leads to significant energy waste. For this example, the electricity waste is estimated around 2500 kWh for the heater. Nevertheless, as the anomaly spans over 18 days, it is hidden in the building’s overall consumption, thus, it is difficult to detect by building administrators without SBS.

### 7.3 Spatial Verification Methodology

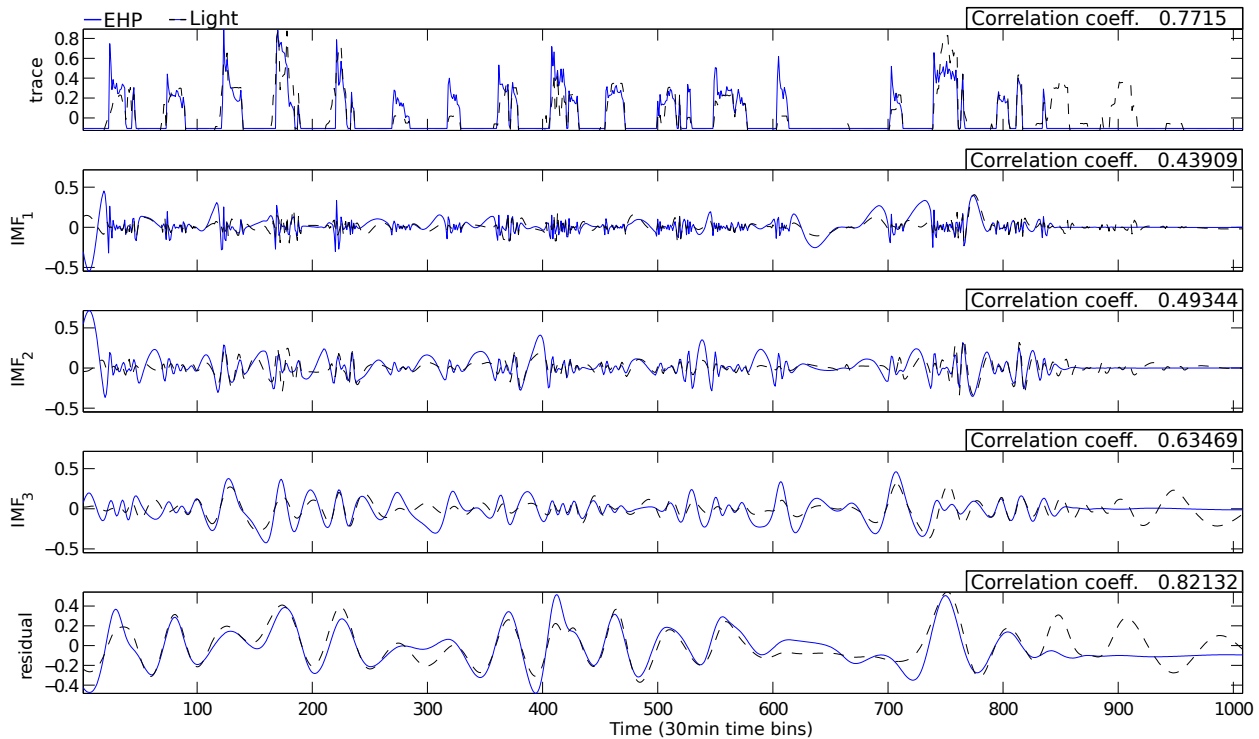


Figure 7.8: Decomposition of the EHP and light trace using bivariate EMD. IMFs correlation coefficients highlight the intrinsic relationship of the two traces.

For this investigation, we focus on a three-week span in the summer of 2011 (from July 4th to July 24th). The dataset captures regular work days, weekends, and one holiday (July 18th). This timeframe captures the typical usage of the equipment, triggered by occupant activity. For the initial analysis, we focus on three sensors; two water pumps and a light feed. The first pump is an “electric heat pump” and is labeled as EHP, the second is a “gas heat pump” and labeled as GHP. The room lighting system serves the same room as the EHP. The GHP serves a different room on the same floor. The expanded portion of our

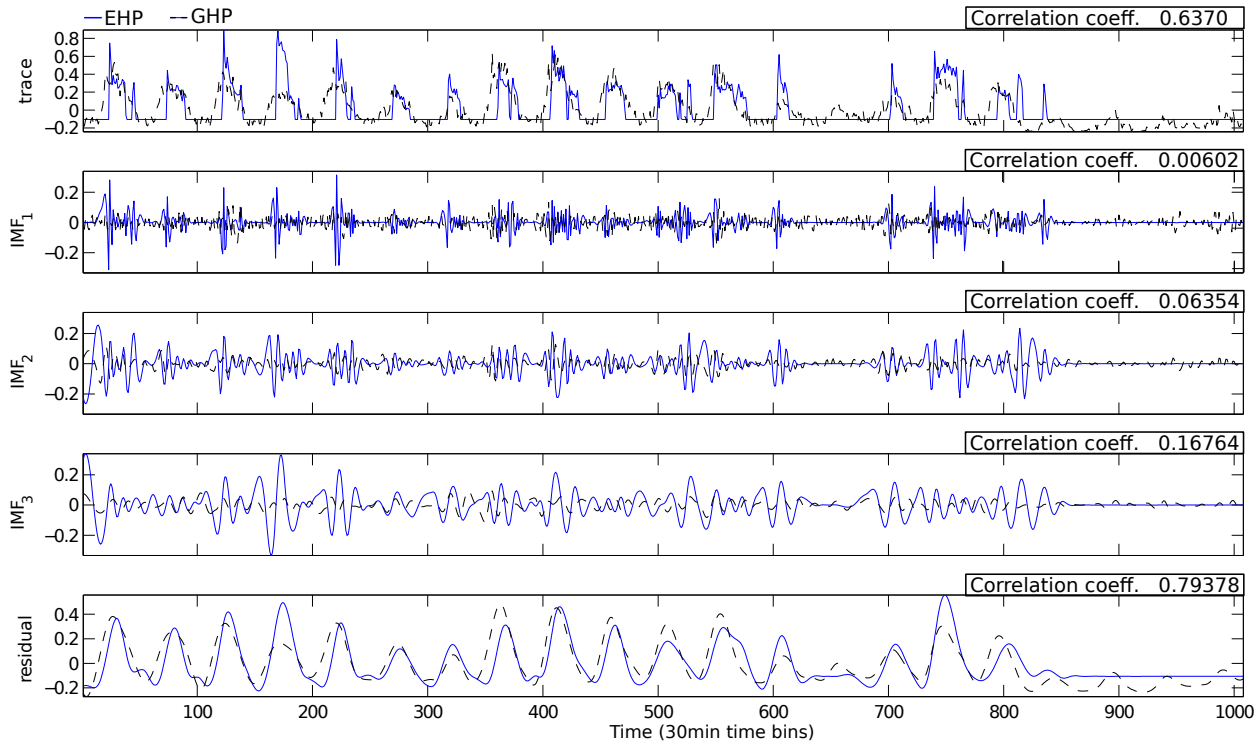


Figure 7.9: Decomposition of the EHP and GHP trace using bivariate EMD. IMFs correlation coefficients highlight the intrinsic independence of the two traces.

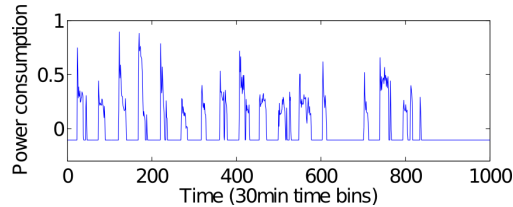


Figure 7.10: Trace from an Electric Heat Pump (EHP) captured in 2011 from July 4th to July 24th. Data is normalized and aggregated into 30 minutes time bins.

analysis pivots around the EHP and does a pairwise comparison between it and all other sensors in the building. Computationally, this approach does not scale to a large number of sensors. For future work, we will examine various heuristics to narrow the search space before running pairwise comparisons.

We use EMD to detrend each of the traces and pay particularly close attention to the high-frequency IMFs. Our hypothesis is that correlating at the higher frequencies will yield more meaningful comparisons. In buildings, metadata is poorly and unsystematically managed

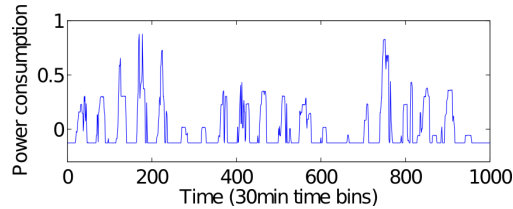


Figure 7.11: Light traces from captured in 2011 from July 4th to July 24th. Data is normalized and aggregated into 30 minutes time bins.

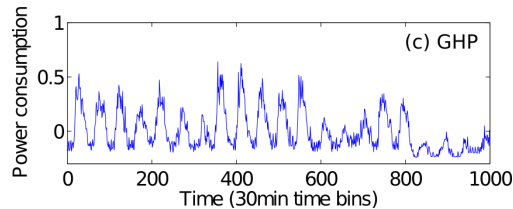


Figure 7.12: Traces from a Gas Heat Pump (EHP) captured in 2011 from July 4th to July 24th. Data is normalized and aggregated into 30 minutes time bins.

within a single system domain. Moreover, with the ever growing number of additional sub-meters, it is important to quickly integrate sensor data from multiple systems to understand the full state of the building. It is also important to understand how sensors are used in concert. Anomalies in usage may indicate underlying problems with the equipment or inefficient/incorrect usage.

Figure ?? shows the raw traces for the three devices discussed in the previous section (EHP, GHP, light). All three exhibit a diurnal usage pattern. On weekends, each draw less power. For our initial analysis, we calculated the pairwise correlation coefficient for all sensors in the set. The correlation coefficient for the EHP and light is 0.7715 and the correlation coefficient for the EHP and GHP is 0.6370. Running correlation across them yields high correlation coefficients, mostly due to their underlying daily usage pattern.

## Distribution

Let  $ts_{j,t}^i$  be a time-series for sensor  $j$  in room  $i$  observed over some time interval  $t$ . For simplicity, we ignore  $t$  in defining subsequent functions and re-introduce it where necessary. For each trace we run EMD and obtain a set of  $n$  IMFs, denoted as follows:

$$\Phi_j^i = EMD(ts_{j,t}^i) = \{IMF_{1 \sim n}\}$$

IMFs are traces themselves, so we divide and re-aggregate them into the four bands,  $B$ , further described in Section ??.

$$B = \{H(igh), M(edium), L(ow), R(esidue)\}$$

Let the re-aggregation of the bands be denoted as:

$$Aggr(\Phi_j^i) = \{IMF_{f,j}^i\}$$

where  $f \in B$ . We pick the *medium* frequency band ( $M$ ) to compute the pairwise corrcoeff of the sensor traces. In order to understand and characterize the boundary between sensors we consider two sets of corrcoeffs for each room; the “intra”-room set and “inter”-room set, as defined:

$$R_{intra,t}^i = \{r(IMF_{M,j,t}^i, IMF_{M,k,t}^i)\}, s.t. \forall j, k \in S_i$$

The intra set only contains pairs of sensors in the same room, so both  $ts_{j,t}^i$  and  $ts_{k,t}^i$  are traces from sensors in room  $i$ .

$$R_{inter,t}^i = \{r(IMF_{M,j,t}^i, IMF_{M,k,t}^{i'})\},$$

$$s.t. \forall j \in S_i, \forall k \in S'_i, i \neq i'$$

By contrast, the *inter* set contains pairs across rooms, meaning  $ts_{j,t}$  is a trace from a sensor in room  $i$  and  $ts_{k,t}$  is a sensor trace from some other room  $i'$ . Note the use of  $t$  in the definitions. We re-introduce  $t$  here to denote that the construction of each set is performed with respect to a specific time interval.

Finally, we examine populations,  $R_{intra}^i$  and  $R_{inter}^i$ , across multiple time intervals (in days):

$$R_{intra}^i = \bigcup_{\forall t} R_{intra,t}^i, s.t. t \in \{1, 3, 5, 7, 14, 21, 28\}$$

$$R_{inter}^i = \bigcup_{\forall t} R_{inter,t}^i, s.t. t \in \{1, 3, 5, 7, 14, 21, 28\}$$

We generate a CDF for each of the two populations with respect to each room. This allows us to closely examine the statistical characteristics of the relationship between sensors in the same space and those in different spaces. Each room offers a potentially different perspective on this relationship.

## Threshold Analysis

In order to understand the statistical properties, we generate two corrcoeff distributions by computing the corrcoeff between pairs of traces within and across each room, as detailed in the previous section. Figure 7.17 shows how we divide the corrcoeff values into two sets. The figure shows two intra and two inter sets. Specifically, we examine how a choice in cut-off threshold affects the ability to separate the sets, when their separation is not known a priori, relative to each room. Our hypothesis is that there exists a computable, statistical boundary between sensors in different rooms.

To test our hypothesis, we choose a threshold value relative to the distribution of corrcoeffs. All pairs with a corrcoeff larger than the threshold will be classified as being in the

same room. To closely analyze the threshold parameter, we generate a receiver operating characteristic (ROC) curve by varying the threshold value. Then, we look for a good trade-off point between the true-positive and false-positive rate; one that maximizes the difference between TPR and FPR. We compare the ROCs generated for our “medium” frequency band IMFs against raw-signal, cross-correlation values, in order to ascertain the extent to which the SBS [13] methodology is advantageous for discovering a statistical separation, analogous to a physical one. We also examine whether there is a uniform boundary between clusters across all the rooms.

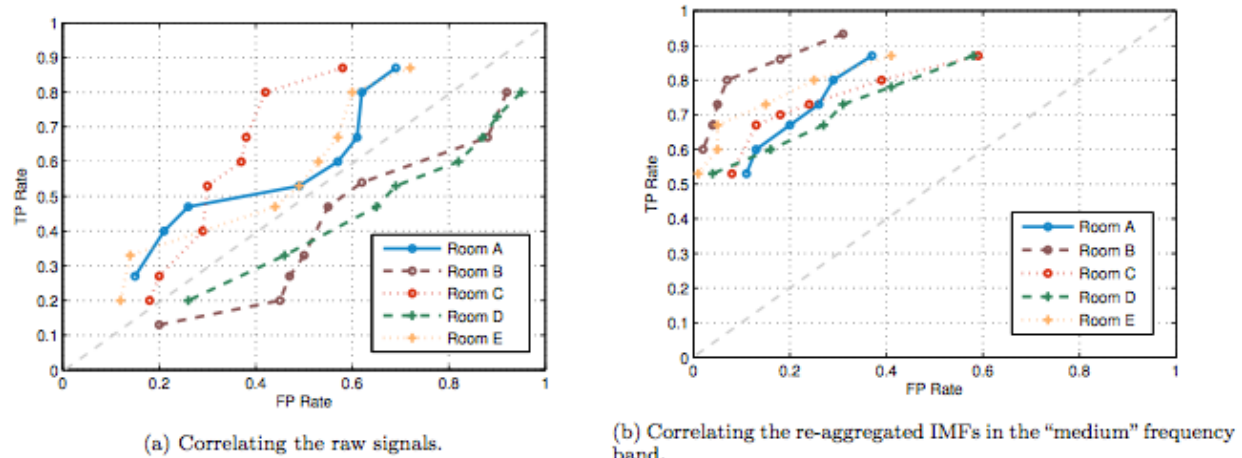


Figure 7.13: The ROC curves depict the sensitivity of the raw signal and mid-frequency IMFs to the threshold value. We choose the 0.2 FPR point as the boundary threshold for each room.

## Experimental Setup

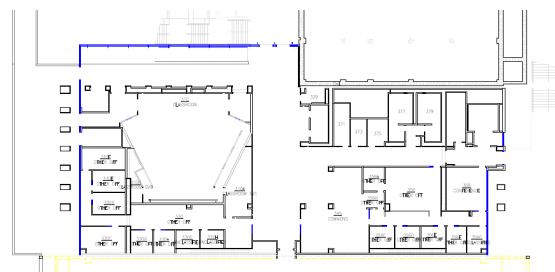


Figure 7.14: We collect data from 15 sensors in 5 rooms sitting on 4 different floors. This is a map of a section of the 3rd floor in Sutardja Dai Hall.

We perform an empirical study on sensor data collected from 15 sensors across 5 rooms on 4 different floors of a Sutardja Dai Hall, as detailed in Table 7.2. Each room has three sensors: a temperature sensor, a  $CO_2$  sensor, and a humidity sensor. The data from these is reported to an sMAP [7] archiver. The data set used comes from a deployment [34] lasting over 6 months on several floors in Sutardja Dai Hall (SDH) at UC Berkeley, where one sensor box – which contains a thermometer, a humidity sensor and a  $CO_2$  sensor – is placed in each room. The box reports data over 6LowPAN [23] to a sMAP archiver every 15 seconds. Due to intermittent data loss, we pick a time span without interruption, starting in January until mid-February, 2013, for evaluation.

Table 7.2: Room Specs

Room#	Orientation	Floor	Type
A	West	2	Computer Lab
B	South	4	Conference Room
C	No Window	2	Classroom
D	North	7	Conference Room
E	South	5	Conference Room

## 7.4 Spatial Verification Results

Our initial results on the Todai dataset were not surprising. The diurnal pattern dominates the comparison between the sensors. Weather is the main driver for this behavior and it affects the readings in almost all of the sensors in our dataset. Cross-correlation on raw sensor data is insufficient for filtering intrinsically related behavior. Upon closer examination of the data we assess the following:

- The main underlying diurnal trend occurs in almost all the traces.
- Occupancy and room activities occur at random times during the day and change at a higher frequency than weather patterns.
- Sensors that serve the same location observe the same activities. Therefore, their underlying measurements should be correlated.

In order to uncover these relationships we must remove low-frequency trends in the traces and compare the readings at high frequencies.

We test our hypothesis in this section by using EMD to remove low-frequency trends in the data and run correlation calculation at overlapping IMF timescales. We discover that EMD allows us to find and compare high-frequency intrinsic behavior that is spatially correlated across sensors. We begin with a small set of three sensors (EHP, GHP, light) and expand our scope to include all the sensors in the dataset.

$\tilde{A}U$	Raw trace	1st IMF	2nd IMF	3rd IMF	Residual
EHP, Light	0.7715	0.43909	0.49344	0.63469	0.82132
EHP, GHP	0.6370	0.0060274	0.063546	0.16764	0.79378

Table 7.3: Correlation coefficients of the analyzed trace and their IMFs uncovered by EMD

## Initial analysis

Lets consider the simple example of Section ?? where we would like to know if the EHP trace is correlated with the two other traces. Recall that the correlation coefficients of the raw feeds was 0.7715 and 0.6370, corresponding to the light and GHP, respectively. As stated in previous section this result is correct but not so meaningful, since most of the traces display the same diurnal pattern. Figure 7.8 and Figure 7.9 show the EMD decomposition of the three traces. For each trace, EMD has retrieved three IMFs that highlight the higher frequencies of the traces.

Figure 7.8 shows the normalized raw trace (top) and EMD output IMFs and residual as well as the correlation coefficients calculated on the IMFs for the EHP and light traces. The correlation coefficients are 0.43909, 0.49344 and 0.63469 corresponding to the IMF1, IMF2, and IMF3, respectively. Notice the high correlation between the high-frequency IMFs. We know that the light and EHP serve the same room, and their high-frequency IMF correlation corroborates our prior knowledge. Figure 7.9 shows a complementary result, for the EHP and GHP comparison. The correlation coefficients for the EHP and GHP IMFs suggest that the two may be independent. In fact, they *are* independent; they serve completely different rooms in the building!

EMD allows us to remove low-frequency trends that add noise to the original analysis. By comparing IMFs, we see both intrinsically correlated and *uncorrelated* behavior. In the next section we expand our analysis and show the effectiveness of our methodology.

## Validation

To validate the effectiveness of our approach, we analyze the same three-week time span for *all* 674 sensors deployed in the building. For each trace  $S$  we compute two scores: (1) the correlation coefficient between  $S$  and the EHP trace and (2) the average value of the IMF correlation coefficients.

Figure 7.15a shows the distribution correlation coefficients. Notice that a large fraction of the dataset is correlated with the EHP trace. *Half* the traces have a correlation coefficient higher than 0.36. As expected, the underlying trend is shared by a large number of device. Although the highest score (i.e. 0.7715) corresponds to the light in the same room that the EHP serves, there are 118 pumps, serving all areas of the building, with a correlation higher than 0.6. Using only these results, it is not clear where the threshold should be set.

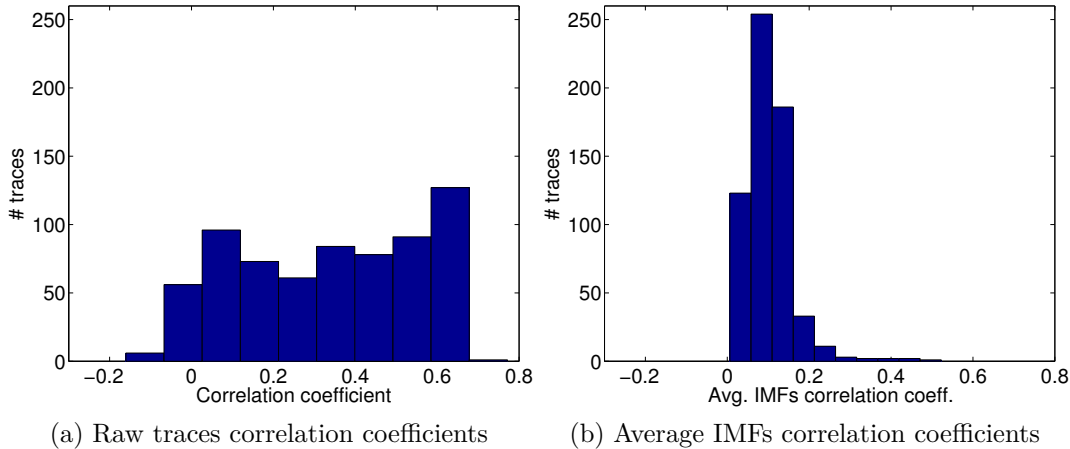


Figure 7.15: Distribution of the correlation coefficients of the raw traces and correlation coefficients average of the corresponding IMFs using 3 weeks of data from 674 sensors.

The distribution is close to uniform, making it difficult to know of how well your threshold discriminates against unrelated traces.

Figure 7.15b shows the distribution of the average correlation value for the IMFs of each trace and the EHP. The number of traces correlated in the high frequency IMFs is significantly smaller than the previous results. It's clear from the distribution that only a small set of devices are *intrinsically correlated* with the EHP. In fact, *only 10 traces out of 674* yielded a score higher than 0.25. This allows us to easily rank traces by correlation.

Upon closer inspection of the 10 most correlated IMF traces, we find that there is a spatial relationship between the EHP and the ten devices. In fact, there is a direct relationship between score and distance from the areas served by the EHP. Figure 7.16 shows a map of the floor that contains the rooms served by this EHP. The EHP directly serves room *C2*. We introduce a correlation threshold to cluster correlated traces by score. We highlight rooms by the threshold setting on the IMF correlation score. When we set the threshold at 0.5 we see that the sensors that have a correlation higher fall within room *C2* – the room served directly by the EHP. As we relax the threshold, lowering it to 0.25 and 0.1 we see radial expansion from *C2*. The trace with the highest score, 0.522, is the trace corresponding to the lighting system *in the same room*. The two highest scores for this floor (i.e. 0.316 and 0.279) are the light and EHP traces from next door, room *C1*. Lower values correspond to sensors measuring activities in other rooms that have no specific relationship to the analyzed trace. The results show a direct relationship between IMF correlation and spatial proximity and *supports our initial hypothesis*.

EMD is useful for finding underlying behavioral relationships between traces of sensor data. However, when we set the timescales smaller than a day, the results were not as strong. The trace has to be long enough to capture the trend. For this data set, the underlying trend is daily, therefore it requires there to be a significant number of samples over many

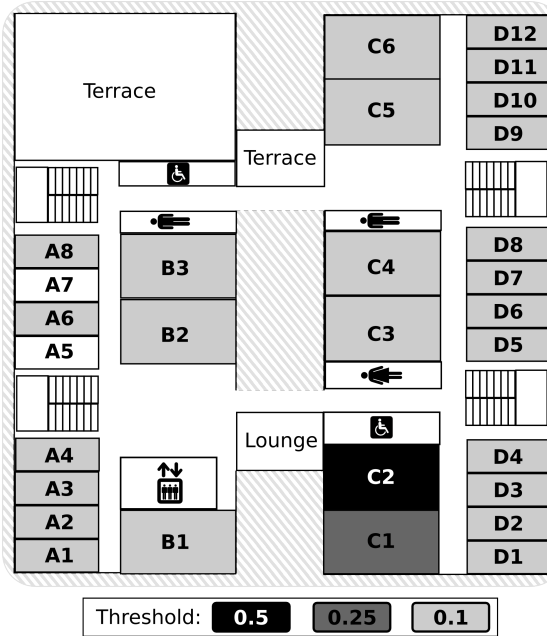


Figure 7.16: Map of the floor where the analyzed EHP serves (room  $C2$ ). The location of the sensors identified as related by the proposed approach are highlighted, showing a direct relationship between IMF correlation and spatial proximity.

days. Although this was a limitation for this dataset, it really depends on the underlying phenomenon that the sensors are measuring. Its underlying trend is ultimately what EMD will be able to separate from the intrinsic modes of the signal.

Figure ?? shows a comparison of two temperature sensor feeds from different rooms and their respective decomposition. Despite strong correlation in the raw time series, the medium frequency IMF shows little correlation. Only the low frequency diurnal pattern is correlated. Alternatively, Figure ?? shows a  $CO_2$  trace and a humidity trace.

While the raw signals appear to be very different, and indeed have modest correlation, the medium frequency components are strongly correlated. We conjecture that the medium frequency band “records” local activity. Occupants and movement in the space affect the levels of various physical phenomenon, namely temperature, humidity,  $CO_2$  levels, etc. Over shorter time spans, noise in the system hides the effects of local activity. Longer time-spans capture long-term trends related to weather or building operation schedules. The medium frequency band captures activities such as meetings and office occupation times. These examples illustrate the basis for an automated process. By isolating a particular component of the signal we seek to strip away common diurnal factors and also eliminate differences in the response of various sensors to environmental factors. We combine this observation with a simple classifier to derive colocation.

## Spatial Clustering Experimental Results

We conduct two sets of experiments. First, we quantify the sensitivity of our method for different threshold values and examine the effect of different time spans on the threshold. We then cluster the traces based on our threshold analysis and compare it with a baseline approach using multidimensional scaling and k-means.

### Baseline and Metrics

As a baseline, after we generate the two distributions described previously, we apply multidimensional scaling (MDS) to the corrcoeff matrix, in order to transform the original high-dimensional relative space to a 3-D space with an absolute origin, and run the k-means clustering algorithm. We choose the true-positive rate (TPR, also known as recall rate) and false-positive rate (FPR) as metrics to evaluate the performance of our method versus the naive approach, which correlates the raw traces. A true-positive (TP) is when a sensor pair in a room is classified as being co-located while a false-positive (FP) is when a sensor that is not in room is classified as being so.

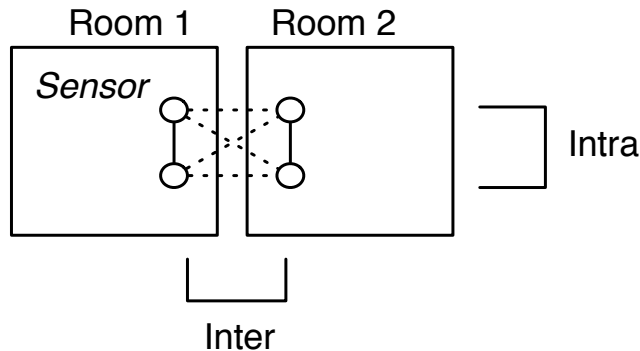


Figure 7.17: Two populations are examined for our threshold analysis. A solid line connects sensors in the same room while a dotted line connects to a pairs in different rooms.

### Characterizing the Boundary

To corroborate our boundary-existence hypothesis, we first need to characterize the boundary between sensors in different rooms. We compute the pairwise correlation coefficients (corrcoeffs) between sensor traces in both of populations depicted in Figure 7.17, over different time spans – ranging from one day to one month. After generating points over different time spans for each room, we accumulate the corrcoeffs to obtain distributions as shown in Figure 7.18, for each of the five rooms.

The dashed vertical lines in Figure 7.18 represent an arbitrary threshold that partitions the distribution into two sets. Pairs of sensors to the right of the line are classified as being

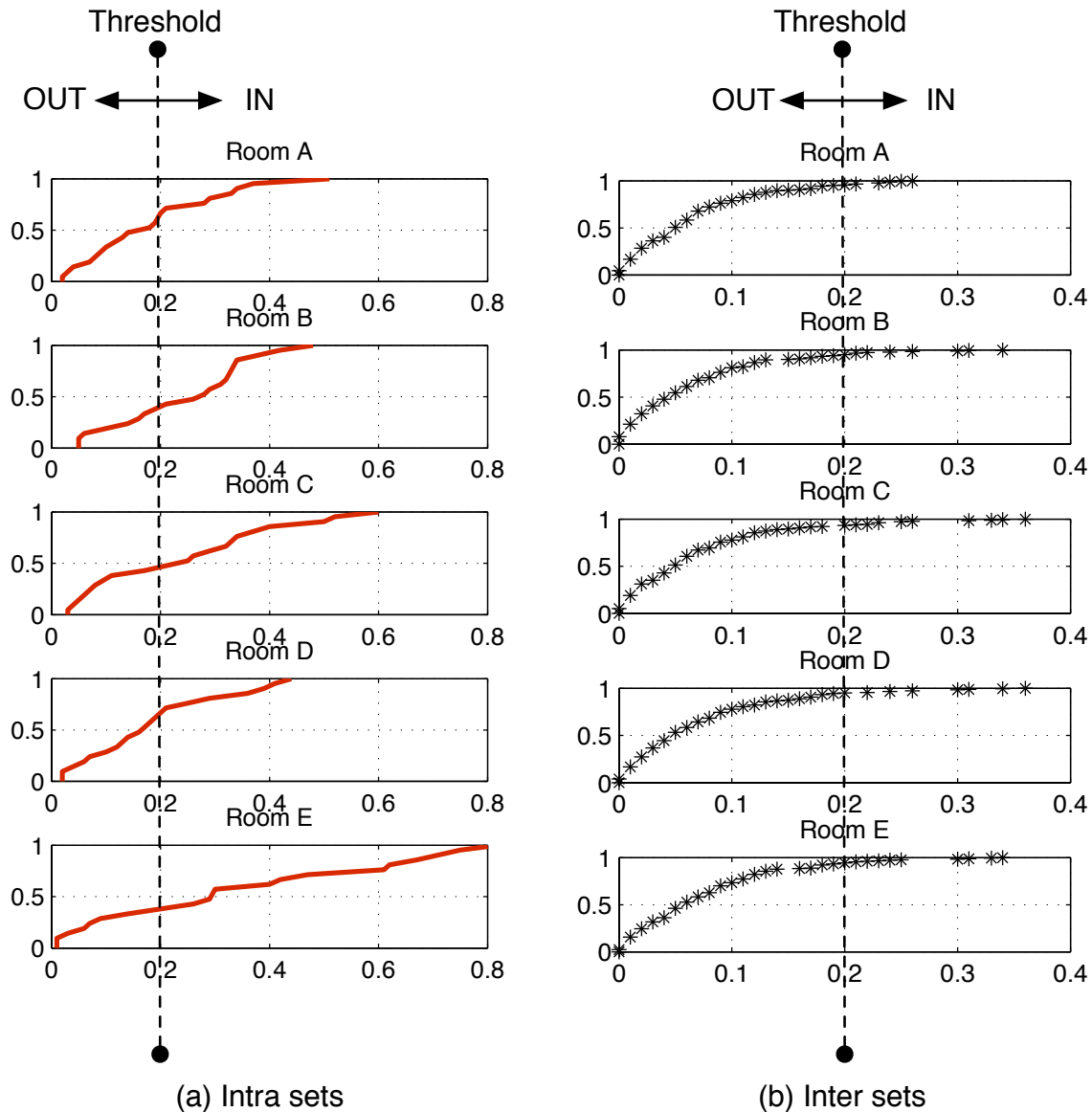


Figure 7.18: CDF of correlation coefficients between IMFs of sensor feeds: the dotted lines point to some threshold which divides the distribution and produces a TPR and FPR.

in the same room. Pairs of sensors to the left are classified as being in different rooms. The CDFs on the left column show the distribution of corrcoeffs for pairs known to be in the same room and the CDFs on the right show the distribution of corrcoeffs in different rooms. Note in the figure, we set the threshold to the same value to both the left and right side, in order to observe the effect of the true/false positive rates. By adjusting the threshold, we get different TPRs/FPRs parameterized by the threshold. Figure 7.13 captures the range

tradeoff in a corresponding ROC curve.

Figure 7.13 illustrates the TPR/FPR sensitivity to different threshold values for our method and the naive approach. A good cluster achieves a high TPR and a low FPR. As we vary the threshold, we see that our approach achieves a TPR between 52%–93% and a FPR between 5%–59%. We can see that the average TPR for the ROC graph on the right is higher than the ROC graph on the left. Moreover, the corresponding average FPR is lower on the right than on the left. In general, as the TPR rises, the FPR also goes up – *a tradeoff exists between maximizing TPR and maintaining a lower FPR*.

The “boundary” is represented as the corrcoeff that produces a “good” TPR with an “acceptable” FPR. In Figure ??, we choose 0.2 FPR as the boundary threshold. This point represents the largest difference between TPR and FPR – an acceptable tradeoff point. Looking at Figure 7.18, the 0.2 FPR corresponds roughly to the 80th-percentile correlation coefficient, on the “inter” set (the set of CDFs on the right). The recall rate for each room – using a 80th-percentile corrcoeff threshold value – ranges between 62%–86% and the threshold value falls into a narrow interval between 0.1 to 0.12. This shows that *we are able to choose a uniform value for all the rooms regardless of the sensor type*.

## Convergence over Time

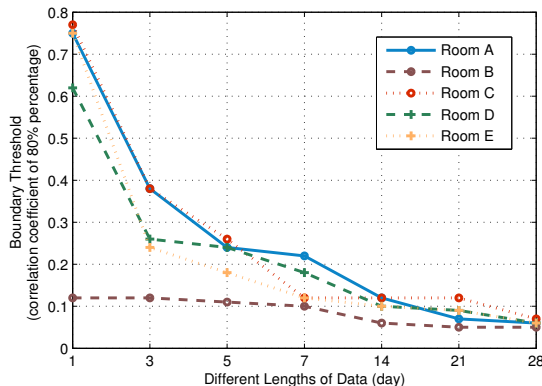


Figure 7.19: The threshold values all converge to a similar value and we can derive the optimal value with as minimal as 14 days data.

Using the threshold the roughly 80th-percentile corrcoeff corresponds to in the distribution, we examine how it affects the classification rate across traces that span different lengths of time. Convergence and consistency across different time spans is critical to automate the parameter selection process. Observe how the threshold values differ quite significantly in Figure 7.19. However, the threshold values gradually converge, as the length of training data increases from one day to one month. The values derived after 14 days of data are

approximately the same as the final convergence value (around 0.07). In other words, we can determine a threshold from two weeks of data.

## Clustering Results

We cluster the sensor traces over the entire one-month period, and use the roughly 80th percentile corrcoeff (0.07) as the boundary threshold. A sensor is classified into the cluster with the largest corrcoeff. The clustering result is shown in Table 7.4. A “1” means the sensor is classified as inside the corresponding room. In general, after obtaining the sensor clusters, we don’t know which room each cluster corresponds to without further information such as the metadata of sensors. The labels “A-E” in Table 7.4 are used to indicate the ground truth of where each sensor is physically placed since we have such information. Overall, the classification accuracy is 93.3%. We do not cluster on the corrcoeffs obtained among raw signals because the 80%-percentile corrcoeff values do not converge across rooms. The reason that we are able to get such a high accuracy, which is seemingly different from the statistics in Figure 7.18 and Figure 7.13, is because the statistics in the two figures are generated out of the corrcoeffs accumulated over different time spans (the same intervals in Figure 7.19) while the clustering here is performed on the corrcoeffs from the entire one-month period.

	<i>A</i>	<i>B</i>	<i>C</i>	<i>D</i>	<i>E</i>	
<i>Sensor A<sub>1</sub></i>	1	0	0	0	0	✓
<i>A<sub>2</sub></i>	1	0	0	0	0	✓
<i>A<sub>3</sub></i>	1	0	0	0	0	✓
<i>B<sub>1</sub></i>	0	1	0	0	0	✓
<i>B<sub>2</sub></i>	0	1	0	0	0	✓
<i>B<sub>3</sub></i>	0	1	0	0	0	✓
<i>C<sub>1</sub></i>	0	0	1	0	0	✓
<i>C<sub>2</sub></i>	0	0	1	0	0	✓
<i>C<sub>3</sub></i>	0	0	1	0	0	✓
<i>D<sub>1</sub></i>	0	0	0	1	0	✓
<i>D<sub>2</sub></i>	0	0	0	1	0	✓
<i>D<sub>3</sub></i>	0	0	1	0	0	✗
<i>E<sub>1</sub></i>	0	0	0	0	1	✓
<i>E<sub>2</sub></i>	0	0	0	0	1	✓
<i>E<sub>3</sub></i>	0	0	0	0	1	✓

Table 7.4: Clustering result using the thresholding method: a “1” means the sensor is classified as inside the room. We get the “✓” and “✗” by comparing the clustering results with ground truth.

To compare with our threshold-based method, we also cluster using a baseline approach. The pairwise corrcoeff for sensors in different rooms can be interpreted as a “distance” between them. A larger coefficient indicates a closer “distance”, and vice versa. However, since the distances between pairs is relative, we use multidimensional scaling [10] to find a

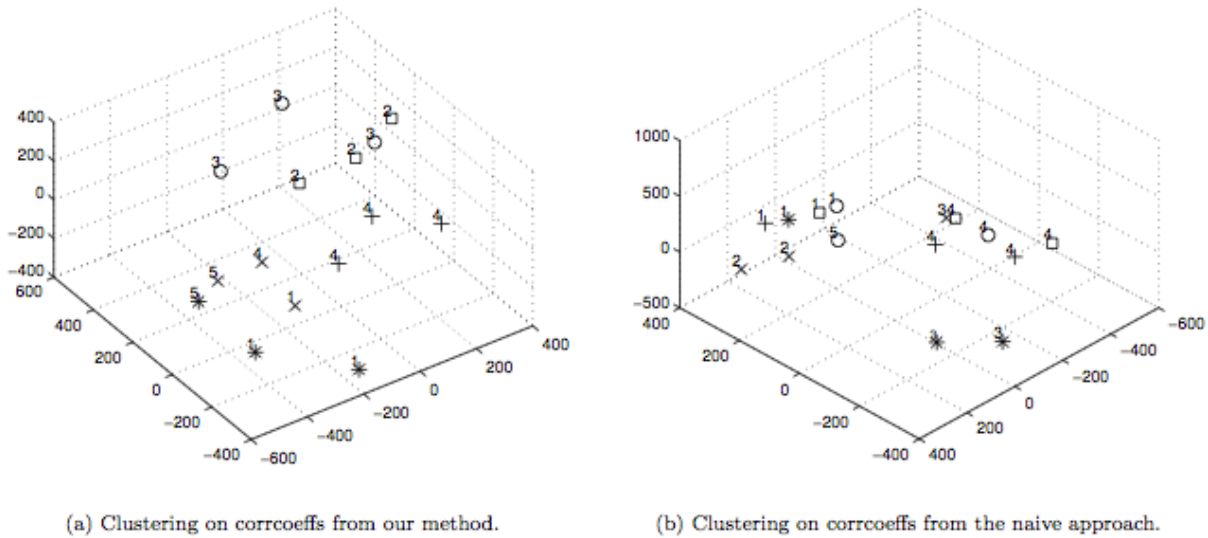


Figure 7.20: Clustering with k-means on the corrcoeff matrix after applying multidimensional scaling (MDS): The EMD-based set achieves an accuracy of 80% while the results with raw-trace is only 53.3% classification accuracy.

common basis in three dimensions, re-map the relative distance metric (feature vector) into this three-dimensional grid and use k-means to classify the traces. We set k to equal the number of rooms, since the goal of the approach is to verify spatial placement at room-level granularity. Generally, we believe that k should equal the number of rooms you wish to classify the sensors into. The clustering results are shown in Figure 7.20. Ground truth is shown through different markers (x, o, +, star, box). Each marker stands for one room. The cluster each sensor assigned to is denoted with a number. The classification accuracy of the baseline approach on corrcoeffs matrix of re-aggregated IMFs is 80%. For raw traces, the baseline approach achieves an accuracy of only 53.3%.

## 7.5 Type Verification Methodology

## 7.6 Type Verification Results

## 7.7 Related Work

SBS is a practical method for mining device traces, uncovering hidden relationships and abnormal behavior. In this paper, we validate the efficacy of SBS using the sensor metadata (i.e. device types and location), however, these tags are not needed by SBS to uncover devices relationships. Furthermore, SBS requires no prior knowledge about the building and

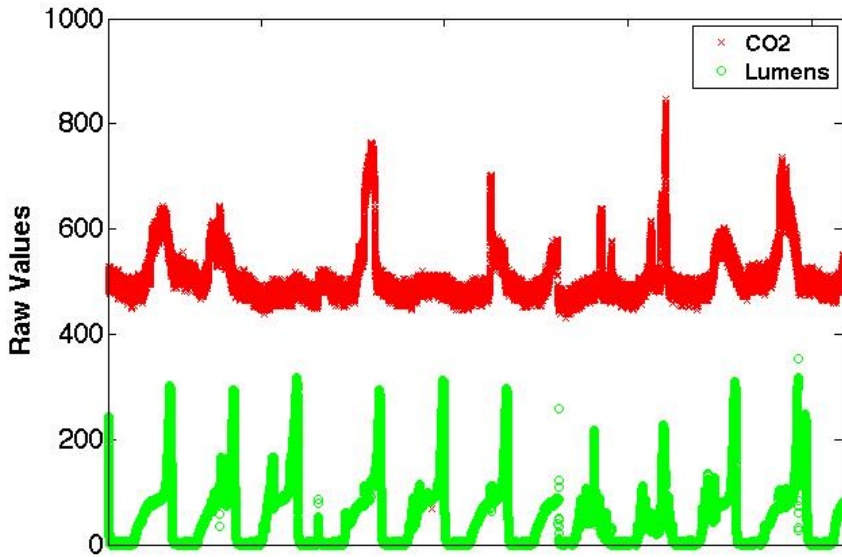


Figure 7.21:

deploying our tool to other buildings requires no human intervention – neither extra sensors nor a training dataset is needed.

SBS is a best effort approach that takes advantage of all the existing building sensors. For example, our experiments revealed that SBS indirectly uncovers building occupancy through device use (e.g. the elevator in the Building 2). The proposed method would benefit from existing sensors that monitor room occupancy as well (e.g. those deployed in [agarwal:ipsn2011, erickson:ipsn2011]). Savings opportunities are also observable with a minimum of 2 monitored devices and building energy consumption can be better understood after using SBS.

SBS constructs a model for normal inter-device behavior by looking at the usage patterns over time, thus, we run the risk that a device that constantly misbehaves is labeled as normal. Nevertheless, building operators are able to quickly identify such perpetual anomalies by validating the clusters of correlated devices uncovered by SBS. The inspection of these clusters is effortless compare to the investigation of the numerous raw traces. Although this kind of scenario is possible it was not observed in our experiments.

In this paper, we analyze only the data at medium frequencies, however, we observe that data at the high frequencies and residual data (Figure 7.4) also permits us to determine the device type. This information is valuable to automatically retrieve and validate device labels – a major challenge in building metadata management.

There has been much research work on sensor stream clustering and trace analysis. Chen and Tu [6] investigate how to cluster data streams in real-time using a density-based approach with a two-tiered framework. The first tier captures the dynamics of a data stream with

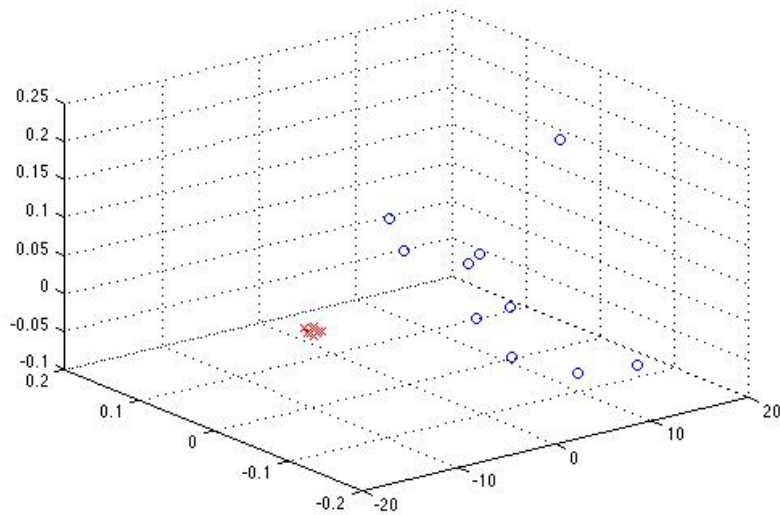


Figure 7.22:

a density decaying technique and then maps it to a grid. The second tier computes a grid density based on how it clusters the grid. Their approach differs from ours in that they focus on decreasing algorithm complexity for real-time sensor stream clustering. We run our analysis on historical traces and use correlation analysis in our clustering algorithm.

Kapitanova et al. [25] describe a technique to monitor sensor operations in the home and identify sensor failures. The classifier is trained on historical sensor data to obtain the relationship between sensors, assuming the number and location of sensors is known. When

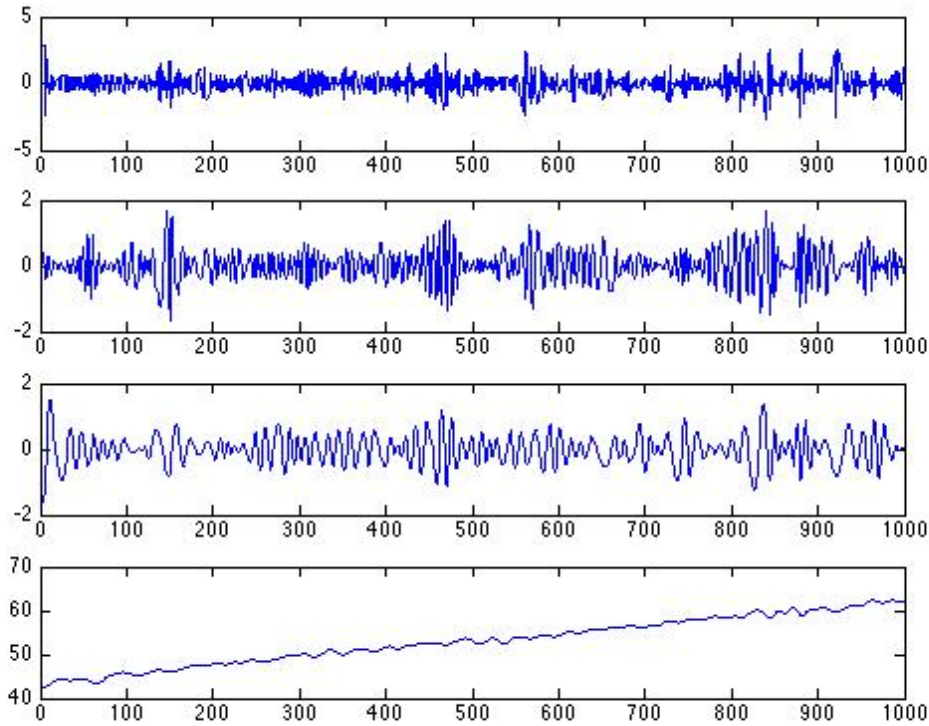


Figure 7.23:

a failure or removal of a sensor occurs, the classifier’s behavior deviates and the event is captured. Our method does not require any prior knowledge and instead tries to cluster feeds to discover their relative placement.

Lu and Whitehouse [28] formulate a new algorithm, particularly leveraging the semantic constraints interpreted from sensor data to determine sensor locations. The algorithm identifies how many rooms are present using motion sensors and determines room position based on physical constraints. Finally, it maps each sensor into the associated room. Our efforts focus on using intrinsic patterns typically pre-existing in building system sensor feeds to uncover physical relationships.

Fontugne et al. [12] propose a new method to decompose sensor signals with EMD. They extract the intrinsic usage pattern from the raw traces and show that sensors close to each other have higher intrinsic correlation. However, they do not explore the observation more deeply by answering whether there is a statistically discoverable boundary between sensor clusters in different rooms, or if there is a uniform threshold in the correlation coefficients able to be generalized to different rooms.

Fontugne et al. [13] carry on the work and propose an unsupervised method to monitor sensor behavior in buildings. They constructed a reference model out of the underlying patterns, obtained with EMD, and use it to compare future activity against it. They report

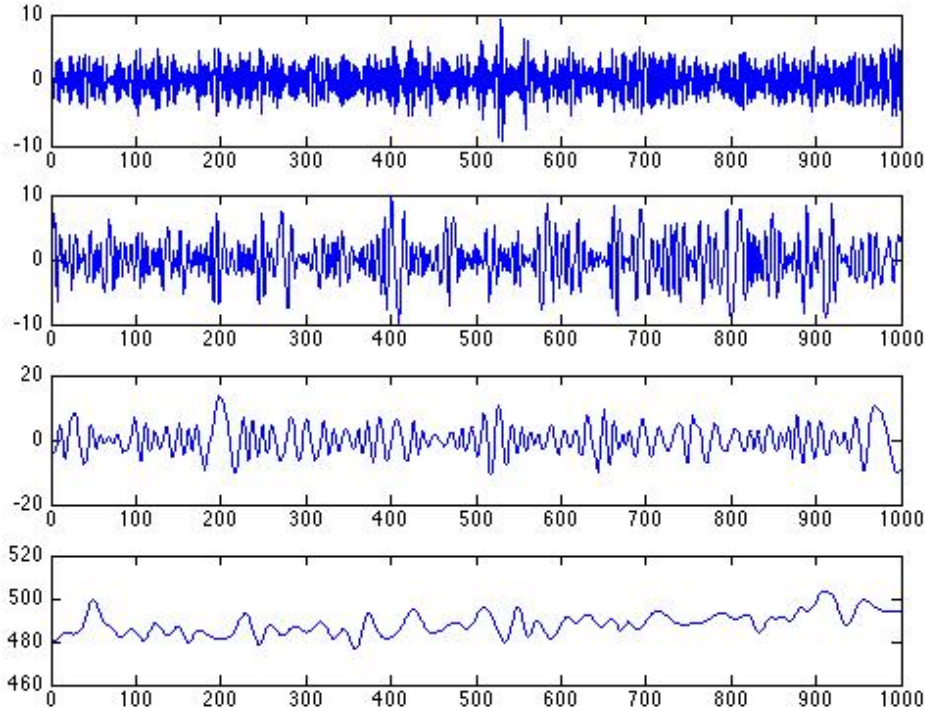


Figure 7.24:

an anomaly whenever a device deviates from the reference. This work exploits EMD as a method to detrend the signals and capture the inter-device relationships.

Much work utilizes EMD on medical data [3], speech analysis [18], image processing [32] and climate analysis [27]. Our method adopts EMD to determine whether a discoverable statistical boundary exists in sensors traces from sensors in different rooms and whether such a boundary can be generalized across rooms with various kinds of sensors.

## 7.8 Summary

### Functional Verification

This paper aims to establish a methodology to identify abnormalities in device power traces and inter-device usage patterns. In addition, we are planning to apply this method to online detection using, for example, a sliding window to compute an adaptive reference matrix that evolves in time. However, designing such system raises new challenges that are left for future work.

The goal of this work is to assist building administrators in identifying misbehaving devices in large building sensor deployments. We proposed an unsupervised method to systematically detect abnormal energy consumption in buildings: the Strip, Bind, and Search

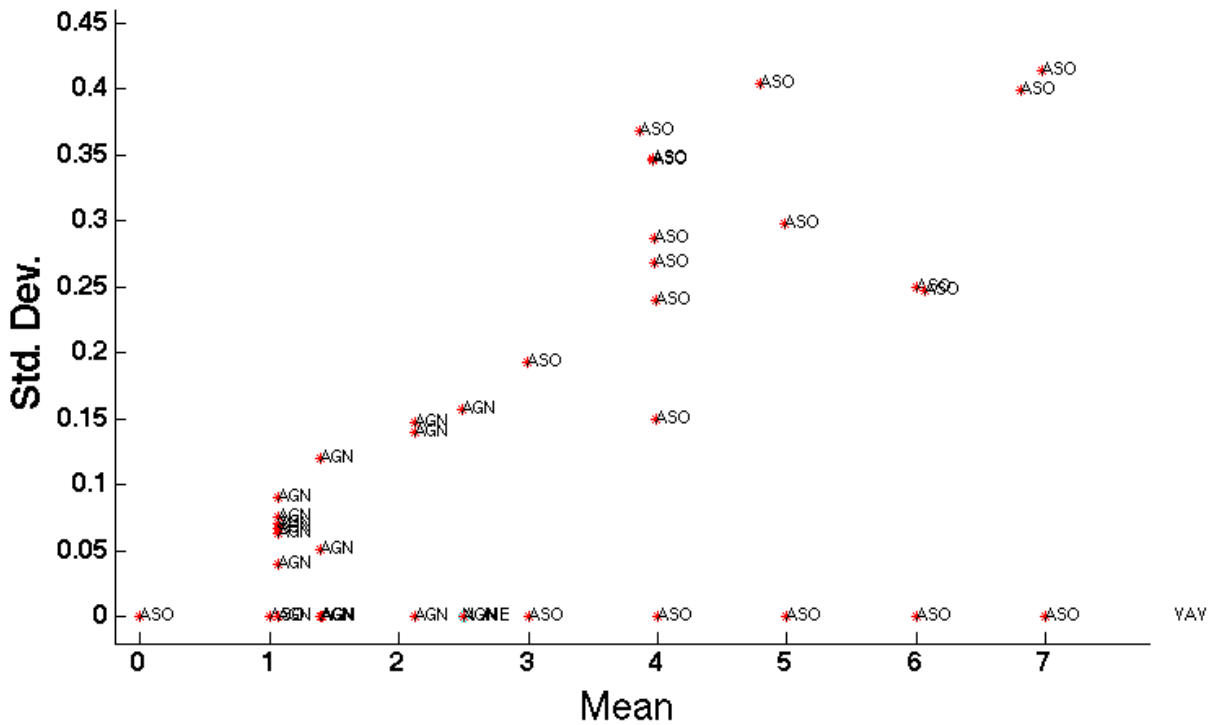


Figure 7.25:

(SBS) method. SBS uncovers inter-device usage patterns by striping dominant trends off the devices energy-consumption trace. Then, it monitors device usage and reports devices that deviate from the norm. Our main contribution is to develop an unsupervised technique to uncover the true inter-device relationships that are hidden by noise and dominant trends inherent to the sensor data. SBS is used on two sets of traces captured from two buildings with fundamentally different infrastructures. The abnormal consumption identified in these two buildings are mainly energy waste. The most important one is an instance of a competing heater and cooler that caused the heater to waste around 2500 kWh.

## Spatial Verification

EMD allows us to effectively identify fundamental relationships between sensor traces. We believe that identifying meaningful usage-correlation patterns can help reduce oversights by the occupants and faults that lead to energy waste. A direct application of this is the identification of simultaneous heating and cooling [31]. Simultaneous heating and cooling is when the heating and cooling system either compete with one another or compete with the incoming air from outside. If their combined usage is incorrect, there is major energy waste. This problem is notoriously difficult to identify, since the occupants do not notice changes

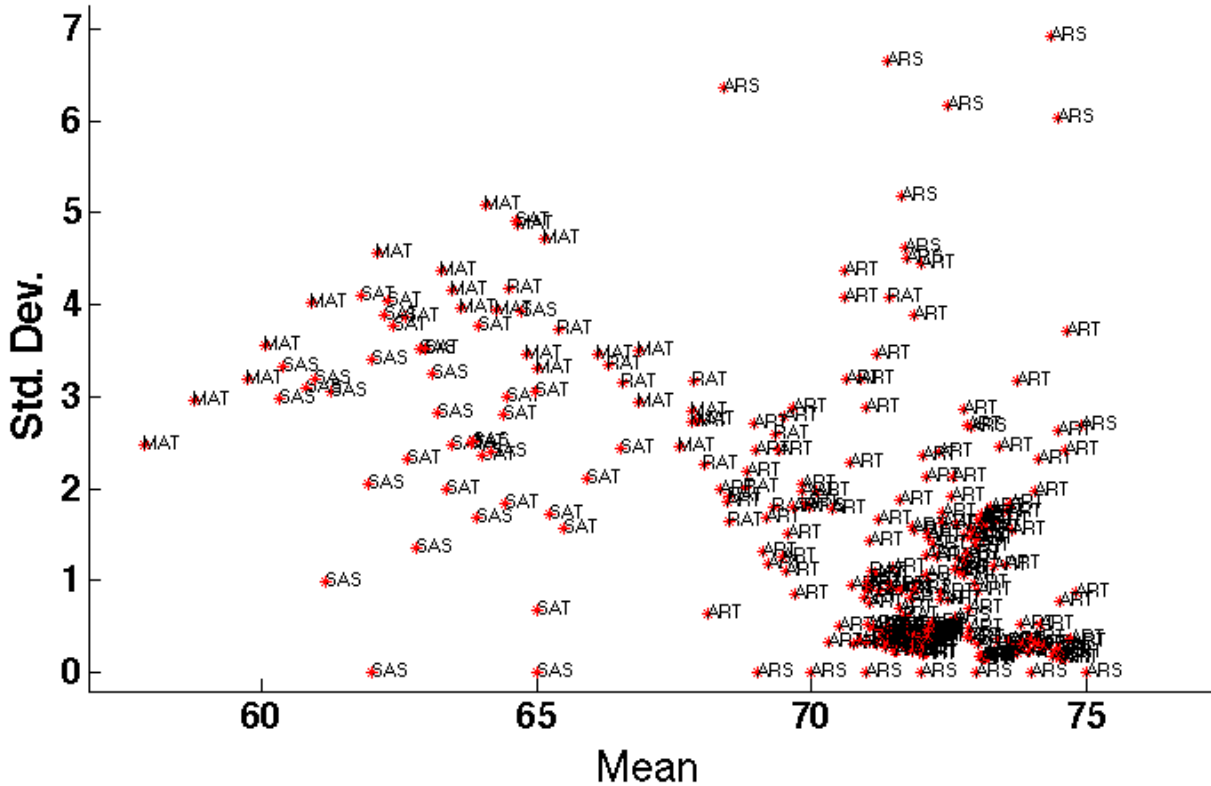


Figure 7.26:

in temperature and building management systems do not perform cross-signal comparisons. For future work, we intend to run our analysis on the set of sensors that will allow us to identify this problem: the outside temperature sensors, the cooling coil temperature, and the air vent position sensor. If their behavior is not correlated as expected, an alarm will be raised.

We can also apply it to other usage scenarios. In our traces, we found an instance where the pump was on but the lights were off; where, typically, they are active simultaneously. The air conditioning was pumping cool air into a room without occupants. With our approach this could have been identified and corrected. In future work, we intend to package our solution to serve these kinds of applications.

This paper set out to examine the underlying relationship between sensor traces to find interesting correlations in use. We used data from a large deployment of sensors in a building and found that direct correlation analysis on the raw traces was not discriminatory enough to find interesting relationships. Upon closer inspection, we noticed that the underlying trend was dominating the correlation calculation. In order to extract meaningful behavior this trend has to be removed. We show that empirical mode decomposition is a helpful

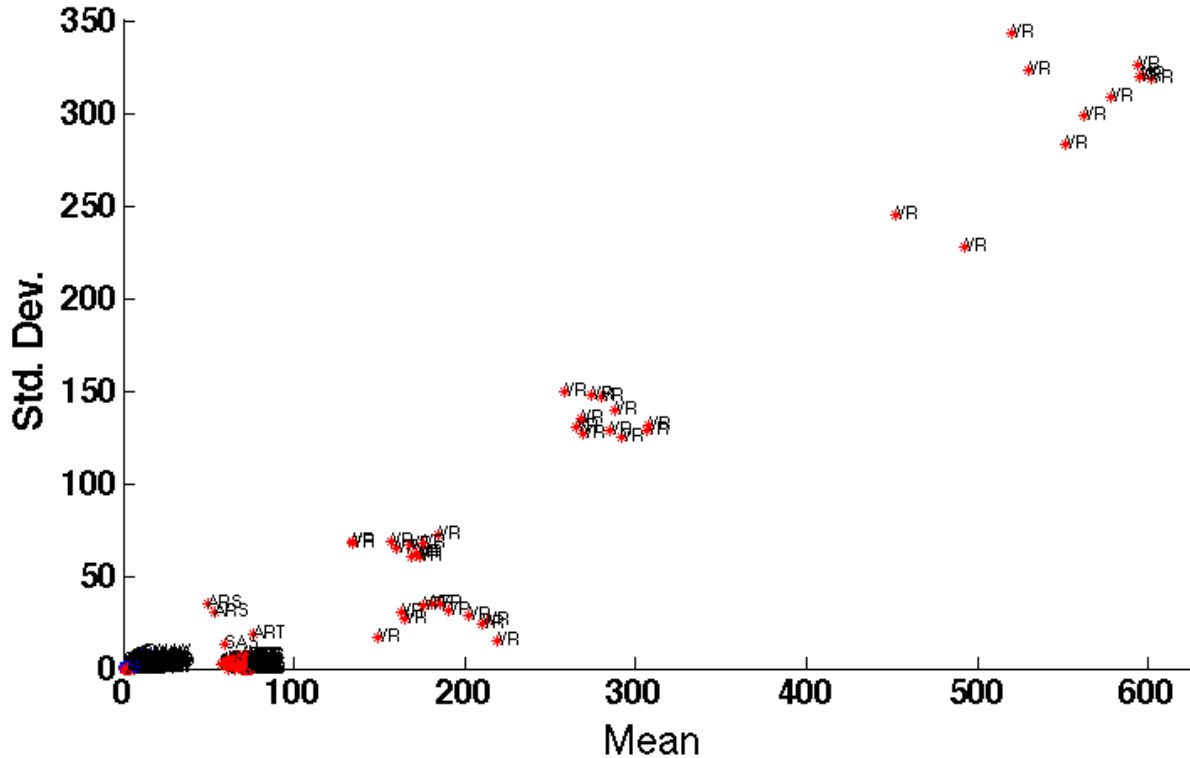


Figure 7.27:

analytical tool for detrending non-linear, non-stationary data; inherent attributes contained in our traces.

We ran our correlation analysis across IMFs, extracted from each trace by the EMD process, and found that the pump and light that serve the same room were highly correlated, while the other pump was not correlated to either. In order to corroborate the applicability of our approach, we compared the pump trace with *all* 674 sensor traces and found a strong correlation between the relative spatial position of the sensors and their IMF correlations. The most highly-correlated IMFs were serving the same area in the building. As we relax the admittance criteria we find that the spatial correlation expands radially from the main location served by the reference trace.

We plan to examine the use of this method in applications that help discover changes in underlying relationships over time in order to identify opportunities for energy savings in buildings. We will use it to build inter-device correlation models and use these models to establish “(ab)normal” usage patterns. We hope to take it a step further and include a supervised learning approach to distinguish between “(in)efficient” usage patterns as well.

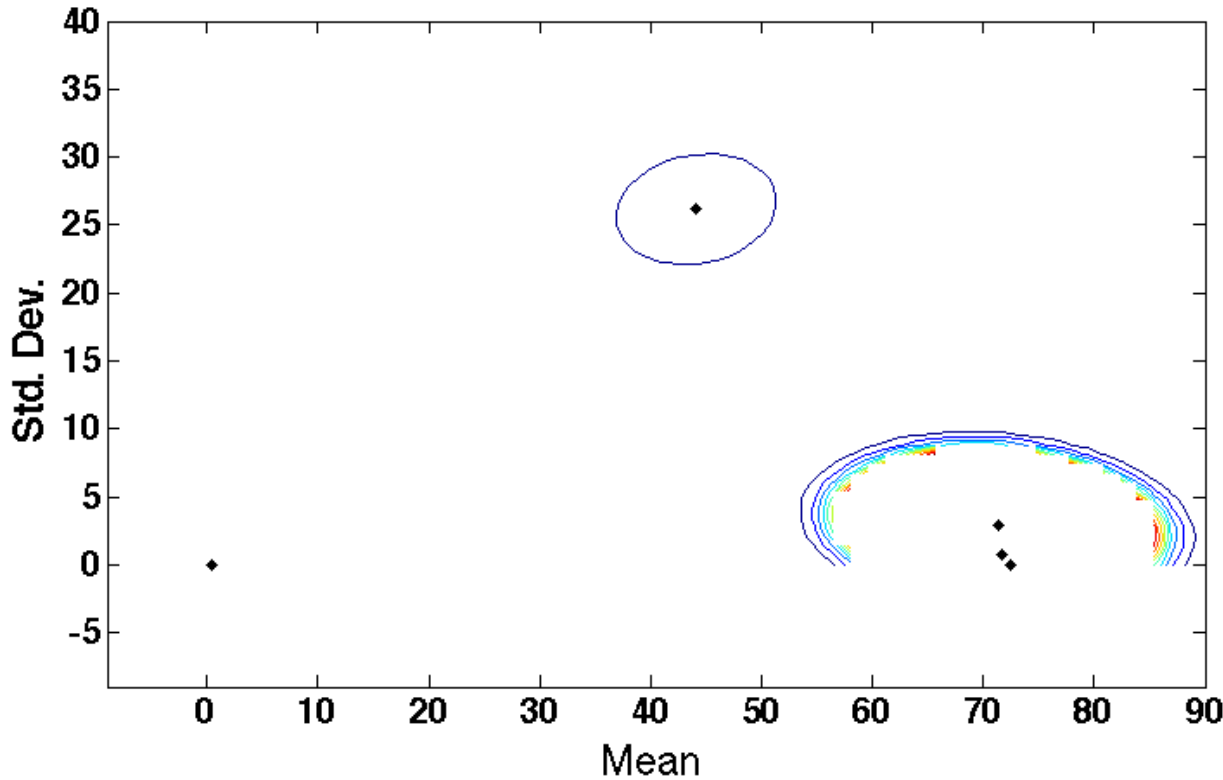


Figure 7.28:

**Bi-modal Distribution** From the results illustrated in Figure 7.18, we observe a bi-modality in the corrcoeff distribution for the two population sets. Sensors in the same room correlate to each other more (typically a corcoeff of 0.4 or higher) than sensors in different rooms. This bi-modal distribution may provide insight for us to understand the boundary and search for an effective discriminator more broadly.

**Across Different Sources** To further validate the effectiveness of the proposed method, we should consider using data from different sources. For example, in room B in Sutardja Dai Hall, there are two different sets of temperature sensors reporting data at different rates and granularities. We demonstrate our ability to classify sensor streams on the same platform (recall the sensor box we used to collect data). It would be more convincing to verify the effectiveness of our method with sensor streams generated from devices on different systems – since separate systems are independent. For instance, we can use temperature data from the second deployment and use the  $CO_2$  and humidity sensor data from the first deployment and compare the results to what we have gathered.

**Generalizability** In our results, the boundary threshold parameter converges to a narrow interval, as the data set expands over a longer time range. This may suggest that our method generalizes across rooms in a building, although further validation in a larger, more representative data set is necessary. This study looked at 5 different rooms with a large physical separation from one another. A more representative data set would consider all the rooms and pay special attention to rooms that share a common orientation and are separated by a single wall or floor slab.

Based on this study, and the previous, related one [12], we conjecture that local activity modulates various types of physical signals – captured by the various kinds of physical sensors embedded throughout the building – and that those signals are attenuated over distance and physical boundaries (such as walls). We believe that this is what drives our observations. If the conjecture is true, the effects will be less pronounced in larger rooms, such as an auditorium or a large laboratory space.

As our approach performs slightly better than traditional learning techniques, we must further evaluate its robustness versus the baseline method; across the entire building and across multiple buildings. In future work, we will examine the two approaches across larger intra-building data sets and compare results across multiple buildings. A key factor is the variance of classification accuracy – smaller variance demonstrates robustness.

We present a new method for spatial placement clustering. We first characterize the corrcoef distribution of medium frequencies IMFs between sensors in the same/different room(s), and then we learn the tradeoff between achieving a higher TPR and maintaining a lower FPR by manipulating a discriminator parameter within these two distributions. For a preliminary sample of relatively well separated rooms, we find that there is a clear boundary between sensor clusters in terms of their spatial placement and the boundary can be probed statistically. We also find a uniform discriminator can be learned and generalized across these rooms. For this initial study, our method is able to classify the sensors of 93.3% accuracy, which is 13% higher than a tradition k-means approach, with a TPR between 62%-86% and a FPR less than 20%.

These results are very encouraging. However, we recognize that they are far from definitive. While the rooms in the study were picked arbitrarily, they are neither comprehensive nor a systematic sampling. While they are clearly separated by our approach, and not by analyses of the raw time series, they do differ substantially in placement and usage. A key question going forward is, “how well will highly similar rooms be separated?” - say, adjacent rooms facing the same side of the building and with similar occupancy. Will these techniques hold, more powerful techniques be required, or is further discrimination intractable? In future work, we will examine how far this method takes us and explore how it may be used in combination with other techniques to improve the results more generally. Automated metadata verification is important to include in the lifecycle of building data management.

## Type Verification

## Chapter 8

### Lessons Learned and Future Work

# Chapter 9

## Conclusion

# Bibliography

- [1] Yuvraj Agarwal et al. “Enabling Building Energy Auditing Using Adapted Occupancy Models”. In: *Buildsys’11*. Seattle, WA, 2011, p. 6.
- [2] American Society of Heating, Refrigerating and Air-Conditioning Engineers. *ASHRAE Standard 135-1995: BACnet*. ASHRAE, Inc., 1995.
- [3] A. Arafat and T. Hasan. “Automatic detection of ECG wave boundaries using empirical mode decomposition”. In: *IEEE International Conference on Acoustics, Speech and Signal Processing (ICASSP)*. 2009.
- [4] Gowtham Bellala et al. “Towards an Understanding of Campus-Scale Power Consumption”. In: *Buildsys’11*. Seattle, WA, 2011, p. 6.
- [5] Vincent D. Blondel et al. “Fast unfolding of communities in large networks”. In: *J.STAT.MECH.* (2008).
- [6] Yixin Chen and Li Tu. “Density-based clustering for real-time stream data”. In: *Proceedings of the 13th ACM SIGKDD international conference on Knowledge discovery and data mining*. KDD ’07. 2007.
- [7] Stephen Dawson-Haggerty et al. “sMAP: a simple measurement and actuation profile for physical information”. In: *Proceedings of the 8th ACM Conference on Embedded Networked Sensor Systems*. SenSys ’10. Zürich, Switzerland, 2010.
- [8] Department of Energy. *2011 Buildings Energy Data Book*. <http://buildingsdatabook.eren.doe.gov/>.
- [9] Department of Energy. *USGBC Exploring A New Kind of LEED Plaque*. <http://www.leeduser.com/blogs/usgbc-exploring-new-kind-leed-plaque-v4-gbci-certification-platinum>.
- [10] R.O. Duda, P.E. Hart, and D.G. Stork. *Pattern Classification*. Wiley, 2001.
- [11] Patrick Th. Eugster et al. “The many faces of publish/subscribe”. In: *ACM Comput. Surv.* 35.2 (June 2003), pp. 114–131. ISSN: 0360-0300. DOI: 10.1145/857076.857078. URL: <http://doi.acm.org/10.1145/857076.857078>.
- [12] Romain Fontugne et al. “Empirical mode decomposition for intrinsic-relationship extraction in large sensor deployments”. In: *Workshop on Internet of Things Applications*. IoT-App’12. 2012.

- [13] Romain Fontugne et al. “Strip, bind, and search: a method for identifying abnormal energy consumption in buildings”. In: *Proceedings of the 12th international conference on Information processing in sensor networks*. IPSN ’13. 2013.
- [14] Ge Gao and Kamin Whitehouse. “The self-programming thermostat: optimizing setback schedules based on home occupancy patterns”. In: BuildSys’09. Berkeley, California, 2009, pp. 67–72. ISBN: 978-1-60558-824-7. DOI: <http://doi.acm.org/10.1145/1810279.1810294>. URL: <http://doi.acm.org/10.1145/1810279.1810294>.
- [15] P. Gardner and L. Ward. *Energy Management Systems in Buildings: The Practical Lessons*. Energy Publications, 1987. ISBN: 9780905332543. URL: [http://books.google.com/books?id=\\\_1wKfAEACAAJ](http://books.google.com/books?id=\_1wKfAEACAAJ).
- [16] Neil Gershenfeld, Stephen Samouhos, and Bruce Nordman. “Intelligent Infrastructure for Energy Efficiency”. In: *Science* 327.5969 (2010), p. 3.
- [17] Neil Gershenfeld, Stephen Samouhos, and Bruce Nordman3. “Intelligent Infrastructure for Energy Efficiency”. In: *Science Magazine* (2010).
- [18] Hai Huang and Jiaqiang Pan. “Speech pitch determination based on Hilbert-Huang transform”. In: *Signal Processing* 86.4 (2006), pp. 792 –803. ISSN: 0165-1684. DOI: <http://dx.doi.org/10.1016/j.sigpro.2005.06.011>. URL: <http://www.sciencedirect.com/science/article/pii/S0165168405002367>.
- [19] N. E. Huang et al. “The empirical mode decomposition and the Hilbert spectrum for nonlinear and non-stationary time series analysis”. In: *Proceedings of the Royal Society of London. Series A: Mathematical, Physical and Engineering Sciences* (1998). URL: <http://dx.doi.org/10.1098/rspa.1998.0193>.
- [20] Norden E. Huang. “Computing frequency by using generalized zero-crossing applied to intrinsic mode functions”. Pat. 6990436. 2006.
- [21] Norden E. Huang et al. “On Instantaneous Frequency”. In: *Advances in Adaptive Data Analysis* 1.2 (2009).
- [22] Norden E. Huang et al. “The empirical mode decomposition and the Hilbert spectrum for nonlinear and non-stationary time series analysis”. In: *Proceedings of the Royal Society of London. Series A: Mathematical, Physical and Engineering Sciences* 454.1971 (1998), pp. 903–995. DOI: 10.1098/rspa.1998.0193. eprint: <http://rspa.royalsocietypublishing.org/content/454/1971/903.full.pdf+html>. URL: <http://rspa.royalsocietypublishing.org/content/454/1971/903.abstract>.
- [23] Jonathan W. Hui and David E. Culler. “Extending IP to Low-Power, Wireless Personal Area Networks”. In: *Internet Computing, IEEE* 12.4 (2008).
- [24] Xiaofan Jiang et al. “Design and implementation of a high-fidelity AC metering network”. In: *Proceedings of the 2009 International Conference on Information Processing in Sensor Networks*. IPSN ’09. Washington, DC, USA: IEEE Computer Society, 2009, pp. 253–264. ISBN: 978-1-4244-5108-1. URL: <http://dl.acm.org/citation.cfm?id=1602165.1602189>.

- [25] Krasimira Kapitanova et al. “Being SMART about failures: assessing repairs in SMART homes”. In: *Proceedings of the 2012 ACM Conference on Ubiquitous Computing*. UbiComp ’12. 2012.
- [26] Younghun Kim et al. “Granger causality analysis on IP traffic and circuit-level energy monitoring”. In: BuildSys’10. Zurich, Switzerland, 2010, pp. 43–48. ISBN: 978-1-4503-0458-0. DOI: <http://doi.acm.org/10.1145/1878431.1878442>. URL: <http://doi.acm.org/10.1145/1878431.1878442>.
- [27] T. Lee and T. B. M. J. Ouarda. “Prediction of climate nonstationary oscillation processes with empirical mode decomposition”. In: *Journal of Geophysical Research: Atmospheres* 116.D6 (2011).
- [28] Jiakang Lu and Kamin Whitehouse. “Smart blueprints: automatically generated maps of homes and the devices within them”. In: *Proceedings of the 10th international conference on Pervasive Computing*. Pervasive’12. 2012.
- [29] Yudong Ma et al. “Predictive Control for Energy Efficient Buildings with Thermal Storage: Modeling, Stimulation, and Experiments”. In: *Control Systems, IEEE* 32.1 (2012), pp. 44–64. ISSN: 1066-033X. DOI: 10.1109/MCS.2011.2172532.
- [30] Sean Meyn et al. “Anomaly detection using projective Markov models in a distributed sensor network”. In: CDC’09. Shanghai, China, 2009.
- [31] Mark Modera et al. “Efficient Thermal Energy Distribution in Commercial Buildings Final Report to California Institute for Energy Efficiency”. In: *Environmental Energy Technologies Division, LBNL Technical Report* (1994).
- [32] H. Mohammadzade et al. “BEMD for expression transformation in face recognition”. In: *IEEE International Conference on Acoustics, Speech and Signal Processing (ICASSP)*. 2011.
- [33] Next10. *Untapped Potential of Commercial Buildings: Energy Use and Emissions*. 2010. URL: [http://next10.org/next10/pdf/NXT10\\_BuildingEfficiencies\\_final.pdf](http://next10.org/next10/pdf/NXT10_BuildingEfficiencies_final.pdf).
- [34] Jay Taneja et al. *Enabling Advanced Environmental Conditioning with a Building Application Stack*. Tech. rep. UCB/EECS-2013-14. EECS Department, University of California, Berkeley, 2013. URL: <http://www.eecs.berkeley.edu/Pubs/TechRpts/2013/EECS-2013-14.html>.
- [35] U.S. Environmental Protection Agency. *Buildings Energy Data Book*. 2010. URL: [http://buildingsdatabook.eren.doe.gov/docs/DataBooks/2010\\_BEDB.pdf](http://buildingsdatabook.eren.doe.gov/docs/DataBooks/2010_BEDB.pdf).
- [36] U.S. Green Building Council. *Leadership in Energy and Environmental Design*. <http://www.usgbc.org/leed/>.